REGULATORY FUNCTIONS OF NOTCH SIGNALING IN EARLY EMBRYONIC VASCULAR DIFFERENTIATION AND VESSEL REMODELING

BY

Jessica N. Copeland

Submitted to the graduate degree program in Pathology and Laboratory Medicine and the Graduate Faculty of the University of Kansas in partial fulfilment of the requirements for the degree of Doctor of Philosophy.

_____
Chairperson: Jay L. Vivian, Ph.D

_____
Dale R. Abrahamson, Ph.D.

_____
Patrick E. Fields, Ph.D.

_____
Linheng Li, Ph.D.

_____
Brenda J. Rongish, Ph.D.

Date defended: February 25, 2011

The Dissertation Committee for Jessica N. Copeland
certifies that this is the approved version of the following dissertation:

REGULATORY FUNCTIONS OF NOTCH SIGNALING IN EARLY EMBRYONIC

VASCULAR DIFFERENTIATION AND VESSEL REMODELING

_____
Chairperson: Jay L. Vivian, Ph.D

Date approved: _____

Abstract

The signaling cascades that direct the morphological differentiation of the vascular system during early embryogenesis are not well defined. Several signaling pathways, including Notch and VEGF signaling, are critical for the formation of the vasculature in the mouse. However, the relationship between the molecular signals and transcriptional networks directing this process are still not well defined. To further understand the role of Notch signaling during endothelial differentiation and the genes regulated by this pathway, both loss-of-function and gain-of-function approaches were analyzed in vivo and in vitro. Conditional transgenic models were used to expand and ablate Notch signaling in the early embryonic endothelium. Embryos with activated *Notch1* in the vasculature displayed a variety of defects, particularly in the yolk sac, and die soon after E10.5. These phenotypes were distinct from endothelial loss-of-function of *Rbpj*, a transcriptional regulator of Notch activity. Gene expression analysis of RNA isolated from the yolk sac of transgenic embryos indicated aberrant expression in a variety of genes in these models. In particular, a variety of secreted factors, including the VEGF family member, *Pgf*, displayed coordinate expression defects in the loss-of-function and gain-of-function models. These data indicate that Notch signaling may have potential nonautonomous roles in the remodeling of the yolk sac capillary plexus. To further understand the role of placental growth factor during endothelial differentiation, an in vivo gain-of-function transgenic model was developed. Embryos with expanded expression of *Pgf* in the vasculature display two distinct phenotypes, which were classified moderate and severe. Most notably, in both classes, the extraembryonic vasculature of the yolk sac displayed remodeling differentiation defects, with few

matured vessels. Gene expression analysis of RNA isolated from the yolk sac of transgenic embryos indicated aberrant expression in a variety of genes. In particular, Notch family members showed increased expression in the gain-of-function model. The data from this model demonstrates regulatory connections between the VEGF and Notch signaling pathways during endothelial differentiation. We propose a role for Notch signaling in elaborating the microenvironment of the nascent arteriole, and suggest that novel regulatory connections exist between Notch signaling and other signaling pathways, particularly the VEGF family, during endothelial differentiation.

Acknowledgements

This work was supported in part by a graduate teaching assistantship with the Department of Pathology and Laboratory Medicine at the University of Kansas Medical Center, an American Heart Association Heartland Affiliate predoctoral fellowship, and the Biomedical Research Training Program.

I would first like to thank my mentor and friend, Jay Vivian. During the past six years you have been there whenever I needed your help and guidance. You have helped me become a better scientist. I am truly indebted to you.

This research and my sanity would not have been possible without the help and friendship of past and present members of the Vivian lab. Lucy, you never complained about anything I asked of you. Thank you. Katie, you were always willing and able to answer my many questions. Thank you. Emily, my whole fourth chapter would not have been possible without you. You were always there when I needed to vent and relax. Thank you.

I would also like to thank and acknowledge my committee members, Drs. Dale Abrahamson, Pat Fields, Linheng Li, and Brenda Rongish. The guidance and suggestions I received in my committee meetings has truly helped to develop both my research and my knowledge.

I would like to thank all those on the first floor of Lied for supplying me with the reagents and help I often needed. I also thank Stanton Fernald of the KU Medical Center Imaging Core for aid in image acquisition, the KUMC Microarray Facility for generating array data sets, the KUMC Transgenic Core for generating my PGF chimeric mice, and the KUMC Flow Core for hep with yolk sac cell sorting.

I would like to thank my parents, Chris and Pat Vitello, who have always supported me and pushed me to do my best in everything. You believed in me even when I didn't believe in myself. I would also like to thank my in-laws, Ken Copeland and Jim and Lisa Sackuvich, along with my many other family members, for supporting me and being there whenever I needed your help.

Most importantly I would like to thank my husband, Andy. For the past six years you have helped me through many things, including my graduate studies. You have been so patient and understanding through it all and were always there when I needed someone to talk to. You are a wonderful husband and father. Thank you.

And finally, to my little girl, Mackenzie, thank you! You help brighten each day. You are truly my inspiration.

Table of Contents

Abstract ..... **iii**

Acknowledgements ..... **v**

Table of Contents ..... **vii**

List of Figures ..... **xiii**

List of Tables ..... **xvi**

Abbreviations ..... **xvii**

Chapter 1 Introduction **1**

1.1 Vasculogenesis 2

1.2 Angiogenesis 5

1.2.1 Sprouting angiogenesis *6*

1.2.2 Intussusceptive angiogenesis *6*

1.2.3 Tumor angiogenesis *10*

1.3 Signaling pathways in vascular development 12

1.3.1 Notch signaling pathway *12*

1.3.1.1 Notch family 12

1.3.1.2 Notch family expression 16

1.3.1.3 Notch signaling in vascular development 18

1.3.1.4 Notch signaling in pathological conditions 21

1.3.2 VEGF signaling pathway *22*

1.3.2.1 VEGF family 22

1.3.2.2 VEGF family expression 25

1.3.2.3 VEGF signaling in vascular development 27

1.3.2.4 VEGF signaling in pathological conditions 28

1.3.3 TGFβ signaling pathway *29*

1.4 Interactions between the signaling pathways 30

Chapter 2 Materials and Methods 32

2.1 Standard solutions and reagents 32

2.2 Animal husbandry 33

2.2.1 Generation of the Z/EG-Pgf transgene *33*

2.2.2 Breeding scheme to obtain mice and embryos *33*

2.2.3 Genotyping of progeny *34*

2.2.4 Animal euthanasia *34*

2.3 Generation and embedding of embryoid bodies 35

2.3.1 Embryoid body formation *35*

2.3.2 Collagen embedding of embryoid bodies *35*

2.3.2.1 Preparation of wells 35

2.3.2.2 Embryoid body embedding 35

2.4 DNA manipulations 36

2.4.1 Genomic DNA isolation *36*

2.4.2 Polymerase Chain Reaction (PCR) *37*

2.5 RNA manipulations 38

2.5.1 RNA isolation *38*

2.5.2 Reverse Transcriptase (RT)-PCR *38*

2.5.3 Real-time PCR *39*

2.5.4 Microarray analysis *39*

2.6 Histology 42

2.7 Immunochemistry 42

2.7.1 Embryo and yolk sac immunochemistry 42

2.7.2 Embryoid body immunochemistry 43

2.8 Immunofluorescence 43

2.8.1 Yolk sac immunofluorescence 43

2.8.2 Fluorescence histology 44

2.8.3 Embryoid body immunofluorescence 45

2.8.4 Endothelial cell immunofluorescence 45

2.9 X-gal staining 46

2.10 Yolk sac endothelial cell purification 47

2.10.1 Preparation of single yolk sac cell suspension 47

2.10.2 Cell sorting with PECAM1 47

2.11 Identification of TFBSs 47

2.12 Microscopy and image acquisition 47

2.13 Statistical analysis 48

Chapter 3 Notch signaling regulates remodeling and vessel diameter in the extraembryonic yolk sac 49

3.1 Introduction 49

3.2 Results 51

3.2.1 Conditional transgenesis to modulate Notch signaling in the early endothelia. 51

3.2.2 Regulated Notch signaling is essential for the growth and development of the

early embryo *55*

3.2.3 Vascular defects in EC-N1ICD and EC-Rbpj-KO embryos *55*

3.2.4 Identification of Notch regulated genes in EC-N1ICD yolk sacs and EC-Rbpj-KO yolk sacs *62*

3.2.5 Notch-Rbpj signaling regulates the vascular expression of key signaling molecules *64*

3.2.6 Putative Notch regulated genes contain potential RBPJ binding sites in the upstream regulatory region *69*

3.3 Discussion 71

Chapter 4 Development of an embryonic stem cell differentiation model for Notch functions in vascular development 78

4.1 Introduction 78

4.2 Results 80

4.2.1 Design and generation of Ainv15-N1-ICD ES cells. *80*

4.2.2 Endothelial cells differentiated from Ainv15-N1-ICD ES cells *85*

4.2.3 Gene regulation in differentiated Ainv15-N1-ICD ES cells *87*

4.2.4 Collagen embedded embryoid bodies mimic sprouting angiogenesis *91*

4.3 Discussion 93

Chapter 5 Overexpression of placental growth factor in the early embryo disrupts vascular differentiation 99

5.1 Introduction 99

5.2 Results 101

5.2.1 Design and generation of a transgene to conditionally modulate the

expression of placental growth factor in the endothelia. *101*

5.2.2 Regulated placental growth factor expression is essential for the growth and development of the early embryo *103*

5.2.3 Expression of PlGF via GFP after CRE excision *105*

5.2.4 Vascular defects in Z/EG-Pgf embryos *107*

5.2.5 Defects in embryo-derived vasculature and gene expression in Z/EG-Pgf transgenic placenta *110*

5.2.6 Overexpression of Pgf in the endothelia induces the expression of Notch signaling family members *112*

5.3 Discussion 114

Chapter 6 General Discussion and Prospectus 123

6.1 Insights into vascular remodeling 124

6.2 Model of role of Notch and VEGF pathways in vascular remodeling 127

6.2.1 Implications of model. *129*

6.2.1.1 Notch/VEGF interaction in embryonic vascular development 129

6.2.1.2 Notch/VEGF interaction in pathological angiogenesis 130

6.3 Future directions 132

6.3.1 Notch signaling in vascular remodeling *132*

6.3.2 Transgenic ES cell model *133*

6.3.3 Placental growth factor activity in vivo *135*

6.3.4 Future transgenic studies *136*

6.4 Concluding remarks 137

References **138**

Appendix I Microarray data of EC-N1ICD yolk sacs **151**

AI-1 Top 50 upregulated genes 151

AI-2 Top 50 downregulated genes 153

Appendix II Microarray data of EC-Rbpj-KO yolk sacs **155**

AII-1 Top 50 upregulated genes 155

AII-2 Top 50 downregulated genes 157

Appendix III Microarray data of Dox treated Ainv15-N1-ICD ES cells **159**

AIII-1 Top 50 upregulated genes 159

AIII-2 Top 50 downregulated genes 161

Appendix IV Microarray data of differentiated Ainv15-N1-ICD ES cells **163**

AIV-1 Top 50 upregulated genes 163

AIV-2 Top 50 downregulated genes 165

Appendix V Curriculum Vitae **167**

List of Figures

Figure 1.1. Vasculogenesis in the Early Embryo 4

Figure 1.2. Intussusceptive Angiogenesis 8

Figure 1.3. Structure of the Notch Ligands and Receptors..... 13

Figure 1.4. Notch Signaling Pathway 15

Figure 1.5. VEGF Signaling Pathway 26

Figure 3.1. Conditional Mouse EC-N1ICD and EC-Rbpj-KO Transgene Constructs..... 53

Figure 3.2. *Tie2-Cre* and *Flk1-Cre* are Expressed in the Endothelia of the Early Embryo...
.....54

Figure 3.3. Embryonic Growth and Vascular Remodeling is Normal in Early EC-N1ICD Embryos..... 57

Figure 3.4. Defects in Growth and Yolk Sac Vasculature Remodeling in EC-N1ICD and EC-Rbpj-KO Embryos 58

Figure 3.5. Defects in Vessel Diameter in EC-N1ICD and EC-Rbpj-KO Embryos..... 60

Figure 3.6. Gene Expression in EC-N1ICD and EC-Rbpj-KO Yolk Sac Tissues 63

Figure 3.7. Gene Expression in Transgenic EC-N1ICD and EC-Rbpj-KO Embryo Yolk Sacs..... 66

Figure 3.8. Histograms Obtained from PECAM1-PE Cy7 Fluorescent Activated Cell Sorting 68

Figure 3.9. Gene Expression in Transgenic EC-N1ICD PECAM1+ Sorted Yolk Sac Tissues 70

Figure 3.10. rVista Visualization of Conserved RBPJ Binding Sites 72

Figure 3.11. Notch Regulates the Expression of Key Genes and the Remodeling of the

Yolk Sac Vasculature 76

Figure 4.1. Generation of an Ainv15-N1-ICD ES Cell Line Specifying an Inducible Notch1-ICD Transgene..... 82

Figure 4.2. Expression Analysis of Undifferentiated Ainv15-N1-ICD ES Cells after Doxycyline Treatment..... 83

Figure 4.3. Schematic of the Differentiation Process of Ainv15-N1-ICD ES Cells into Endothelial Cells..... 86

Figure 4.4. Expression Analysis of Ainv15-N1-ICD Embryoid Bodies and Differentiated Cells 88

Figure 4.5. Expression Analysis of Select Genes in Differentiated Ainv15-N1-ICD ES Cells as Analyzed by Real-time PCR..... 92

Figure 4.6. Collagen Embedded EBs Mimic Sprouting Angiogenesis but are Unresponsive to Treatment..... 94

Figure 5.1. Conditional Mouse Z/EG-Pgf Transgene Construct..... 102

Figure 5.2. *LacZ* Expression in Embryonic and Adult Tissues in the Z/EG-Pgf Transgene 104

Figure 5.3. Defects in Growth and Vascular Remodeling in Z/EG-Pgf Embryos 106

Figure 5.4. Resulting PlGF Expression in the Early Embryo and Placenta after *Tie2-Cre* Mice were Crossed with Z/EG-Pgf Mice 108

Figure 5.5. Defects in Vessel Diameter in Z/EG-Pgf Embryos..... 111

Figure 5.6. Defects in Embryonic-Derived Vasculature and Gene Expression in Z/EG-Pgf Moderate and Severe Placentas..... 113

Figure 5.7. Gene Expression in Z/EG-Pgf Moderate Yolk Sac Tissues..... 115

Figure 5.8. PlGF Modulates the VEGF Response and Regulates the Expression of Notch Family Members 121

Figure 6.1. Model of Role of Notch and VEGF Pathways in Vascular Remodeling 128

List of Tables

Table 1.1. Notch Family Expression in the Developing Embryo 17

Table 1.2. Phenotype of Mice with Mutations in Notch Family Members 19

Table 2.1. Primer Pairs for RT-PCR 40

Table 2.2. Taqman Primer Sets for Real-time PCR 41

Table 3.1. Microarray Expression of Genes Encoding Secreted Factors in EC-N1ICD and EC-Rbpj-KO Yolk Sac Tissues 67

Table 4.1. Expression Analysis of Select Genes as Analyzed by Microarray in Undifferentiated Ainv15-N1-ICD ES Cells in Response to Dox Treatment 84

Table 4.2. Expression Analysis of Select Endothelial Genes as Analyzed by Microarray in Differentiated Ainv15-N1-ICD Cells Compared to Undifferentiated ES cells 90

Table 5.1. Expression of Select Genes in Z/EG-Pgf Moderate Yolk Sac Tissues 116

Abbreviations

bHLH	basic helix-loop-helix
BME	beta mercaptoethanol
BMP	bone morphogenic protein
bp	base pair
BSA	bovine serum albumin
°C	degrees centigrade
CDS	coding DNA sequences
ChIP	chromatin immunoprecipitation
CR	cysteine-rich region
CSL	CBF1/Rbpjk/KBF2
DA	dorsal aorta
DAB	3, 3-diaminobenzidine tetrahydrochloride
DAPI	4-6-Diamidino-2-phenylindole
Dll	delta-like
DMEM	Dulbecco's modified Eagle's medium
DMF	dimethylformamide
DMSO	dimethyl sulfoxide
DNA	deoxyribonucleic acid
dNTP	deoxyribonucleotide triphosphate
Dox	doxycycline
dpc	day post coitum
DSL	delta/serrate/lag-2
DTT	dithiothreitol
E	embryonic (day)
EB	embryoid body
EC	endothelial cell
EC-CPM	EC collagen prep media
ECFP	enhanced cyan fluorescent protein
ECM	extracellular matrix

ECR	evolutionary conserved region
EGF	epidermal growth factor
EGFP	enhanced green fluorescent protein
ES	embryonic stem
EtOH	ethanol
FBS	fetal bovine serum
FGF	fibroblast growth factor
FITC	fluorescein isothiocyanate
g	gram
GAPDH	glyceraldehydes 3-phosphate dehydrogenase
GCN5	K(lysine) acetyltransferase 2A
GFP	green fluorescent protein
GSI	gamma secretase inhibitor
H&E	hematoxylin and eosin
HAT	histone acetylase
HDAC1	histone deacetylase 1
HERP	HES-related basic helix-loop-helix protein
HES	hairy and enhancer of split
HEY	hairy/enhancer-of-split related with YRPW motif 1
HIF	hypoxia-inducible factor
HPRT	hypoxanthine phosphoribosyl transferase
HRE	hypoxia-responsive element
HRP	horseradish peroxidase
IA	intussusceptive angiogenesis
IACUC	Institutional Animal Care and Use Committee
IAR	intussusceptive arborization
IBR	intussusceptive branching remodeling
Ig	immunoglobin G
IMG	intussusceptive microvascular growth
Jag	jagged

kb	kilobase
KDR	kinase insert domain protein receptor
KO	knock out
L	liter
LNR	lin-12/Notch
M	molar
MAEC	mouse aortic endothelial cells
MAPK	mitogen-activated protein kinase
mg	milligram
$MgCl_2$	magnesium chloride
min	minute
ml	milliliter
mM	millimolar
mRFP	monomeric red fluorescent protein
NEXT	Notch extracellular truncation
ng	nanogram
NICD	Notch intracellular domain
NLS	nuclear localization signals
ORF	open reading frame
PEST	proline(P), glutamic acid(E), serine(S), threonine(T)
PBS	phosphate buffered saline
PBSMT	phosphate buffered saline, milk, triton X-100
PCAF	P300/CBP-associated factor
PCR	polymerase chain reaction
PI3K	phosphatidylinositol-3-kinase
PECAM	platelet endothelial cell adhesion molecule
Pgf	placental growth factor (gene)
PKC	protein kinase C
PLCy	phospholipase C gamma
PlGF	placental growth factor (protein)

RAM	RBP-Jkappa-associated module
Rbpj	recombination signal binding protein for Ig kappa J
RNA	ribonucleic acid
RT-PCR	reverse transcriptase PCR
RtTA	reverse tetracycline transactivator
SA	sprouting angiogenesis
SD	standard deviation
SE	standard error
Sec	second
SKIP	Ski interacting protein
SMA	smooth muscle actin
SOP	standard operating procedure
Su[H]	suppressor of hairless
TE	tris edta
TFBS	transcription factor binding sites
TGF-β	transforming growth factor-β
TM	transmembrane domain
TS	trophoblast stem
WT	wildtype
x g	times gravity
X-Gal	bromo-chloro-indolyl-galactopyranoside
µl	microliter
µM	micromolar
µg	microgram
VEGF	vascular endothelial growth factor
VRF	VEGF-related factor

Chapter 1

Introduction

The formation of a vascular system is essential for the growth and development of the early embryo, as it functions to transport nutrients and waste throughout the developing embryo. In the mouse, a linear heart tube forms from cardiac progenitors and begins to beat by E8 (Ji et al. 2003; Lucitti et al. 2007). Concurrent with heart formation, the vascular system initially forms in two distinct regions, intraembryonic and extraembryonic, through the process of vasculogenesis (Risau and Flamme 1995; Drake and Fleming 2000). This early vascular plexus is remodeled and refined in the presence of flow between E8.5 and E9.5 - through proliferation, sprouting, pruning, and vessel enlargement - to form the more complex vascular system found in the adult (Risau 1997; Djonov et al. 2000; Lucitti et al 2007). Mural cells (smooth muscle cells and pericytes) are recruited to and surround the remodeled vessels and extracellular matrix is generated to provide support and contractility. Vascular smooth muscle cells surround the larger blood vessels (arteries and veins) while the pericytes are associated with small caliber vessels (arterioles, capillaries, and venules) (Li et al. 2003; Hellstrom et al. 1999). These processes also occur in the adult, during wound healing, reproductive cycling, and tumor progression. A greater understanding of these processes in vivo will provide insights into heart disease and the control of tumor progression (Jain 2003).

Several signaling cascades are required for the morphological differentiation of the embryonic vasculature, including vascular endothelial growth factor (VEGF) signaling, Notch signaling, and TGFβ signaling (Carmeliet et al. 1996; Tallquist et al.

1999; Krebs et al. 2000). However, the relationship between the molecular signals and transcriptional networks directing endothelial differentiation are still not well defined. In this chapter, I summarize the current understanding of several signaling pathways relevant to my work and address outstanding questions that remain.

1.1 Vasculogenesis

During the early stages of embryonic development, the extraembryonic yolk sac vasculature, primitive endocardium, and embryonic dorsal aorta all form through the process of vasculogenesis (Risau and Flamme 1995; Patan 2000). This process is described as the formation of a network of simple endothelial tubes via the aggregation of angioblasts (Rossant and Howard 2002). Angioblasts are precursors to endothelial cells that express only a subset of endothelial cell markers and have yet to form a lumen (Risau and Flamme 1995). In the extraembryonic region a subset of the primitive mesodermal cells from the splanchnopleuric mesoderm differentiate into the angioblast cells and aggregate into blood islands by approximately E7.0. The peripheral cells of the blood islands will differentiate to form the endothelial cells lining the vasculature, whereas the inner cells will become hematopoietic stem cells, the precursors of blood cells (Risau and Flamme 1995; Patan 2000). It was initially believed that the angioblasts and the blood cells of the blood islands were derived from a common precursor, the hemangioblast, based on the observations that CD34 and PECAM1 are expressed on both endothelial cells and hematopoietic cells in the mouse (Risau and Flamme 1995; Choi et al. 1998). However, direct clonal analysis of blood island formation has shown that each island consists of multiple progenitors (Ueno and Weissman 2006). To analyze the origins of

the hematopoietic and endothelial progenitors in the blood islands, three separate ES clones expressing the fluorescent markers EGFP, ECFP, and mRFP1 in the *Rosa26* locus were injected into E3.5 blastocysts to generate tetrachimera mice. Fluorescence imaging of embryos at E8 indicated that the origin of the blood islands is polyclonal; the endothelial and hematopoietic progenitors arise from distinct lineages (Ueno and Weissman 2006). By E8.5 the blood islands form lumenized vessels composed of endothelial cells, which fuse, forming the primitive polygon—shaped vascular plexus of the yolk sac, and blood flow commences (Patan 2000; Lucitti 2007; Figure 1.1).

Concurrent with the formation of the yolk sac vasculature, in the embryo proper the linear heart tube is formed form mesoderm-derived cardiac precursors and begins to beat by early E8.0 (Ji et al. 2003; Lucitti et al. 2007). Also within the embryo, angioblasts derived from the splanchnic mesoderm at approximately E7.5 migrate and establish cell-cell contacts with other angioblasts to develop blood vessels, initially in the formation of the two ventral and dorsal aortae. These vessels will later fuse to form the single, lumenized aorta seen in the adult (Patan 2000; Drake and Fleming 2000). In contrast to extraembryonic vascular development, the initial intraembryonic vasculature is formed in the absence of hematopoiesis; blood cells from the yolk sac and other areas of hematopoiesis in the embryo will later populate the lumen of these vessels (Risau and Flamme 1995). The distal portions of the dorsal aortae give rise to the vitelline arteries, which fuse with the yolk sac vessels to form the circulatory loop between the intra- and extraembryonic regions (Patan 2000).

Vasculogenesis also occurs in other regions of the embryo. In the allantois, endothelial cell precursors are seen at approximately E7.0-7.5 and a vascular plexus

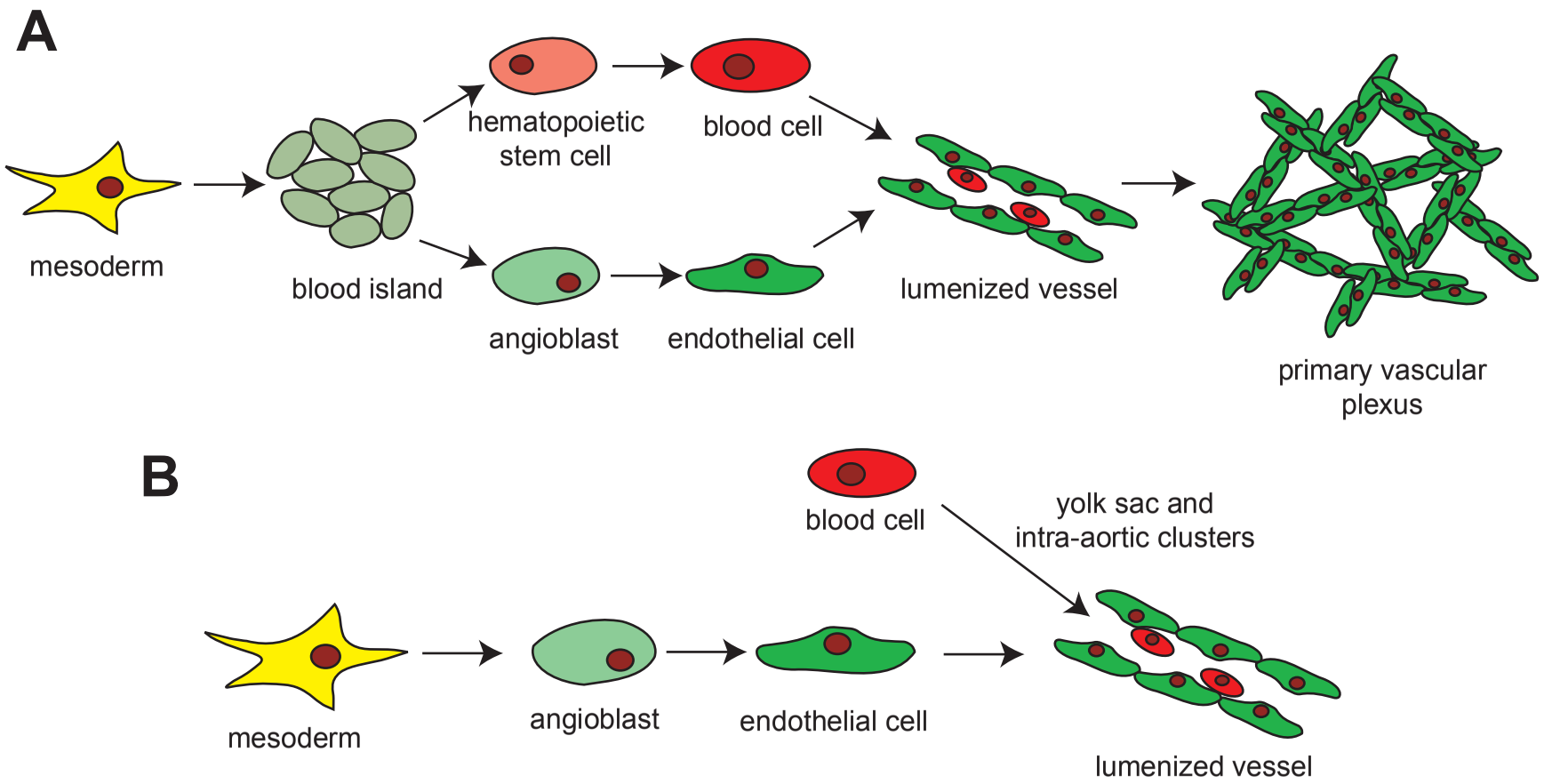

Figure 1.1. Vasculogenesis in the Early Embryo
(A) Schematic representation of vascular formation in the extraembryonic region of the developing embryo. Note that the developing vasculature forms concurrent with the hematopoietic cells although from distinct lineages. (B) Schematic representation of vascular formation in the intraembryonic region of the developing embryo. Note that the vessels form independent of the blood cells. Blood cells from other areas, including the yolk sac will later populate these vessels.

forms by E8.3. This primitive vasculature gives rise to the umbilical vessels (Patan 2000; Drake and Fleming 2000). It has also been shown that the vascularization of the kidney and liver occurs by vasculogenesis and that the development of the lung also involves vasculogenesis (Drake 2003).

1.2 Angiogenesis

For many years the belief was that the vasculature formed initially through the process of vasculogenesis followed directly by angiogenesis, which is described as the formation of blood vessels from pre-existing ones (Risau 1997). It has more recently been shown that this process is context dependent and not quite so straightforward particularly in the yolk sac. Early in vascular development, while the primary plexus is still forming, this plexus undergoes a remodeling or rearrangement without a network expansion. This occurs through the fusion of vascular segments and migration of endothelial cells to form larger vessels, resulting in a more completely structured secondary plexus with different types and calibers of vessels, including arteries, veins and capillaries (Patan 2000; Rossant and Howard 2002). The vasculature is also remodeled via the sprouting of endothelial cells from existing vessels, which migrate and proliferate to form other vessels (Risau 1997; Patan 2000). Based on these early findings, along with others, it is now widely accepted that angiogenesis is split into two broad processes, sprouting angiogenesis (SA) and intussusceptive angiogenesis (IA) (Risau 1997; Patan 2000; Djonov et al. 2000).

1.2.1 Sprouting angiogenesis

Sprouting angiogenesis was first described during second century Greece by the physician Galen (Galen, De foetuum formatione) and later during the beginning of the 20th century in vivo in the sprouting capillaries in the chicken chorioallantoic membrane (CAM) (Patan 2000). It is described as the expansion of the vasculature via the formation of new vessels composed of endothelial cells derived from an existing vessel. This process is the primary mode of angiogenesis and occurs simultaneously with IA early in development, in the yolk sac and embryo, and later during organogenesis (Risau 1997; Patan 2000). Sprouting angiogenesis consists of a number of steps including the degradation of the basement membrane of an existing vessel, followed by the invasion of the endothelial cells into the surrounding matrix. These endothelial cells proliferate and then migrate, forming 'sprouts' which join with other sprouts and lumenize to form an immature blood vessel. Mural cells and extracellular matrix stabilize the vessel and blood flow commences in the sprout (Patan 2000; Hillen and Griffioen 2007). Sprouting angiogenesis occurs in a number of physiological conditions, including embryonic vascular development, wound healing, and the female reproductive system. It also occurs in many pathological conditions, such as rheumatoid arthritis, diabetes, and tumor progression among others (Patan 2000; Jain 2003; Hillen and Griffioen 2007).

1.2.2 Intussusceptive angiogenesis

Intussusceptive angiogenesis is simply defined as the internal division of the primary capillary plexus without sprouting. Observations of vessel remodeling in the yolk sac, particularly in the chick embryo, suggest that the formation of large diameter vessels

from pre-existing capillary-derived endothelial cells occurs via the process of intussusceptive angiogenesis (Patan 2000; Djonov et al. 2000). This process is readily perceived by examination of the avascular space ('pillars'), in which adjacent pillars 'fuse' during this remodeling process. This process involves the collapse of capillary microvessels, and the endothelial cells from the capillary are then recruited into the nascent vessels to result in a larger diameter vessel (Djonov et al. 2000). New vascular segments are formed when endothelial cells on opposing capillary walls protrude into the lumen and contact one another. Once this contact has been made, the cells are perforated centrally and a 'pillar' is formed. The endothelial cells retract and the pillar is increased by the invasion of fibroblasts, collagen, and pericytes. The pillars are continuously formed and joined together to expand and remodel the capillary plexus (Djonov et al. 2003).

The process of intussusceptive angiogenesis is divided into three phases, intussusceptive microvascular growth (IMG), intussusceptive arborization (IAR), and intussusceptive branching remodeling (IBR). Each phase involves the formation of pillars; however they differ in the direction and arrangement of the pillars, which results in different vascular arrangements (Makanya et al. 2009). Intussusceptive microvascular growth greatly expands the primary capillary plexus through the delineation of new vascular segments resulting in organ-specific angioarchitecture. Intussusceptive arborization also expands the capillary plexus through the insertion of new pillars, remodeling the plexus into the vascular tree pattern. Intussusceptive branching remodeling further remodels the vascular tree to meet the perfusion demands of the local environment (Figure 1.2; Makanya et al. 2009).

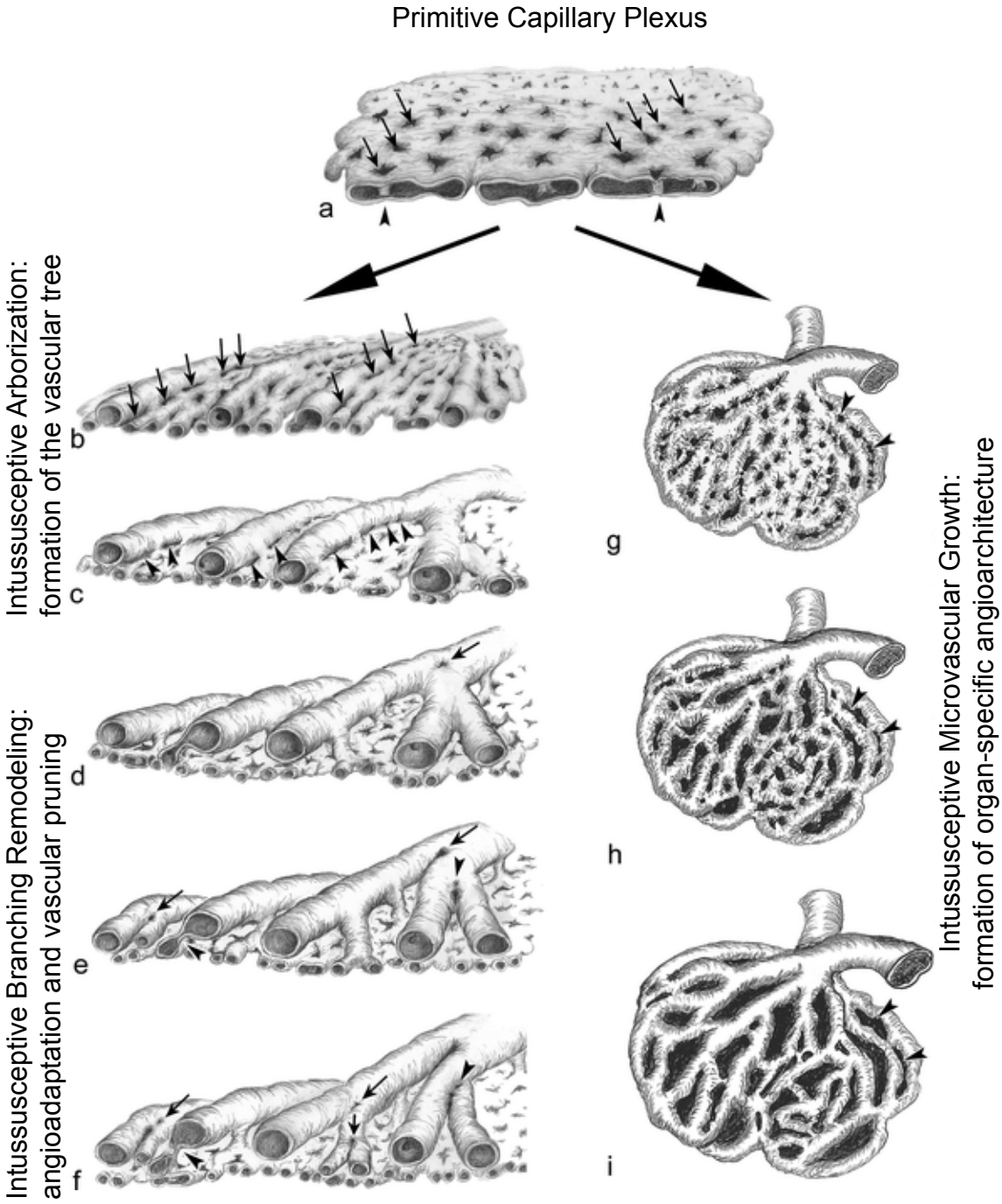
Primitive Capillary Plexus
a
Intussusceptive Arborization:
formation of the vascular tree
b
c
Intussusceptive Branching Remodeling:
angioadaptation and vascular pruning
d
e
f
g
h
i
Intussusceptive Microvascular Growth:
formation of organ-specific angioarchitecture

Figure 1.2. Intussusceptive Angiogenesis
A schematic drawing showing the phases and phenotypes of intussusceptive angiogenesis (not drawn to scale). (A) The initial capillary plexus is a disorganized meshwork without a definite phenotype. The development of this meshwork proceeds through insertion of new pillars (arrows), which result in rapid expansion of the capillary plexus. Arrowheads indicate intraluminal appearance of the pillars. (B-C) From the disorganized capillary meshwork, IAR segregates the various vessel generations by formation of 'vertical' pillars in rows (arrows in B) and narrow tissue septa formed by pillar reshaping and pillar fusions segregate the new vascular entities. Subsequently, the formation of 'horizontal pillars' and folds (arrowheads in C) separates the new vessels from the capillary plexus. (D-F) The vasculature is finally adapted by IBR to suit the local perfusion demands. This entails modification of the branching angles and the diameters of the vessels by insertion of trans-luminal pillars at branching points (arrows). Expansion and fusion of such pillars relocate the branching angle proximally with a concomitant change in blood flow properties. Part of the vascular remodeling by IBR involves severance of putative superfluous vessels, a process known as vascular pruning, which entails formation of eccentric pillars across the target branch (arrowheads in E, F), their subsequent augmentation and fusion resulting in ablation of the vessel. (G-I) Demonstration of intussusceptive microvascular growth (IMG) in the kidney glomerulus. Regardless of the organ, IMG proceeds through pillar initiation (arrowheads in G), pillar expansion (arrowheads in H), and ultimate fusion (arrowheads in I). In this way, the primordial simple capillary network is greatly expanded with delineation of new vascular segments and, depending on the pillar fusion pattern, the organ-specific angioarchitecture is formed (From Makanya et al. 2009).

IA only occurs in areas of pre-existing vasculature formed through either vasculogenesis or sprouting angiogenesis and is important for vasculature remodeling of a number of tissues (Makanya et al. 2009). In the CAM, during the first phase of development (E5-E7) the blood vessels grow via SA, while in the second (E8-E12) and final phase the vasculature is expanded and remodeled by IA (Schlatter et al. 1997; Burri et al. 2004). IA is established following initial growth by sprouting angiogenesis in the rat mammary vasculature (Djonov et al. 2001). IA is suspected to play a role in a number of pathological conditions, including psoriasis, rheumatic disease, and retinopathy, but has to date only been characterized in tumor angiogenesis (Makanya et al. 2009).

Sprouting angiogenesis and intussusceptive angiogenesis act in parallel and are similar processes which both result in the remodeling and maturation of the primary capillary plexus. The main difference is that sprouting angiogenesis results in new vessels via migration of endothelial cells, while intussusceptive angiogenesis is the expansion of the vasculature through the splitting of existing vessel lumens.

1.2.3 Tumor angiogenesis

The tumor microenvironment is a complex mixture of cell types and molecules such as ECM, endothelial cells, tumor cells, and immune cells among others (Nyberg et al. 2008). Initial tumor growth is limited due to a lack of oxygen and nutrients. Further outgrowth of the tumor requires the formation of new vessels from the pre-existing vasculature of the surrounding stroma and the remodeling of these vessels to form the tumor vascular network. This progression from an avascular phase to a vascular phase is termed the “angiogenic switch” (Hillen and Griffioen 2007; Deshpande et al. 2010).

Tumor angiogenesis is a tightly controlled, complex process. Similar to physiological angiogenesis, this process is dependent on a balance of promoters and inhibitors to regulate the growth of tumor blood vessels. An increase in the positive regulators shifts the growth toward a pathological state (Patan 2000). The tumor vasculature is an unstable, evolving network of vessels, unlike normal vasculature, which is stable once formed (Jain 2003).

Several mechanisms have been implemented in the formation and remodeling of the tumor vasculature including both sprouting angiogenesis and intussusceptive arborization. Sprouting angiogenesis is the initial growth of blood vessels from the existing vessels surrounding the tumor. This process is important for both tumor growth and metastasis, as it is an unlimited process supplying oxygen and nutrients to the tumor cells. Intussusceptive arborization is the rapid expansion of the vasculature via endothelial cell migration and vessel remodeling without endothelial cell proliferation (Hillen and Griffioen 2007; Deshpande et al. 2010). The process of IA in tumor angiogenesis is similar to that seen in the embryo, however there are differences. In the tumor, the formation of pillars occurs more frequently and in shorter periods of time than in the embryo (Patan 2000). Following anti-angiogenic treatment or radiotherapy, as a mechanism for tumor recovery, vessel remodeling switches from SA to IA, restoring tumor vascularization and growth (Hlushchuk et al. 2008). Based on recent knowledge of the pathways involved in tumor angiogenesis, promising anti-angiogenic therapies have been developed, although much work remains to fully understand the complex process of tumor development.

1.3 Signaling pathways in vascular development

1.3.1 Notch signaling pathway

Notch signaling is an evolutionarily conserved pathway originally discovered in *Drosophila* over 90 years ago. Haploinsufficiency of the gene resulted in notches in the wing, hence the name (Mohr 1919). It has since been shown to influence a broad spectrum of cell fate and developmental processes, including proliferation, differentiation, and apoptosis (Artavanis-Tsakonas et al. 1999). Notch has been shown to suppress undifferentiated precursors from differentiating in neurogenesis, myogenesis, and hematopoiesis, among others, and can also determine cell fate and tissue patterning (Weinmaster 1998).

1.3.1.1 Notch family

The Notch family consists of four type1 transmembrane receptors, Notch 1 – 4 and five type 1 cell surface ligands Delta-like (Dll) -1, -3, and -4 and Jagged (Jag) -1 and -2 (Mumm and Kopan 2000). The receptors and ligands both consist of an extracellular domain, a transmembrane domain (TM), and an intracellular domain. In the receptors, the extracellular domain contains a signal sequence followed by 29 to 36 epidermal growth factor (EGF)-like repeats and 3 lin-12/Notch (LNR) motifs. The C-terminal intracellular domain contains a RAM domain (~ 118 amino acids), 6 or 7 cdc10/ankyrin repeats, 1 or 2 putative nuclear localization signals (NLS), a glutamine rich stretch, and a PEST domain (Figure 1.3). In the trans-Golgi network the full-length receptor is processed by a furin-like convertase creating a heterodimeric receptor, which then localizes to the cell surface (Karsan 2005; Figure 1.4). In the ligands, the extracellular domain contains an

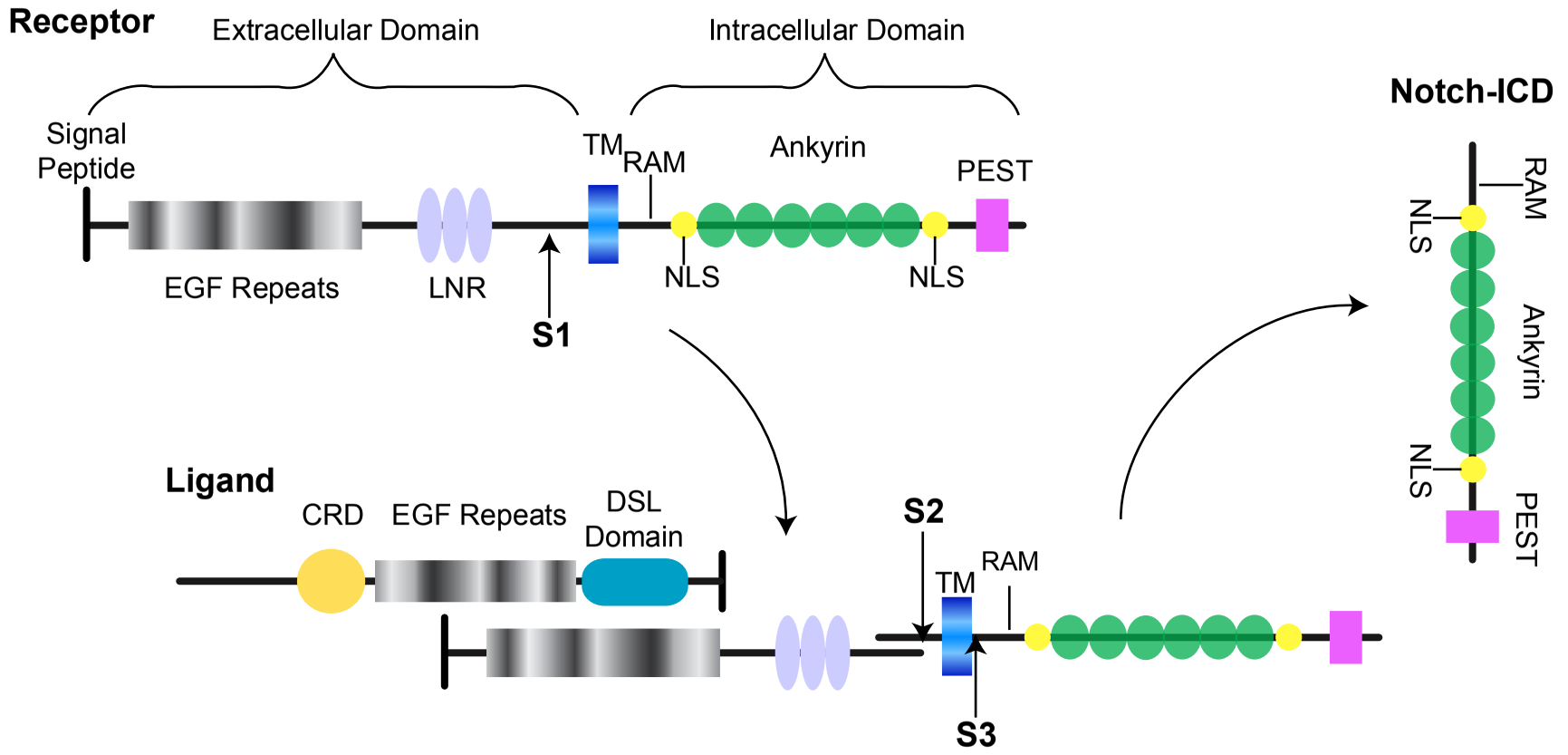

Figure 1.3. Structure of the Notch Ligands and Receptors
Schematic representation of the structure and processing of the Notch ligands and receptors. The Notch ligands consist of a DSL Domain, EGF repeats (twice as many in Jag), and a cysteine-rich domain in the extracellular domain. The Notch receptors contain multiple EGF repeats and 3 LNR motifs in the extracellular domain and a RAM domain, 6-7 Ankyrin repeats, 1-2 NLS, and a PEST domain in the intracellular domain. In the trans-Golgi network the full length Notch receptor is cleaved at S1. Upon ligand binding, the Notch receptor is clipped at S2, which allows the cleavage event by γ-secretase within the TM resulting in the Notch-Intracellular Domain (Notch-ICD). EGF, epidermal growth factor; TM, transmembrane domain; PEST, proline, glutamate, serine, threonine-rich; NLS, nuclear localization signals; LNR, Lin/Notch repeats; CRD, cysteine-rich domain; DSL, delta serrate LAG-2.

N-terminal domain followed by a DSL domain and multiple tandem EGF-like repeats. The Jagged ligands contain approximately twice the number of EGF repeats than Delta and also contain a cysteine-rich region (CR). The intracellular domain contains multiple lysine residues and a c-terminal PDZ (PSD-95/Dlg/ZO-1)-ligand motif (Figure 1.3; D'souza et al. 2008).

Upon ligand binding the receptor is further processed by a disintegrin-metalloprotease in the extracellular region resulting in a product termed NEXT (Notch EXtracellular Truncation). A final cleavage within the TM domain by a γ-secretase-like protease, thought to be the Presenilins, releases the Notch IntraCellular Domain (NICD) (Mumm and Kopan 2000). The NICD translocates to the nucleus mediated by the NLS, where it binds directly to the DNA-binding protein RBPJ, also termed CSL (CBF1/Rbpjk/KBF2 in mammals, Suppressor of hairless (Su[H]) in *Drosophila* and *Xenopus*, and Lag-1 in *C. elegans*), through the RAM domain (Weinmaster 1998) (Figure 1.4). In the absence of Notch, RBPJ acts as a transcriptional repressor at its DNA binding site GTGGGAA (Tun et al. 1994), forming a complex with the SMRT/NcoR/histone deacetylase 1 (HDAC1) or CIR/HDAC/SAP30 complexes, and Ski interacting protein (SKIP). When the NICD translocates to the nucleus it displaces the SMRT or CIR/HDAC complex. Mastermind, a transcriptional coactivator protein, then acts on the complex. The conserved histone acetylase (HATs), PCAF, GCN5, and p300, are recruited to the corepressor complex, allowing for the activation of downstream genes (Mumm and Kopan 2000; Kovall 2007). A number of Notch target genes have been identified to date, including members of the hairy/Enhancer of split-related genes, the HES (Jarriault et al. 1995; Kageyama and Ohtsuka 1999), HERP (Iso et al. 2003), and

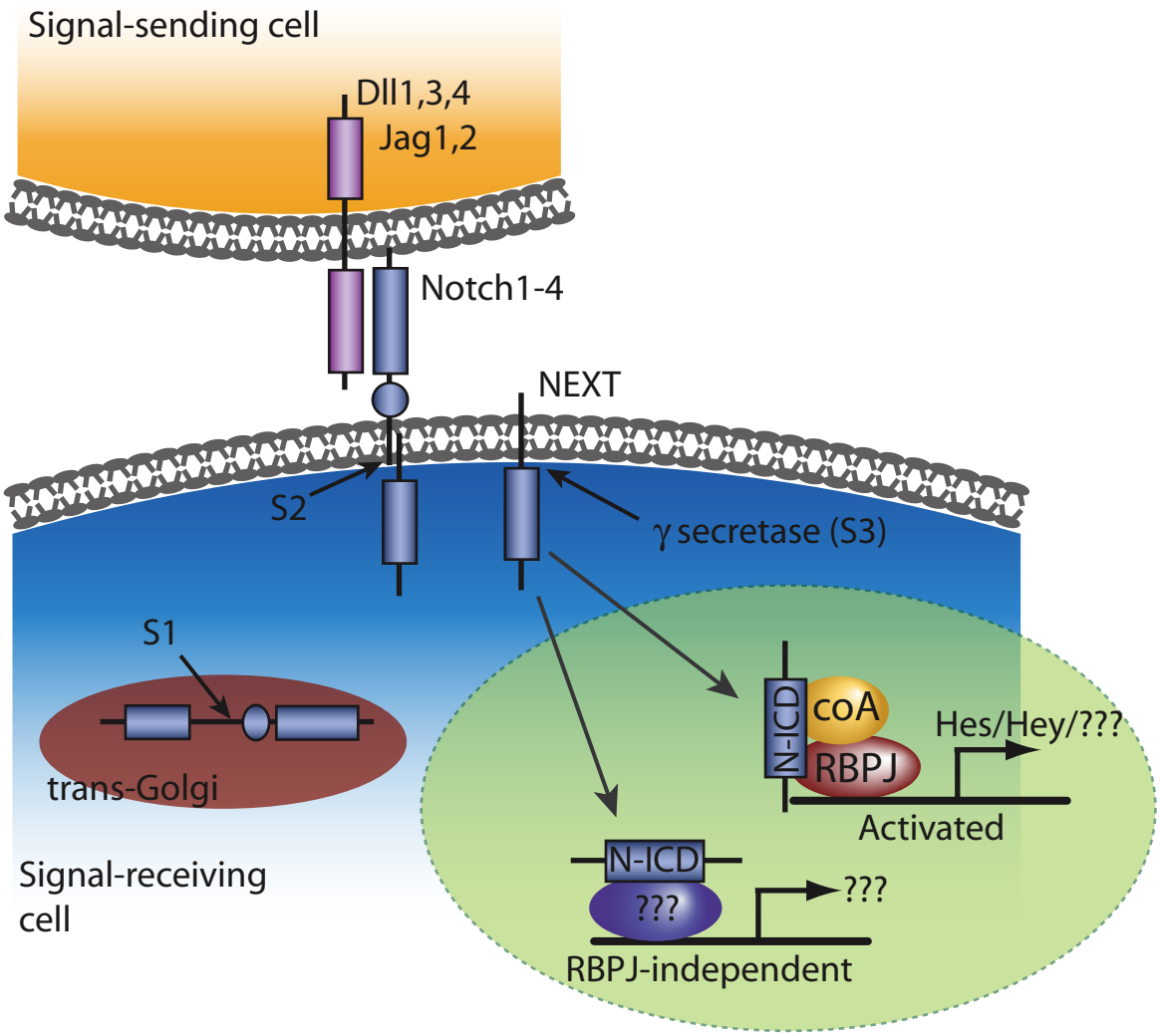

Figure 1.4. Notch Signaling Pathway
(A) Schematic representation of the Notch signaling pathway. The Notch ligand first undergoes a cleavage (S1) in the trans-Golgi network. Then, upon ligand binding, the ligand is again cleaved (S2), resulting in the Notch ExtraCellular Truncation (NEXT). This product is then cleaved by a γ-secretase (S3), resulting in the Notch IntraCellular Domain (NICD). This will translocate to the nucleus where it will interact with the binding factor RBPJ activating transcription of a subset of genes.

HEY (Maier and Gessler 2000) families, which are basic helix-loop-helix (bHLH) transcription factors. These genes are activated upon binding of the NICD-RBPJ complex and in turn act to repress the expression of other downstream target genes (Figure 1.4). They act by binding to N- or E- box elements and recruiting corepressors to the binding site, acting as effectors of Notch signaling (Iso et al. 2003). Thus, a number of different ligand, receptors, and effectors act in concert to direct Notch signaling in its many roles.

1.3.1.2 Notch family expression

Embryonic expression of Notch family members, including ligands and receptors, as well as downstream targets, has been examined in some detail. All Notch family members show expression at some point in the very early embryo, during preimplantation development. Expression was analyzed in oocytes, zygotes, 2-cell embryos, morulae, blastocysts, and hatched blastocysts using nested PCR (Table 1.1). Of the ligands, *Notch1* and *Notch2* are detected in oocytes and all throughout preimplantation development, *Notch3* only in the 2-cell embryo and hatched blastocyst, and *Notch4* from the 2-cell stage on. The Notch ligands, *Jag1*, *-2* and *Dll3* are expressed in the oocytes through the late blastocyst stage, while *Dll4* is not present until the 2-cell stage, and *Dll1* is expressed in the 2-cell embryo and weakly in the blastocyst and hatched blastocyst. The Notch transcription factor, *Rbpj*, is also expressed in the oocyte stage and all throughout preimplantation development. All Notch family members showed expression in both embryonic stem (ES) cells and trophoblast stem (TS) cells (Cormier et al. 2004).

The vascular expression pattern of the Notch family members has also been

Table 1.1. Notch Family Expression in the Developing Embryo

Gene	Preimplantation	Embryonic Vasculature
Ligand		
Dll1	2-cell embryo, blastocyst, hatched blastocyst, ES cell, TS cell	ND
Dll3	oocyte, zygote, 2-cell embryo, morulae, blastocyst(E3.5), hatched blastocyst, ES cell, TS cell	ND
Dll4	2-cell embryo, morulae, blastocyst(E3.5), hatched blastocyst, ES cell, TS cell	Arterial endothelium, capillaries
Jag1	oocyte, zygote, 2-cell embryo, morulae, blastocyst(E3.5), hatched blastocyst, ES cell, TS cell	Arterial endothelium, Arterial SMC
Jag2	oocyte, zygote, 2-cell embryo, morulae, blastocyst(E3.5), hatched blastocyst, ES cell, TS cell	Arterial endothelium
Receptor		
Notch1	oocyte, zygote, 2-cell embryo, morulae, blastocyst(E3.5), hatched blastocyst, ES cell, TS cell	Arterial endothelium
Notch2	oocyte, zygote, 2-cell embryo, morulae, blastocyst(E3.5), hatched blastocyst, ES cell, TS cell	ND
Notch3	2-cell embryo, hatched blastocyst, ES cell, TS cell	Arterial SMC
Notch4	2-cell embryo, morulae, blastocyst(E3.5), hatched blastocyst, ES cell, TS cell	Arterial endothelium, capillaries
Rbpj	oocyte, zygote, 2-cell embryo, morulae, blastocyst(E3.5), hatched blastocyst, ES cell, TS cell	96
Effector		
Heyl	ND	ND
Hey1	ND	Dorsal aorta, allantois

ND, not described; ES, embyronic stem; TS, trophoblast stem; SMC, smooth muscle cell.

studied in depth in mouse embryos (Leimeister et al. 1999; Leimeister et al. 2000; Villa et al. 2001; Table 1.1). Except for *Notch2*, which was not expressed in either arteries or veins, and *Dll3 and Dll1*, which were not detected at this early time point, all of the ligands and receptors exhibited arterial specific expression; none were detected at high levels in the veins of the early vasculature. Interestingly, *Notch3* is expressed in the smooth muscle cells of the dorsal aortae and not in the endothelial cells, *Jag1* is expressed in smooth muscle cells in addition to the endothelia, and *Notch4* and *Dll4* are the only members to exhibit expression in the capillaries (Villa et al. 2001). The expression of the downstream targets of Notch, *Hey1*, *Hey2*, and *HeyL* has also been examined. In the early embryo *HeyL* is expressed in a number of tissues, including the branchial arch mesenchyme, peripheral nervous system, and somites, while later in development it is also expressed in the smooth muscle cells of the digestive tract and the vasculature (Leimeister et al. 2000). In the early embryo, *Hey1* and *Hey2* are coexpressed in the somites and otic vessels. *Hey1* also exhibits expression in a number of tissues, including the dorsal aorta, allantois, and floor plate of the neural tube, among others. *Hey2* is widely expressed as well, including in the spinal nerves and first branchial arch (Leimeister et al. 1999).

This expression pattern indicates that the Notch signaling may play an important role during preimplantation development in the mouse and later in the formation of the vascular system, specifically in the specification of the arteries.

1.3.1.3 Notch signaling in vascular development

Mutations in both the ligands and receptors of the Notch family lead to defects in the vasculature, many of which are embryonic lethal (Table 1.2). Mutant mice lacking

Table 1.2. Phenotype of Mice with Mutations in Notch Family Members

Gene Mutation	Lethality	Vascular Phenotype
Ligand		
Dll4 overexpression	E10.5	Reduction in vascular sprouting, enlarged vessels
Dll4 deletion	E11.5	Vascular remodeling defects, reduction in vessel diameter, arteriovenous malformations
Jag1 deletion	E11.5	Imapired remodeling in the yolk sac, reduction in vessel diameter
Receptor		
Notch1	E11.5	Vascular remodeling defects in embryo, yolk sac, and placenta
Notch1 conditional	E10.5	Vascular defects in the yolk sac, placenta, and embryo proper
Notch1 overexpression	E10.5	Immature vasculature, impaired remodleing, arteriovenous malformations, cardiac defects
Notch4	Viable	No vascular phenotype
Notch4 overexpression	E10	Enlarged vessels, arterious malformations
Notch1/*Notch4*	E9.5	More severe phenotype than Notch1 deletion
Rbpj	E10.5	Similar to defects in Notch mutation,vascular remodeling defects, reduction in vessel diameter
Effector		
Hey1	Viable	No vascular phenotype
Hey1/Hey2	E11.5	Vascular remodeling defects, massive hemmorhage, lack of vessels in placenta

Notch1 do not survive post E11.5 and harbor defects in vascular remodeling in the embryo, yolk sac, and placenta (Swiatek et al. 1994). Mice with a conditional deletion of *Notch1* in the endothelial cells exhibited vascular defects in the yolk sac, placenta, and embryo proper, and died at approximately E10.5 (Limbourg et al. 2005). Deletion of *Notch4* has no visible effect and embryos are viable; however, *Notch1*$^{-/-}$*Notch4*$^{-/-}$ double mutants have more severe vascular phenotypes than the *Notch1*$^{-/-}$ and are embryonic lethal at E9.5 (Krebs et al. 2000; Iso et al. 2003). Mice lacking *Jag1* (Xue et al. 1999) and mice with a heterozygous deletion of *Dll4* (Krebs et al. 2004; Gale et al. 2004) exhibit growth retardation, defects in vascular remodeling, and lethality by E11.5. Activated expression of Notch family members also leads to vascular defects. Mice with activated expression of *Notch1* in the endothelia, under the control of *Tie2*, display an immature vasculature with impaired remodeling, arteriovenous malformations, and cardiac defects and are embryonic lethal at E10.5 (Venkatesh et al. 2008; Krebs et al. 2010). Mice with an activated form of *Notch4* in the endothelium also display enlarged vessels, arteriovenous malformations and embryonic lethality (Uyttendaele et al. 2001; Carlson et al. 2005). Similarly, overexpression of the ligand *Dll4* in the endothelium leads to a reduction in vascular sprouting, enlarged vessels and lethality by E10.5 (Trindade et al. 2008).

Other genes crucial to Notch signaling also display defects in vascular remodeling. Mice with a conditional deletion of *Rbpj* in the endothelia display vascular defects similar to those seen in other Notch mutants, including an absence of vascular remodeling and a reduction in vessel diameter (Krebs et al. 2004). Mice lacking *Hey1* have no apparent phenotype and are viable; however mice with a double knockout of *Hey1* and *Hey2* exhibit defects in growth and vascular remodeling and lethality by E11.5 (Fischer et al. 2004).

In mouse studies, both loss-of-function and gain-of-function of members of the Notch families lead to abnormalities in the vasculature and embryonic lethality. These and other data indicate a definite role for Notch signaling in the control of endothelial differentiation in the early embryo. However, the downstream targets of these signaling pathways remain largely undefined, particularly during early embryogenesis. Much work remains to establish the complex hierarchy of signaling cascades involved in vascular differentiation.

1.3.1.4 Notch signaling in pathological conditions

Notch signaling has recently been found to play a role in tumor angiogenesis. The ligand *Dll4* is strongly expressed in tumor vessels (Mailhos et al. 2001). In tumors VEGF-A induces *Dll4* expression in sprouting endothelial cells, which in turn signals through Notch acting as a negative regulator of growth. Inhibition of Dll4/Notch signaling resulted in increased vessel density, but decreased vessel function. Tumor hypoxia was increased and tumor growth retarded (Noguera-Troise et al. 2006). High levels of *Notch1* and *Jag1* expression are found in breast cancer and prostate cancer (Santagata et al. 2004; Reedijk et al. 2005). Based on these findings the inhibition of Notch signaling, via γ-secretase inhibitors or antibodies neutralizing DLL4, could be a strategy for cancer treatment.

The importance of Notch signaling is also indicated by its role in congenital disorders. Mutations in the *Notch3* gene lead to cerebral autosomal dominant arteriopathy with subcortical infarct and leukoencephalopathy (CADASIL). CADASIL is an autosomal dominant inherited disorder characterized by recurrent ischemic strokes,

cognitive impairment, and migraine. *Notch3* mutations in CADASIL patients are found in the cysteine residues of the EGF-like repeats, with over 100 different mutations reported (Tang et al. 2009). In mice, *Notch3* mutant embryos are viable, however adults exhibited arterial defects (Krebs et al. 2003). How *Notch3* mutations lead to CADASIL and possible treatments for the disorder remain unknown. Mutations in *Jag1* or in *Notch2* lead to Alagille Syndrome (AGS). AGS is an autosomal dominant disorder associated with abnormalities of the heart, eye, kidney, and skeleton and most commonly impaired development of the intrahepatic bile ducts (Niessen and Karsan 2007). AGS is also characterized by vascular anomalies and abnormal intracranial vessel development (Kamath et al. 2004), which likely result due to the role of Jag1/Notch signaling in vasculogenesis. There is no known cure for AGS.

1.3.2 VEGF signaling pathway

Another group of important, and one of the best characterized, signaling molecules involved in vascular differentiation is the vascular endothelial growth factor (VEGF) family. VEGF was initially shown to be an endothelial cell-specific mitogen, an inducer of angiogenesis, and a mediator of vascular permeability (Park et al. 1994). The VEGF family is now known to play a crucial role in the formation of the vasculature in the early embryo as well as in the adult during wound healing and pathological angiogenesis. The VEGF family is also an important component in lymphangiogenesis (Tjwa et al. 2003; Lohela et al. 2009).

1.3.2.1 VEGF family

The VEGF family includes VEGF-A (also referred to as VEGF), VEGF-B,

VEGF-C, VEGF-D, placental growth factor (PlGF), and the more recently identified ORF encoded VEGF-E and snake venom-isolated VEGF-F (Lohela et al. 2009). The VEGFs are dimeric glycoproteins belonging to the platelet-derived growth factor (PDGF)/VEGF superfamily, characterized by their cysteine-knot motif. The monomers are oriented side-by-side and head-to-tail, held together by a single disulfide bond. (Tjwa et al. 2003; Lohela et al. 2009). VEGF-A, also known as vascular permeability factor has six isoforms generated by alternative splicing of the mRNA. In the human they are $VEGF_{121}$, $VEGF_{145}$, $VEGF_{165}$ (the most predominant), $VEGF_{183}$, $VEGF_{189}$, and $VEGF_{206}$; the mouse and rat isoforms are one amino acid shorter. VEGF-A expression is tightly regulated by hypoxia at the transcriptional level via the hypoxia-inducible transcription factors (HIF-1 and -2), which bind the hypoxia-responsive element (HRE) in the VEGF-A promoter (Tjwa et al. 2003). VEGF-B, also known as VEGF-related factor (VRF), consists of two isoforms generated by alternative splicing, VEGF-B_{167} and VEGF-B_{186}, which differ only in the C-terminal sequence. VEGF-B has a 44% sequence identity to VEGF-A. VEGF-C and VEGF-D are closely related; their amino acid sequence contains a central region with homology to VEGF-A, however they also consist of long N- and C-terminal extensions, the C-terminal being rich in cysteine residues (Achen and Stacker 1998). PlGF was discovered in human placenta shortly after the discovery of VEGF-A, in the early 1990s. There are three isoforms in the human, formed via alternative splicing, PlGF-1 ($PlGF_{131}$), PlGF-2 ($PlGF_{152}$), and PlGF-3 ($PlGF_{203}$). PlGF-2 contains 21 basic amino acids in the C-terminus, which are lacking the PlGF-1 and -3, that allow for binding to heparin. PlGF-2 is the only splice isoform found in mice. PlGF has approximately 46% sequence identity to VEGF-A and can form homodimers and

heterodimers with VEGF-A (Achen and Stacker 1998; Tjwa et al. 2003).

The VEGF family consists of three related tyrosine kinase receptors, FLT1 (VEGFR1), KDR (VEGFR2, FLK1), and FLT4 (VEGFR3). Each contains seven immunoglobulin (Ig)-like folds in the extracellular region, a split tyrosine kinase domain and one transmembrane domain. All three are modified via N-linked glycosylation postranslationally (Matsumoto and Claesson-Welsh 2001). There is also a soluble form of FLT1 (sFLT1), resulting from alternative splicing, which lacks the seventh Ig-like domain, the cytoplasmic domain, and the transmembrane domain (Kendall and Thomas, 1993; Park et al. 1994). Neuropilin-1 has also been identified as a relatively high affinity receptor for VEGF-A (Achen and Stacker 1998).

VEGF-A binds to both FLT1 and KDR. Although VEGF-A binds with a higher affinity to FLT1, the angiogenic signal is thought to result from the binding of VEGF to KDR. FLT1 and sFLT1 are believed to act as 'sink' receptors, regulating the binding of VEGF-A to KDR (Neufeld et al. 1999; Tjwa et al. 2003). VEGF-A binding induces the autophosphorylation of the receptor at four major sites and activates downstream signaling cascades, including the MAPK pathway and PI3K-AKT pathway among others. As a result VEGF signaling influences vascular permeability, proliferation, survival, migration, and cell mobilization (Rossant and Howard 2002; Kerbel 2008).

The VEGF family homolog, PlGF, is also believed to be an inducer of vascular development. PlGF binds with high affinity to FLT1 (Park et al. 1994). PlGF is upregulated during pathological angiogenesis (Carmeliet et al. 2001) and stimulates vascular leakage (Park et al. 1994). PlGF may stimulate vascular formation by signaling through FLT1 (Neufeld et al. 1999) or by acting as a 'decoy', limiting VEGF-A binding

to the 'FLT1-sink' and thereby increasing the amount of VEGF-A available to activate KDR (Park et al. 1994). VEGF-B also binds with high affinity to FLT1. VEGF-B does not affect vascular development in the embryo, however it appears to be important in pathological settings, specifically in the regulation of lipid metabolism in cardiac muscle (Lohela et al. 2009). VEGF-C and VEGF-D bind both KDR and FLT4. It has been shown that the binding of VEGF-C to FLT4 regulates the formation of lymphatic vessels, not blood vessels, in the early embryo. Although VEGF-D does bind to with high affinity to FLT4 its role has not been elucidated (Lohela et al. 2009) (Figure 1.5).

1.3.2.2 VEGF family expression

The members of the VEGF family are broadly expressed in the developing embryo and in the adult. *Vegfa* is expressed in the giant cells during early embryogenesis and is found in most organs in later stages. Visualization via a LacZ knock-in reporter allele of *Vegfa* indicated strong expression in the extraembryonic visceral endoderm during early implantation and in the definitive endoderm at E8.0 (Miquerol et al. 1999). *Vegfa* also shows increased expression in regions of hypoxia. *Vegfb* expression overlaps with that of *Vegfa* in most tissues; however it is not regulated by hypoxia. It exhibits expression in the developing heart of the early embryo and, while widely expressed in the adult it is predominant in the adult cardiac and skeletal tissue. *Vegfc* and *Vegfd* have similar expression profiles in many tissues of the embryo and adult, although *Vegfc* is particularly expressed in areas surrounding lymphatic vessels and *Vegfd* is predominant in the lung, heart, and skin tissues. *Pgf* is expressed in the trophoblast cells and vascular endothelium of the placenta throughout the development of the embryo and in certain

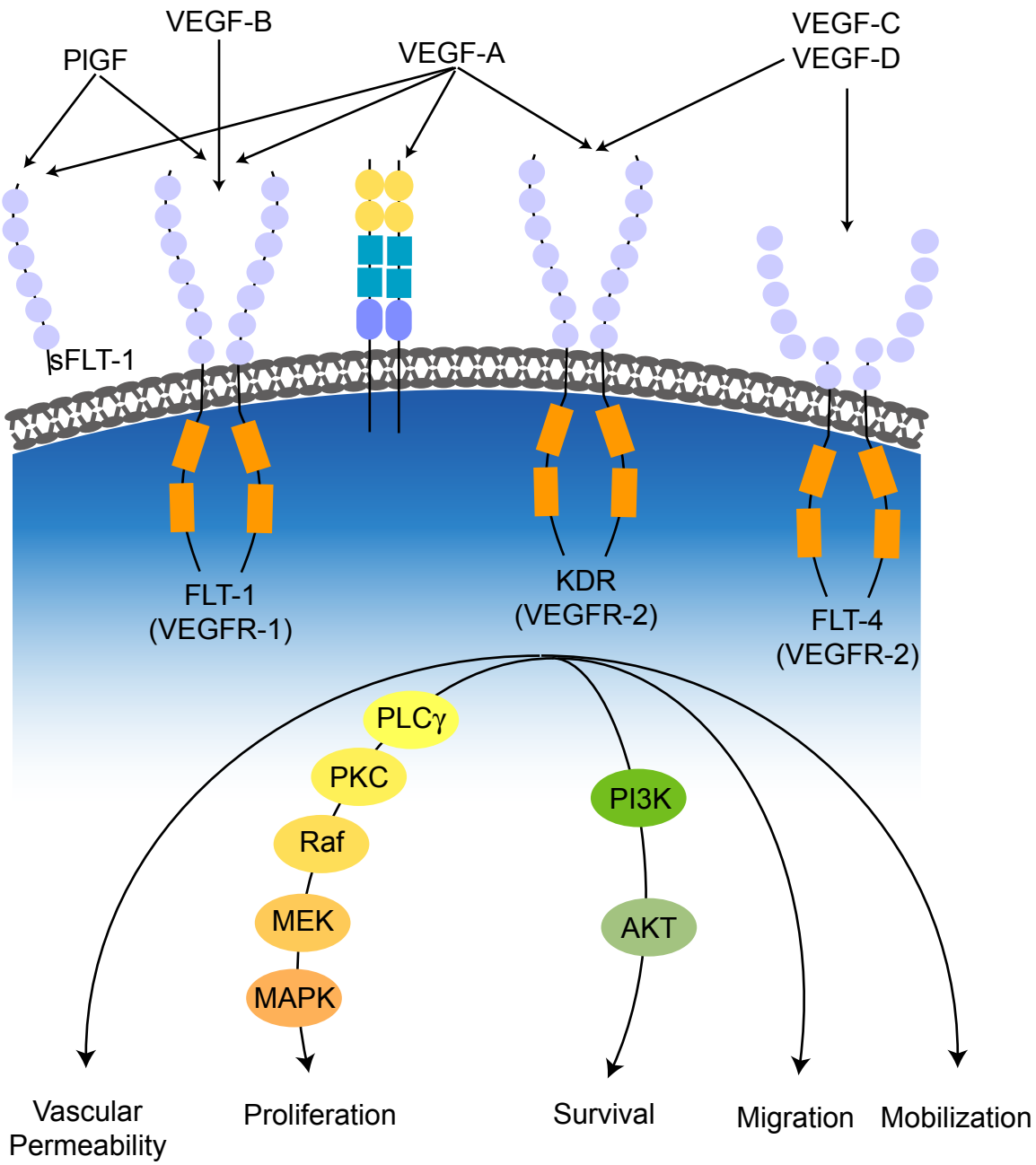

Figure 1.5. VEGF Signaling Pathway
Schematic representation of the VEGF signaling pathway. The main angiogenic signal arises through the binding of VEGF-A to KDR. Via the MAPK pathway and PI3K-AKT pathway, among others, VEGF-A mediates endothelial cell proliferation, migration, mobilization, permeability, and survival.

tumors (Vuorela et al. 1997; Achen and Stacker 1998; Matsumoto and Claesson-Welsh 2001).

The receptors, *Flt1* and *Kdr*, are expressed in the endothelial cells of most tissues in the mouse and human. *Kdr* is first found in the mesodermal precursors of the blood islands and then in the peripheral angioblast cells of the blood islands. *Flt1* appears in angioblasts at approximately E8.5. Both are expressed in adult endothelial cells, however they are lacking in certain tissues, including the brain. *Flt1* and *Kdr* expression is increased in pathologies such as tumors and hyperthyroidism. *Flt4* is expressed in the developing vasculature of the embryo by E8.0; however it is restricted to the venous endothelium. In the adult it is expressed in the lymphatic vasculature and vascular and nonendothelial tumors (Matsumoto and Claesson-Welsh 2001).

1.3.2.3 VEGF signaling in vascular development

In both heterozygous and homozygous *Vegfa* deficient embryos blood vessel formation was abnormal and the embryos died early in development (Carmeliet et al. 1996; Ferrara et al. 1996). Mice lacking *Kdr* lack endothelial cells and blood vessels, and die between E8.5 and E9.5, while *Flt1* knockout mice, which also die at E8.5, have a normal level of endothelial cells but lack functional vessels (Shalaby et al. 1995; Fong et al. 1995). Mice lacking placental growth factor have impaired pathological angiogenesis, likely through the attenuation of the response to VEGF-A (Luttun et al., 2002), while mice overexpressing placental growth factor under the control of the keratin 14 promoter displayed increased vascularization and permeability in the vasculature of the skin (Odorisio et al., 2002). Deletion of *Vegfc* in mice leads to embryonic lethality due to the

absence of lymph vessels; however no vascular defects have been identified (Karkkainen et al. 2004).

It has long been established that the VEGF pathway is crucial for the development of the vascular system in the early embryo, specifically through the binding of VEGF-A to KDR. However, evidence supports a role for other family members in this regulation. Work remains to determine the precise function of the VEGF pathway and its interaction with other signaling pathways.

1.3.2.4 VEGF signaling in pathological conditions

Members of the VEGF family have been implicated in many pathological conditions. VEGF-A and KDR are inducers of tumor angiogenesis (Kim et al. 1993; Carmeliet et al. 2001). FLT1 is also important for tumor angiogenesis and is involved in rheumatoid arthritis and atherosclerosis (Zhao et al. 2004). VEGF-A induces vascular permeability via activation of KDR and subsequent signaling involving Src-kinases (Eliceiri et al. 1999). PlGF has been shown to stimulate vascular leakage, likely by attenuating the response to VEGF-A (Park et al. 1994; Luttun et al. 2002) and while it is minimally expressed in quiescent adult vasculature it is upregulated during tumor angiogenesis enhancing the angiogenic activity of VEGF-A (Carmeliet et al. 2001). In *Pgf*-deficient mice, tumor angiogenesis and growth are reduced (Carmeliet et al. 2001), while mice overexpressing *Pgf* in the skin exhibit increased melanoma growth (Marcellini et al. 2006). PlGF has also been shown to regulate inflammation and edema formation in adult mice (Oura et al. 2003).

Vascularization in tumors has been diminished by the use of VEGF-A

neutralizing antibodies, a dominant negative mutant of KDR, and the expression of VEGF-A antisense RNA (Kim et al. 1993; Millauer et al. 1994; Saleh et al. 1996). Based on this knowledge a number of therapies have been developed, including KDR inhibitors, and a VEGF-A neutralizing antibody (Wedge et al. 2000; Wood et al. 2000; Hurwitz et al. 2004). Further study of the VEGF signaling pathway could lead to additional therapeutics to manipulate the vasculature in pathological conditions.

1.3.3 TGFβ signaling pathway

Compared to the signaling pathways discussed in the previous sections, the role of the TGFβ signaling family in vascular differentiation is less defined. There are almost 30 members of the TGFβ family, including the TGFβs, bone morphogenic proteins (BMPs), activins, and inhibins. There are two types of receptors, type I and type II. Ligand binding to type II receptors leads to the phosphorylation and activation of type I receptors. These in turn phosphorylate the Smads, which convey the signal to the nucleus thus activating the target genes. The members critical to vascular development appear to be the ligand TGFβ1 and the receptors TGFβRII (type II) and ACVRL1 (ALK1) (type I). Mice with a deletion of TGFβ1 have defective vascular development in the yolk sac and have 50% embryonic lethality by E10.5. Knockout of *TgfβRII* or *Acvrl1* also leads to vascular defects in the embryo and yolk sac as well as embryonic lethality. It has been shown that TGFβ is important for the stabilization of the vasculature via the production of extracellular matrix (ECM) and the differentiation of vascular smooth muscle cells. Disruption of these processes may be the cause of the vascular defects seen in mutant mice (Jain 2003; Holderfield and Hughes 2008).

1.4 Interactions between the signaling pathways

These and other data indicate a definite role for VEGF, Notch and TGFβ signaling in the control of endothelial differentiation in the early embryo, however the interactions and many of the downstream targets of these signaling systems remain unknown. VEGF was shown to upregulate the expression of *Notch1* and *Dll4* in human arterial endothelial cells in vitro (Liu et al. 2003) and the expression of *Dll4* in vivo in the mouse retina (Lobov et al. 2007). VEGF has also been shown to act as an upstream component of Notch in the signaling cascade directing the differentiation of the zebrafish vasculature (Lawson et al. 2002). During the process of sprouting angiogenesis, Notch and VEGF are thought to act in concert to control the migration and proliferation of the endothelial cells involved. VEGF-A upregulates the expression of *Dll4* in the tip cell which is thought to activate Notch in the stalk cell and Notch in turn downregulates the expression of the VEGF receptors. Thus the tip cell becomes migratory and the stalk cell remains connected to the blood vessel (Siekmann et al. 2008). TGFβ has been shown to downregulate the transcription of KDR via a GATA site in the promoter. In addition to other interactions, TGFβ/BMP signaling can either act with Notch to induce the expression of target genes or Notch can inhibit TGFβ/BMP signaling; it is all rather complex and context dependent (Holderfield and Hughes 2008).

Taken together the data indicate specific and vital roles for both the Notch and VEGF signaling pathways in the formation of the vasculature in the early embryo and in pathological angiogenesis in the adult. The process of vascular morphogenesis includes a number of processes involving many cell types. It is a complex process involving multiple signaling pathways that must be tightly regulated both spatially and temporally.

While the morphological phenotypes of a number of mutations have been examined in detail, studies of the gene expression defects and, in turn, the genetic interactions between the pathways are lacking. Crosstalk between the pathways is essential for the proper development of the vasculature in the early embryo, however the specific interactions remain unknown. These discrepancies prompt in-depth in vitro and in vivo studies to further examine the role of Notch signaling in the development of the vasculature and how this pathway interacts with other pathways central to this process.

Chapter 2

Materials and Methods

2.1 Standard solutions and reagents

Doxycycline

1 μg/ml in water, stored at -20°C

InSolution gamma-secretase Inhibitor X (GSI-x)

1 μM in Dimethyl sulfoxide (DMSO), stored at -20°C

VEGF-A

30 ng/μl in PBS, 0.1% BSA, stored at -20°C

FGF-2

20 ng/μl in PBS, 0.1% BSA, 1 mM DTT, stored at -20°C

Endothelial Cell Differentiation Media (EC media)

85 ml DMEM, 10 ml ES serum for endothelial cell differentiation (Stem Cell Technologies, Inc), 1 ml glutamine, 1 ml Pen/Strep, 1 ml BME stock, filter sterilized, stored at 4°C

ECVF media

EC Differentiation media, 90 ng/ml VEGF-A, 40 ng/ml FGF-2, stored at 4°C

PBSMT

Phosphate buffered saline, 3% nonfat dry milk, 0.1% Triton X-100, filter sterilized, stored at 4°C

PBT

Phosphate buffered saline, 0.2% BSA, 0.1% Triton X-100, filter sterilized, stored at

4°C

Blocking Solution for Immunofluorescence

Phosphate buffered saline, 3% BSA, 5% donkey serum (Jackson ImmunoResearch Laboratories, Inc), filter sterilized, stored at 4°C

EC Collagen Prep Media (per 6 well plate)

4.5 ml DMEM, 2.7 ml EC Differentiation Media, 190 µl Pen/Strep, 52 µl VEGF-A, 37 µl FGF2 stock, stored at 4°C

2.2 Animal husbandry

2.2.1 Generation of the Z/EG-Pgf transgene

The Z/EG-Pgf construct was generated by inserting the *Pgf* CDS fragment into the Z/EG expression vector (Novak et al. 2000). The resulting Z/EG-Pgf transgene contained a β-geo cassette flanked by *loxP* sites under the control of the β-actin promoter, followed by the *Pgf* cDNA and a GFP cassette. The transgene was introduced into E14 embryonic stem (ES) cells via electroporation and clones were analyzed. The B1 clone was used to generate chimeric mice by injection into C57Bl/6 host blastocysts. The resulting male chimeras were bred to wild type C57Bl/6 females and the resulting pups were assessed for germline transmission via coat color and genotyping.

2.2.2 Breeding scheme to obtain mice and embryos

The generation of $Rosa^{Notch}$ mice (Murtaugh et al. 2003), *loxP*-flanked *Rbpj* (Tanigaki et al. 2002) and *Tie2-Cre* mice (Koni et al. 2001) has been described previously. *Tie2-Cre* mice and *loxP*-flanked *Rbpj* mice were mated to obtain *Tie2-Cre;*

Rbpj$^{f/+}$ males. Breeding pairs of *Tie2-Cre* males and *Rosa*^{Notch} females or *Tie2-Cre; Rbpj*$^{f/+}$ males and *Rbpj*$^{f/+}$ females, or *Tie2-Cre* males and *ZEG-Pgf* females were mated and the presence of a vaginal plug was taken as 0.5 dpc. Embryos were dissected from the decidual tissue at E8.5, E9.5, or E10.5 and treated according to the intended protocol. Placentas were separated from the embryos along with the mesometrial portion of the decidua and prepared for histology.

2.2.3 Genotyping of progeny

The genotypes of all offspring were analyzed by PCR on genomic DNA isolated from ear punches, yolk sac samples, or embryonic tissue depending on the intended protocol. Genomic DNA was isolated using the DNeasy Blood & Tissue Kit (Qiagen). The *Tie2-Cre* transgene presence was tested with the primers Cre-R3, 5'-AAT GCT TCT GTC CGT TTG-3' and Cre-F3, 5'-GGA TTA ACA TTC TCC CAC C-3', giving a 458-bp band (Steenhard et al. 2010). PCR genotyping for *Rosa*^{Notch} mice was performed as described (Soriano 1999). The wild type, floxed, and deleted *Rbpj* alleles were genotyped as described (Souilhol et al. 2006). Z/EG-Pgf mice were genotyped with primers iZ/EG 3' UP, 5'-AAG GTG AAC TTC AAG ATC CGC C-3' and iZ/EG 3' LOW – 5'-ACC TTT GTT CAT GGC AGC CAG-3', yielding a 469-bp band.

2.2.4 Animal euthanasia

All mice used in this study were sacrificed by asphyxiation with carbon dioxide followed by cervical dislocation to confirm mortality or by cervical dislocation alone according to IACUC standard operating procedure (SOP).

2.3 Generation and embedding of embryoid bodies

2.3.1 Embryoid body formation

ES cells were collected in EC differentiation media at 60 cells/μl. Cells were plated in 20 μl drops (1200 cells/drop) onto the lid of a 10 cm bacterial dish. PBS (10-20 ml) was added to the bottom of the dish to prevent hanging drops from drying out. Cells were grown in an incubator undisturbed for 4 days

2.3.2 Collagen embedding of embryoid bodies

2.3.2.1 Preparation of wells

The following collagen solution was prepared on ice in the hood:

EC-CPM	3.3 ml
Collagen stock	1.2 ml (neutralize with ~60 μl 0.4M NaOH in 20 μl units)
PBS	3.3 ml

Next, 1ml collagen solution was added to each well of a 6-well plate and incubated at 37°C for 1 hour to set. After 1 hour any liquid remaining on the top of the collagen was aspirated.

2.3.2.2 Embryoid body embedding

The following collagen solution was prepared:

EC-CPM	4.4 ml
Collagen stock	1.6 ml (neutralized with ~80 μl 0.4M NaOH in 20 μl units)
PBS	4.4 ml

The collagen solution was aliquoted in 1.5 ml aliquots into six 15 ml conical tubes. Embryoid bodies from hanging drops were collected onto a 10 cm dish. Then, 10 embryoid bodies were picked with a P1000 and placed into each tube. The volume of each tube was added onto a well with preset collagen and incubated for 1 hour at 37°C to set the collagen. After 1 hour 4 ml of ECVF media was added to each well. Embryoid bodies were incubated depending on the intended treatment.

2.4 DNA manipulations

2.4.1 Genomic DNA isolation

Genomic DNA was isolated from mouse and embryonic tissues using the DNeasy Blood and Tissue Kit (Qiagen). Following the protocol mouse ear clips and embryonic tissues were incubated overnight in 180 µl Buffer ATL and 20 µl proteinase K. The following morning the samples were vortexed and 200 µl Buffer AL and 200 µl ethanol (96-100%) was added to the samples and mixed thoroughly. The entire sample was pipetted into the DNeasy Mini spin column and centrifuged at 6000 x g for 1 minute. Next, 200 µl Buffer AW1 was added to the column and again centrifuged for 1 minute at 6000 x g. Then 500 µl Buffer AW2 was added and the sample was centrifuged for 3 minutes at 20,000 x g. The column was placed in a clean 1.5 ml microcentrifuge tube and then 80 µl or 60 µl (respectively) Buffer AE was added directly onto the column membrane. The sample was incubated at room temperature for 1 minute and then centrifuged for 1 minute at 6000 x g to elute. Samples were stored at -20°C until needed.

2.4.2 Polymerase Chain Reaction (PCR)

PCR primers (Integrated DNA Tecnologies, Inc) were dissolved in TE buffer to a stock concentration of 1 μg/μl; primers were stored at -20°C. PCR reactions were done with GoTaq Polymerase (Promega) on a DNA Engine Dyad Thermal Cycler (MJ Research (now Bio-Rad)). PCR reactions were analyzed in 1% agarose gels.

A typical PCR cocktail:

5X GoTaq Flexi PCR Buffer	5.0 μl
25 mM magnesium chloride	2.0 μl
dNTPs	0.2 μl
primer (forward)	0.1 μl
primer (reverse)	0.1 μl
GoTaq Polymerase	0.1 μl
water	16.5 μl
template	1 μl
total volume	25 μl

Typical conditions for PCR (annealing temp and cycle number varied):

95°C	5 mins	
95°C	30 secs	
58°C	30 secs	30 cycles
72°C	30 secs	
72°C	5 mins	
4°C	hold	

2.5 RNA manipulations

2.5.1 RNA isolation

For RNA isolation of embryonic tissues, embryos were dissected at E9.5. The uterus and decidua were carefully removed and discarded. The yolk sac and the placenta were separated from the embryo for RNA isolation and the embryo was used for genotyping. RNA was also isolated from ES cells, EBs, and differentiated endothelial cells. Total RNA was isolated using an RNeasy mini kit (Qiagen). Following the protocol, Buffer RLT was added to the sample (350 μl for embryonic tissues and 600 μl for cells). Samples were vortexed and heated for a short amount of time to lyse the RNA. One volume of 70% ethanol was added to the lysate and mixed immediately by pipetting. Up to 700 μl of the sample was transferred to an RNeasy spin column and centrifuged for 30 seconds at 8000 x g and the flow was discarded (repeated for samples larger than 700μL). Next, 700 μl Buffer RW1 was added and again the sample was centrifuged for 30 seconds at 8000 x g and the flow was discarded. Then 500 μl Buffer RPE was added and centrifuged for 30 seconds at 8000 x g, followed by another 500 μl Buffer RPE and centrifuged for 2 minutes at 8000 x g. The spin column was placed in a new 1.5 ml collection tube and 30 μl RNase-free water was added directly to the spin column membrane and centrifuged for 1 minute at 8000 x g. Samples were stored at -20°C until needed.

2.5.2 Reverse Transcriptase (RT)-PCR

cDNA was generated using SuperScript III reverse transcriptase (Invitrogen). Semiquantitative RT-PCR was performed using a number of primers from IDT

(Integrated DNA Technologies, Inc) (Table 2.1), with ribosomal protein L7 (5'-GAA GCT CAT CTA TGA GAA GGC-3' and 5'-AAG ACG AAG GAG CTG CAG AAC-3') as a control. The above protocol for PCR was followed with the annealing temperature and number of PCR cycles optimized for each reaction.

2.5.3 Real-time PCR

RNA was isolated from ES cells, EBs, differentiated endothelial cells, yolk sac tissues, or placentas using an RNeasy mini kit (Qiagen). cDNA from endothelial cells was generated using SuperScript III reverse transcriptase (Invitrogen) and quantitative real-time PCR analysis was performed using Taqman primer sets (Table 2.2) with the 7500 Real Time PCR system (Applied Biosystems). Gene expression was normalized to GAPDH.

2.5.4 Microarray analysis

RNA was isolated from ES cells, EBs, differentiated endothelial cells, yolk sac tissues, or placentas using an RNeasy mini kit (Qiagen). RNA was initially analyzed with the Mouse Genome 430 A Array from Affymetrix. EC-N1ICD and EC-Rbpj-KO microarray data were deposited to the Gene Expression Omnibus (GSE22418).

Table 2.1. Primer Pairs for RT-PCR

Gene	Forward Primer	Reverse Primer	Anneal Temp	Cycle Number	Product (bp)
Hey1	TCCGCCACCATGAAGAGAGC	AACTTCGGCCAGGCATTCCC	63	30	627
Heyl	GAAACGGCGCAGAGACCGCATCAACA	TCCCAGGATGGCGAGCTGACTGTTCA	61	30	436
Notch1	TGCCTGTGCACACCATTCTGC	CAATCAGAGATGTTGGAATGC	57	27	247
Notch4	AAGCGACACGTACGAGTCTGG	ATAGTTGCCAGCTACTTGTGG	61	30	297
Dll4	AACTGTCCTTATGGCTTTGT	CACACTCGTTCCTCTCTTCT	61	30	520
Jag1	CCAGCCAGTGAAGACCAAGT	TCAGCAGAGGAACCAGGAAA	61	30	398
Flk1	GCCAATGAAGGGGAACTGAAGAC	TCTGGCTGCTGGTGATGCTGTC	63	27	538
Vegfa	CCTCCGAAACCATGAACTTTCTGCTC	CAGCCTGGCTCACCGCCTTGGCTT	57	30	593
Vegfb	GTCAAACAACTAGTGCCCAG	TGTCTGGGTTGAGCTCTAAG	57	30	447
Vegfc	CGTTCTCTGCCAGCAACATTAC	TGGCCTTTTCCAATACGATGG	57	30	570
Pgf	CAGCCAACATCACTATGCAG	GGGTGACGGTAATAAATACG	61	30	268
Tgfb2	GGAAAAAAACCAGTGGGAAGACCC	AAGCTGTTCGATCTTGGGCG	57	27	398

Table 2.2. Primers for Real Time-PCR

Gene	Assay ID	Amplicon Length
Ankrd1	Mm00496512_m1	63
Cdh5	Mm00486938_m1	69
CD34	Mm00519283_m1	61
Dll4	Mm00444619_m1	71
Flk1	Mm01222419_m1	81
Gapdh	Mm99999915_g1	107
Hey1	Mm00468865_m1	80
Heyl	Mm00516555_m1	83
Jag1	Mm00496902_m1	61
Notch1	Mm00435245_m1	96
Notch4	Mm00440536_g1	63
Nrarp	Mm00482529_s1	74
PECAM1	Mm01242584_m1	71
Pgf	Mm00435613_m1	75
Rhox5	Mm00476718_m1	59
Tgfb2	Mm00436952_m1	101
Vegfc	Mm00437313_m1	137
ZEG-Pgf	Mm00435611_m1	91

2.6 Histology

Untreated whole-mount embryos, whole-mount PECAM stained embryos, and placentas were fixed in 4% paraformaldehyde overnight, dehydrated into 70% ethanol and embedded in paraffin wax. Embryos were then sectioned on the transverse generally in 8-10 μM sections. For histological observation, Hematoxylin & Eosin or Nuclear Fast Red staining was conducted on the paraffin sections and sections were observed or immunofluorescence was performed.

2.7 Immunochemistry

2.7.1 Embryo and yolk sac immunochemistry

Embryos with or without the surrounding yolk sac were fixed in 4% paraformaldehyde/PBS overnight at 4^{o}C. The following day they were rinsed in PBS, dehydrated in methanol, and bleached in 1 ml of 1.5% H_2O_2 in methanol for 4-5 hours at room temperature. Embryos were then rehydrated through methanol into PBS, blocked in PBSMT for 2 hours at room temperature and incubated with PECAM1 (1:50; catalog no. 557355; BD Pharmingen) overnight at 4^{o}C. Embryos were washed 5 times for 1 hour each with PBSMT and incubated with HRP-coupled anti-rat IgG (1:100; catalog no. 14-16-12; KPL, Inc) overnight at 4^{o}C. Embryos were again washed 5 times in PBSMT with a final wash in PBT. Then embryos were incubated in developing solution (0.3 mg/ml DAB, 0.5% $NiCl_2$ in PBT) for 20 minutes at room temperature followed by the addition of H_2O_2 at a 0.03% final concentration. Once the color developed (approximately 10 minutes), the embryos were rinsed in PBT and then PBS and fixed overnight in 2%

paraformaldehyde/0.1% gluteraldehyde/PBS at 4°C. Embryos were then rinsed in PBS and either equilibrated into 70% glycerol for imaging or dehydrated in ethanol for paraffin embedding.

2.7.2 Embryoid body immunochemistry

EBs embedded in collagen were allowed to differentiate for 6 days in the appropriate media and then removed using a Pasteur pipette and treated in the same manner as the yolk sacs for immunochemical staining.

2.8 Immunofluorescence

2.8.1 Yolk sac immunofluorescence

Embryos were dissected at E9.5 in PBS. The uterus and decidua were carefully removed and discarded. The yolk sac was separated from the embryo by severing the vitelline arteries and the embryo was used for genotyping. The yolk sacs were collected in separate wells of a 24 well plate and then fixed in 1 ml of 3% paraformaldehyde/PBS for 15 minutes on ice. Then the yolk sacs were permeabilized in 1 m of PBS containing 0.02% Triton X-100 for 30 minutes. Yolk sacs were transferred to separate 1.5 ml Eppendorf tubes containing 500 μl of blocking solution (5% donkey serum in PBS) for 2 hours at room temperature. Blocking solution was changed once at 1 hour. Yolk sacs were then incubated with PECAM1 (1:33; catolog no. 557355, BD Pharmingen) overnight at 4°C. Embryos were washed 5 times for 1 hour each with blocking solution and incubated with FITC-conjugated AffiniPure Anti-Rat IgG (1:75; catalog no. 712-095-153, Jackson ImmunoResearch Laboratories, Inc) overnight at 4°C. Embryos were

again washed 5 times in blocking solution with a final 20-minute wash in PBS. The yolk sacs were transferred via Pasteur pipette to a drop of *SlowFade* Gold antifade reagent (Invitrogen) on a glass slide and covered with a cover slip.

2.8.2 Fluorescence histology

Embryos were prepared following the above protocol for histology. Tissues were deparrafinized via the following:

1. Incubate slides in xylene for 10 min
2. Repeat 10 min xylene incubation
3. Incubate in each of the following for 2 min:
    a. 100% EtOH
    b. 100% EtOH
    c. 75% EtOH
    d. 50% EtOH
    e. 25% EtOH
    f. cold tap water

Antigen retrieval was performed on appropriate sections by immersing the slides in 10 mM calcium citrate for 20 minutes in a steam chamber. Sections were washed first with water and then 2 times with PBS. Sections were then blocked with blocking solution for 2 hours at room temperature. Sections were stained with α-smooth muscle actin (1:250 dilution; catalog no. A2547; Sigma-Aldrich, Inc), CD34 (no antigen retrieval step) (1:75; catalog no. 553731; BD Pharmingen), or GFP (1:100; catalog no. NB100-1770; Novus Biologicals) for 1 hour or overnight at 4°C. Sections were washed 3 times

with blocking solution and then stained with Alexa Fluor 546 goat anti-mouse IgG (1:250; catalog no. A11003; Invitrogen), FITC-conjugated AffiniPure Anti-Rat IgG (1:75; catolog no. 712-095-153; Jackson ImmunoResearch Laboratories, Inc), and Alexa Fluor 546 donkey anti-goat IgG (1:250; catalog no. A11056; Invitrogen) respectively for 30 minutes at room temperature in the dark. Sections were again washed 3 times with blocking solution. A small amount of ProLong Gold antifade reagent with DAPI (Invitrogen) was applied and the samples were covered with a cover slip, allowed to set, and imaged. Slides were stored at 4°C.

2.8.3 Embryoid body immunofluorescence

EBs embedded in collagen were allowed to differentiate for 6 days in the appropriate media and then removed using a Pasteur pipette and treated in the same manner as the yolk sacs for immunofluorescence staining with CD34 (1:50; catalog no. 553731; BD Pharmingen) and FITC-conjugated AffiniPure Anti-Rat IgG (1:75; catalog no. 712-095-153; Jackson ImmunoResearch Laboratories, Inc). The EBs were transferred to a grease lined glass slide, covered with a cover slip and imaged.

2.8.4 Endothelial cell immunofluorescence

For immunofluorescence, differentiated endothelial cells were plated on Type I collagen chamber slides at a concentration of 5×10^4 and incubated for 24 hours. The cells were then treated in the same manner as the yolk sacs for immunofluorescence staining with CD34 (1:20; catalog no. 553731; BD Pharmingen) and FITC-conjugated AffiniPure Anti-Rat IgG (1:75; catalog no. 712-095-153; Jackson ImmunoResearch

Laboratories, Inc). Chambers were carefully removed, slides were grease-lined and cells were covered with a cover slip and imaged.

2.9 X-gal staining

Untreated whole-mount E8.5 embryos with surrounding yolk sac and adult organs and tissues were fixed on ice for 10 min and 30 min respectively in the following solution per established procedures (Venuti et al. 1995):

25% glutaraldehyde	80 μl
10% paraformaldehyde in 1X PBS	2 ml
10X PBS pH 7.4	800 μl
water	7.1 ml

The samples were then washed 3 times in 1X PBS pH 7.4 and stained overnight at 37°C in the following solution:

K ferricyanide 50mM	1.0 ml
K ferrocyanide 50mM	1.0 ml
10X PBS	1.0 ml
1M MgCl2	20 μl
X-Gal in DMF (20mg/ml)	0.5 ml
water	6.5 ml

Solution was mixed well and filter sterilized (0.22 μM) prior to addition of samples. Samples were rinsed in PBS and fixed overnight in 3.7% paraformaldehyde. The following day, the samples were again rinsed, imaged and stored in 70% EtOH for paraffin embedding.

2.10 Yolk sac endothelial cell purification

2.10.1 Preparation of single yolk sac cell suspension

Embryonic day 9.5 embryos were obtained from timed matings. Yolk sacs were incubated in 0.1% collagenase (Stem Cell Technologies, Inc)/PBS/20% FBS at 37°C for 30 minutes. The digested yolk sacs were aspirated through a 27 gauge needle. Genotyping was performed on DNA isolated from corresponding embryo tissues.

2.10.2 Cell sorting with PECAM

Single cell suspensions from yolk sacs were incubated for 30 minutes at 4°C with anti-PECAM1 antibody conjugated to PE Cy-7 (eBioscience, Inc.). The PECAM1+ cells were isolated by cell sorting using a BD FACSAria™ cell sorter (BD Biosciences, USA). Sorted cells were prepared for RNA isolation using the RNeasy mini kit (Qiagen) and genes were analyzed via real time PCR.

2.11 Identification of TFBSs

The ECR browser (Ovcharenko et al. 2004) was used to determine the location of potential RBPJ binding sites. The evolutionary conserved regions of the mouse, human, and rat were examined upstream and flanking the transcription start site of each gene for the presence of the RBPJ binding sequence (GTGGGAA) (Tun et al. 1994).

2.12 Microscopy and image acquisition

Images were acquired with a Nikon SMZ800 dissecting microscope for whole embryos and a Nikon ECLIPSE 55i for embryonic sections using a Leica DFC480 camera and Leica FireCam 3.0 software. Images for yolk sac and cell

immunofluorescence were acquired with an Olympus 1X71 microscope and Olympus DP71 camera using Olympus DP71 controller software. Adobe Photoshop CS2 was used for photograph editing.

2.13 Statistical analysis

Data bars represent the means +/- standard error of the mean. RNA analyses of yolk sac tissues were performed with an n of 5. RNA analyses of differentiated ES cells were performed in triplicate. The statistical significance of the data was determined using a t-test with a p-value of < 0.05 considered statistically significant.

Chapter 3

Notch signaling regulates remodeling and vessel diameter in the extraembryonic yolk sac

3.1 Introduction

In mice, the vascular system, essential for nutrient and waste transport, initially forms in intraembryonic and extraembryonic regions. In the extraembryonic yolk sac at approximately embryonic day E7.0-7.5, angioblasts are formed from the differentiation of mesodermal cells. These angioblasts differentiate into endothelial cells, elaborate cell contacts, and lumenize into simple tubes; resulting in the formation of a capillary plexus network (Risau and Flamme 1995; Drake and Fleming 2000). The simple plexus of the yolk sac is remodeled and refined after E8.5 to form the larger diameter vessels. During this process, extensive movements of endothelial cells within the plexus occur through a process termed intussusceptive arborization (Djonov et al. 2000), reallocating cells from the capillaries to larger vessels, to assemble a more complex vasculature network (Risau 1997; Patan 2000). This process forms the vitelline arteriole and venule, which participate in the contiguous blood flow with the embryonic vasculature, concomitant with the initiation of flow after E9.0 (Patan 2000, Ji et al. 2003). More work needs to be done to define the shared and distinct regulatory paths that control vascular differentiation in the various sites of development and in the adult.

Both vasculogenic and angiogenic processes are highly regulative, and under the control of a number of signaling pathways, including the vascular endothelial growth factor (VEGF) pathway, the Notch pathway, and the transforming growth factor-β (TGFβ) pathway, among others (Tallquist et al. 1999; Carmeliet 2000; Yancopoulos et al. 2000; Krebs et al. 2000). The Notch signaling pathway is evolutionary conserved and a

determinant of cell fate (Artavanis-Tsakonas et al. 1999). The Notch receptors are activated upon ligand binding, which initiates the proteolysis of its intracellular domain (N-ICD). The N-ICD translocates to the nucleus where it interacts with a family of DNA-binding proteins, termed recombination signal-binding protein for immunoglobulin kappa J region (RBPJ; also known as C-promoter binding factor 1, CBF1), forming a transcriptional activator complex at the regulatory elements of target genes, thereby directing changes in gene transcription (Mumm and Kopan 2000).

Much work has been done to define the roles of the Notch signaling pathway during vascular differentiation. *Notch1*, *Notch4*, *Dll4*, *Jagged1*, and *Jagged2* are all expressed in the arterial endothelium of vertebrates, *Notch4* being solely expressed in the endothelia of mouse embryos (Uyttendaele et al. 1996; Villa et al. 2001). Mutations in Notch family receptors, ligands, and effectors lead to defects in the vasculature of the placenta, embryo and yolk sac, many of which are embryonic lethal (Swiatek et al. 1994; Krebs et al. 2000; Uyttendaele et al. 2001; Iso et al. 2003; Krebs et al. 2010). Although Notch clearly plays important roles in the formation of the early embryonic vasculature, very little is known about the nature of the downstream targets in vivo, and how changes in Notch activity elicit the observed morphological processes. In vitro analysis has indicated novel Notch targets, including receptors of the VEGF family, FLT4 (VEGFR-3) and FLT1 (VEGFR-1) (Shawber et al. 2007; Funahashi et al. 2010). Given that several signaling cascades are required for the morphological differentiation of the embryonic vasculature, it is likely that these pathways interact during vascular development.

To better define the activity of Notch signaling in vascular differentiation, a detailed morphological and molecular analysis was performed using developmental models in which the Notch signaling pathway is altered. A gain-of-function Notch1 transgenic model showed that expanded Notch1 signaling in the early vasculature results in defects in embryo growth, defective differentiation during remodeling of the yolk sac

vasculature, altered patterns of gene expression, and ultimately embryonic lethality. These phenotypes were compared to embryos lacking Notch signaling in the endothelia, via a tissue-specific loss of RBPJ function. Embryos lacking endothelial *Rbpj* exhibited distinct growth, vascular, and gene expression defects compared to the Notch1 gain-of-function model. Gene expression analysis in the yolk sacs of these models demonstrated altered patterns of expression of a distinct subset of Notch targets. Additionally, several secreted ligands, including the TGFβ ligand, TGFβ2 and the VEGF ligands, VEGFC and placental growth factor (PlGF), were altered in these models, suggesting a role for an altered VEGF signaling pathway in the observed phenotypes of these models. Our data suggest a model in which Notch signaling in the endothelia is critical for elaborating a specialized local environment of the developing arterial vasculature, by influencing the expression of secreted factors, which may be important in autocrine or paracrine signaling to direct further morphological differentiation of the vasculature during remodeling.

3.2 Results

3.2.1 Conditional transgenesis to modulate Notch signaling in the early endothelia

To further understand the functions of Notch signaling in early vascular development, genetic models were employed to modulate Notch activity in the embryonic endothelia. These models employ endothelial-specific Cre-mediated recombination in vivo. To activate and expand Notch1 signaling in the endothelia, a transgenic line $Rosa^{Notch}$ (Murtaugh et al. 2003) was used, which harbors a NOTCH1 intracellular domain (N1ICD) cDNA downstream of a floxed STOP fragment targeted to the *Rosa26* locus. Removal of the STOP cassette through *loxP*-mediated recombination,

via an endothelial Cre expressing transgene, results in expression of N1ICD in endothelial cells (designated as EC-N1ICD embryos; Figure. 3.1A). To delete Notch signaling in the early endothelia, a mouse line was used which harbors a conditional allele of *Rbpj* (*Rbpj*^{f} mice) (Tanigaki et al. 2002). Crossing these mice to an endothelial-specific Cre transgenic mice results in the deletion of exons 6 and 7, which encode the DNA binding domain of *Rbpj*, abrogating the activity of RBPJ only in endothelial cells (designated as EC-Rbpj-KO embryos; Figure 3.1B). The conditional deletion would be predicted to disrupt both Notch1 and Notch4 signaling, which have known redundant functions in early embryonic vascular differentiation (Krebs et al. 2000). Ablation of *Rbpj* in the endothelia was used to assure a complete disruption of Notch signaling in the developing vasculature.

Tie2-Cre (Koni et al. 2001) or *Flk1-Cre* (Motoike et al. 2003) transgenic mice were crossed to either *Rosa*^{Notch} or *Rbpj*^{f} mice. Each of these transgenes expresses the *Cre* recombinase gene and directs expression principally to the vascular endothelium. Identical phenotypes were observed when the *Flk1-Cre* and *Tie2-Cre* transgenic lines were crossed to the *Rosa*^{Notch} and *Rbpj*^{f} models (data not shown). Previous work has demonstrated that these Cre expressing transgenes exhibit restricted endothelial expression of Cre recombinase activity to the endothelial and hematopoietic lineages (Motoike et al. 2003). The early embryonic expression and recombinase activity of the *Tie2-Cre* and *Flk1-Cre* transgenes was confirmed by crossing of these transgenes to a conditional *lacZ* reporter (Soriano 1999). Both transgenes showed specific expression within the early endothelial and hematopoietic lineages at E8.5 (Figure 3.2).

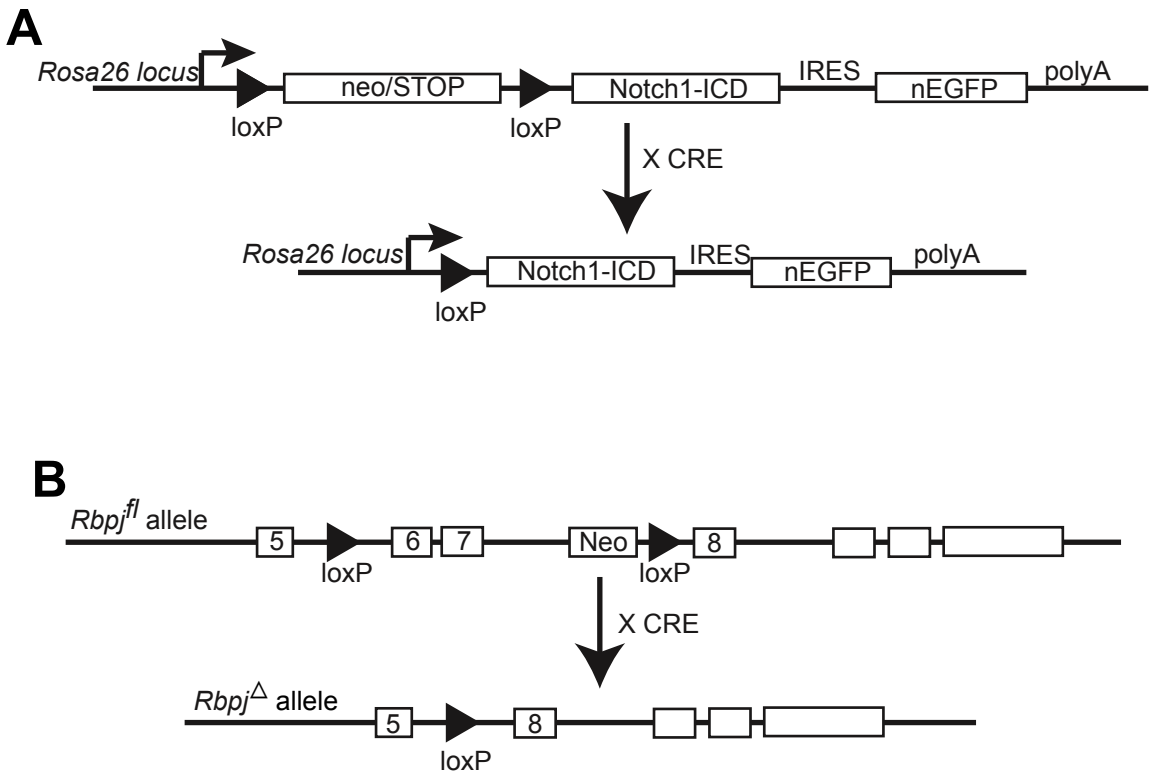

Figure 3.1. Conditional Mouse EC-N1ICD and EC-Rbpj-KO Transgene Constructs
(A) Upon crossing of mice that carry the *Rosa*^{Notch} transgene to a transgenic mouse that expresses CRE in the endothelia (*Tie2-Cre*), recombination removes the neomycin cassette and induces expression of the Notch1 intracellular domain only in endothelial cells. (B) Upon crossing of mice that carry the *Rbpj*^{f} transgene to a transgenic mouse that expresses Cre in the endothelia, recombination will remove the neomycin cassette along with exons 6 and 7, which encode for the DNA binding domains of RBPJ, abrogating the promoter activity of RBPJ only in endothelial cells.

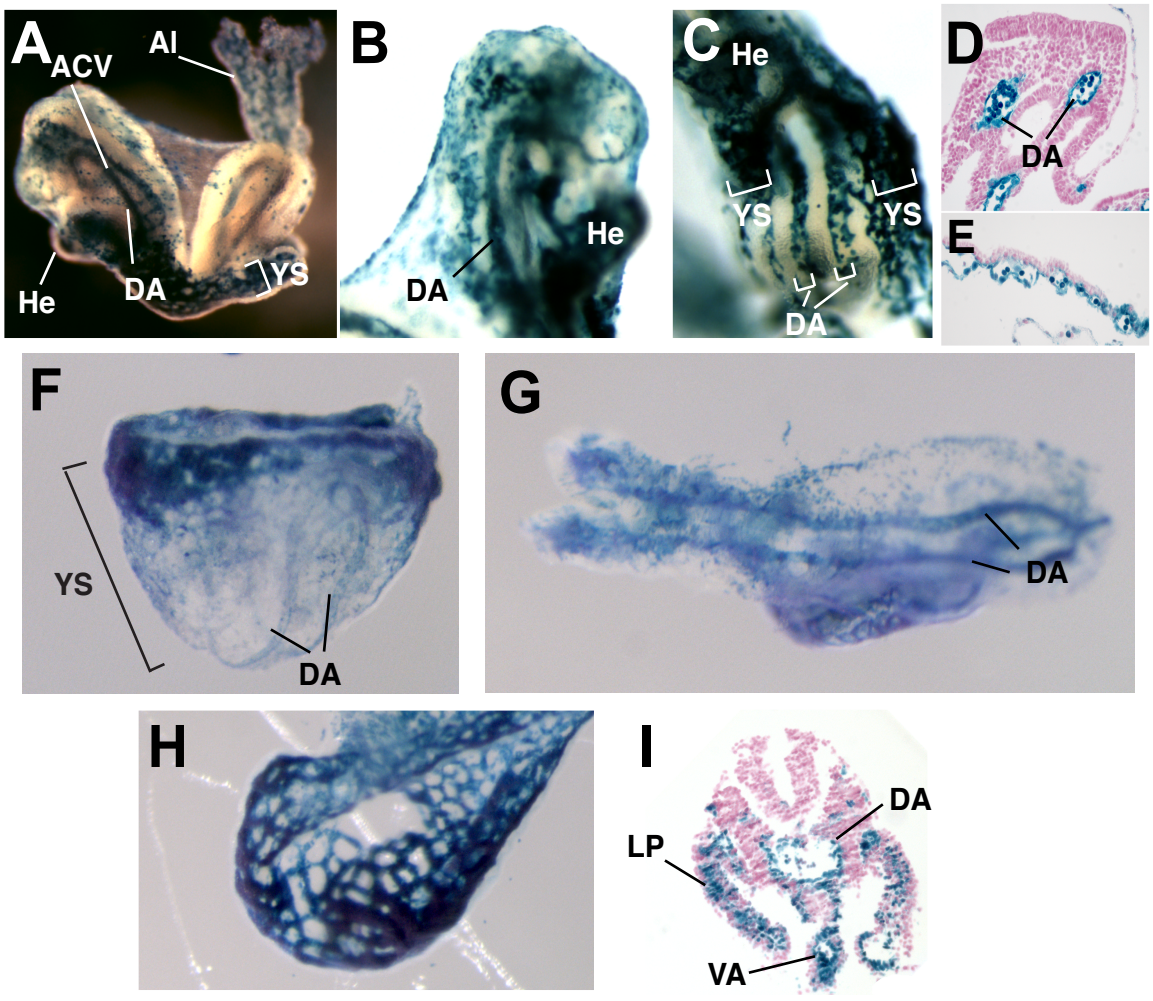

Figure 3.2. *Tie2-Cre* and *Flk1-Cre* are Expressed in the Endothelia of the Early Embryo

(A-E) X-Gal staining of embryos from R26R cross with *Tie2-Cre* transgene. (A-C) Whole mount E8.5 embryos. (D, E) Histological sections of E8.5 embryos. (F-I) X-Gal staining of embryos from R26R cross with *Flk1-Cre* transgene. (F) Whole mount E8.0 embryo with surrounding yolk sac. (G) Whole mount E8.5 embryo. (H) Yolk sac from a E8.5 embryo. (I) Histological section of E8.5 embryo. Note expression in the endothelia of dorsal aorta (DA), heart (He), anterior cardinal vein (ACV), yolk sac (YS), allantois (Al), lateral plate (LP), and vitelline artery (VA).

3.2.2 Regulated Notch signaling is essential for the growth and development of the early embryo

To activate Notch1 signaling throughout the embryonic endothelia, female mice heterozygous for the *Rosa*^{Notch} transgene were crossed with male mice hemizygous for the *Tie2-Cre* transgene, and the resulting embryos were analyzed. At E8.5 the EC-N1ICD mice were morphologically normal and identical to the wild type siblings (Figure 3.3) with open neural folds and a vascularized allantois characteristic of this time point. Compared to stage-matched wild type embryos at E9.5, EC-N1ICD embryos exhibited an enlarged heart and a reduction in overall size (Figure 3.4A-B). Growth defects were much more pronounced at E10.5 (data not shown), and no viable embryos were observed after E10.5.

To ablate Notch signaling in the embryo, *Tie2-Cre* mice were used in a two-generation cross to generate *Tie2-Cre*; *Rbpj*$^{f/f}$ embryos (EC-Rbpj-KO), which lack RBPJ binding activity in the endothelia. The EC-Rbpj-KO embryos displayed severe growth retardation defects at E9.5 similar to those observed in the EC-N1ICD embryos (Figure 3.4C). The morphological analysis of the gain-of-function and loss-of-function embryos were consistent with other models (Krebs et al. 2000; Uyttendaele et al. 2001; Krebs et al. 2004; Krebs et al. 2010) and confirmed that the appropriate Notch signaling in the endothelia of the early embryo is critical for proper growth and development of the embryo.

3.2.3 Vascular defects in EC-N1ICD and EC-Rbpj-KO embryos

A detailed comparison of the vasculature was performed to define the vascular defects in the embryonic and extraembryonic vasculature of EC-N1ICD and EC-Rbpj-KO embryos. At E8.5, no overt defects were observed in the developing vasculature of either the EC-N1ICD or EC-Rbpj-KO. In particular, the vascular plexus of the EC-

N1ICD yolk sac, visualized by histochemical staining of endothelial cells with an antibody to PECAM1 (CD31), appeared unaffected when compared to stage-matched wild type embryos (Figure 3.3; data not shown). The most severe defects were seen in the yolk sac of the developing embryo beginning at approximately E9.5. Gross morphological examination of the vasculature of the yolk sac by whole mount light microscopy showed that at E9.5 the EC-N1ICD yolk sac was the same size as the stage-matched wild type control; however these embryos lacked large diameter vessels (Figure 3.4D-E), indicating a failure in appropriate blood vessel remodeling occurring at this time point (Patan 2000). The EC-N1ICD yolk sac vessels did contain blood cells, although the blood tended to pool near the proximal end of the yolk sac adjacent to the chorioallantoic plate (Figure 3.4E). EC-Rbpj-KO embryos also lacked vascular remodeling in the yolk sac, failing to form the large vitelline blood vessels (Krebs et al. 2004; Figure 3.4F).

Immunofluorescence of PECAM1 stained E9.5 yolk sac revealed the failure of this remodeling in both the EC-N1ICD and EC-Rbpj-KO embryos in greater detail. In the EC-N1ICD embryos, no distinction between large caliber vessels and capillaries was observed (Figure 3.4H); instead, the vasculature consisted of vessels with an enlarged surface area with greatly decreased avascular inter-vessel space compared to wild type controls, as assessed by lack of PECAM1 expression ('pillars'; Figure 3.4G-H, arrows). In contrast to the EC-N1ICD vessel defects, the EC-Rbpj-KO embryos exhibited a qualitatively different vessel phenotype in the yolk sac. Although EC-Rbpj-KO embryos also exhibited a lack of vascular remodeling, the yolk sac of these embryos displayed numerous small avascular intervessel spaces (Figure 3.4I, arrow). These results indicated that the yolk sac vasculature of the EC-Rbpj-KO embryos failed to form the large vitelline blood vessels, reminiscent of the simple vascular plexus seen at E8.5.

Histological sectioning of yolk sac tissue was performed to visualize the vessels in cross-section via PECAM1 immunochemistry and hematoxylin and eosin staining. In

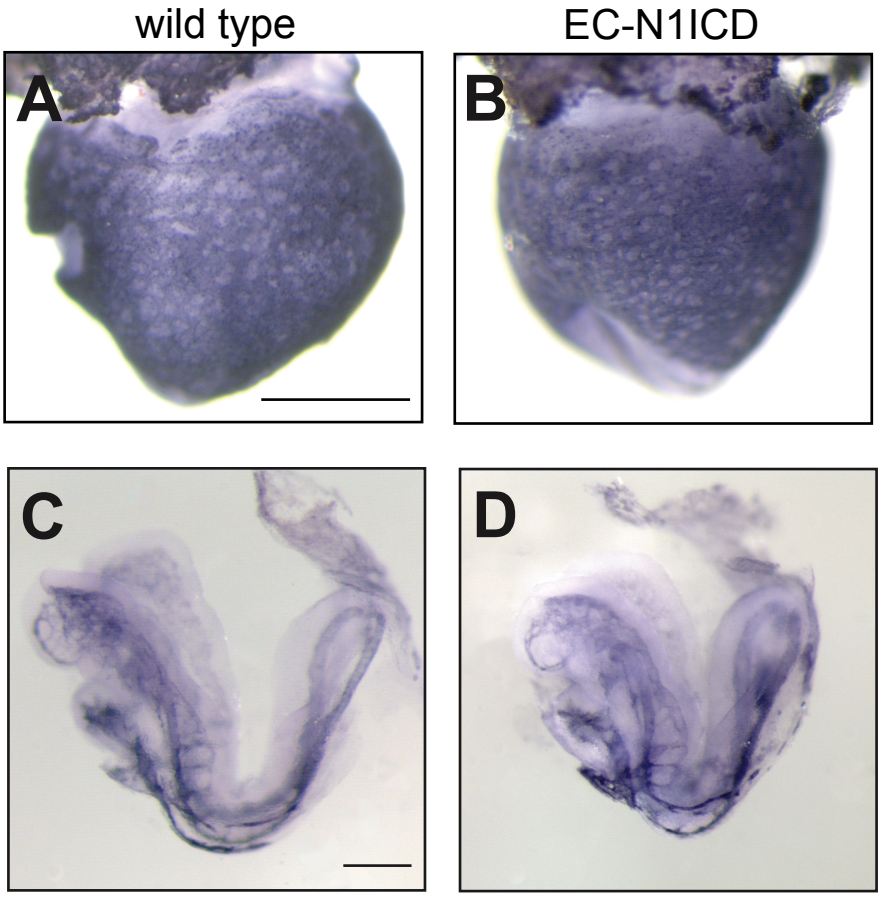

Figure 3.3. Embryonic Growth and Vascular Remodeling is Normal in Early EC-N1ICD Embryos

(A, B) Whole mount E8.5 wild type (A) and EC-N1ICD littermate (B) embryos with surrounding yolk sac stained with an antibody to PECAM1. EC-N1ICD yolk sac vasculature appeared normal. (C, D) Lateral view of E8.5 wild type embryo (C) and EC-N1ICD littermate (D) stained with an antibody to PECAM1. EC-N1ICD embryos appeared normal. Scale bars are 500 μm (A, B) and 250 μm (C, D).

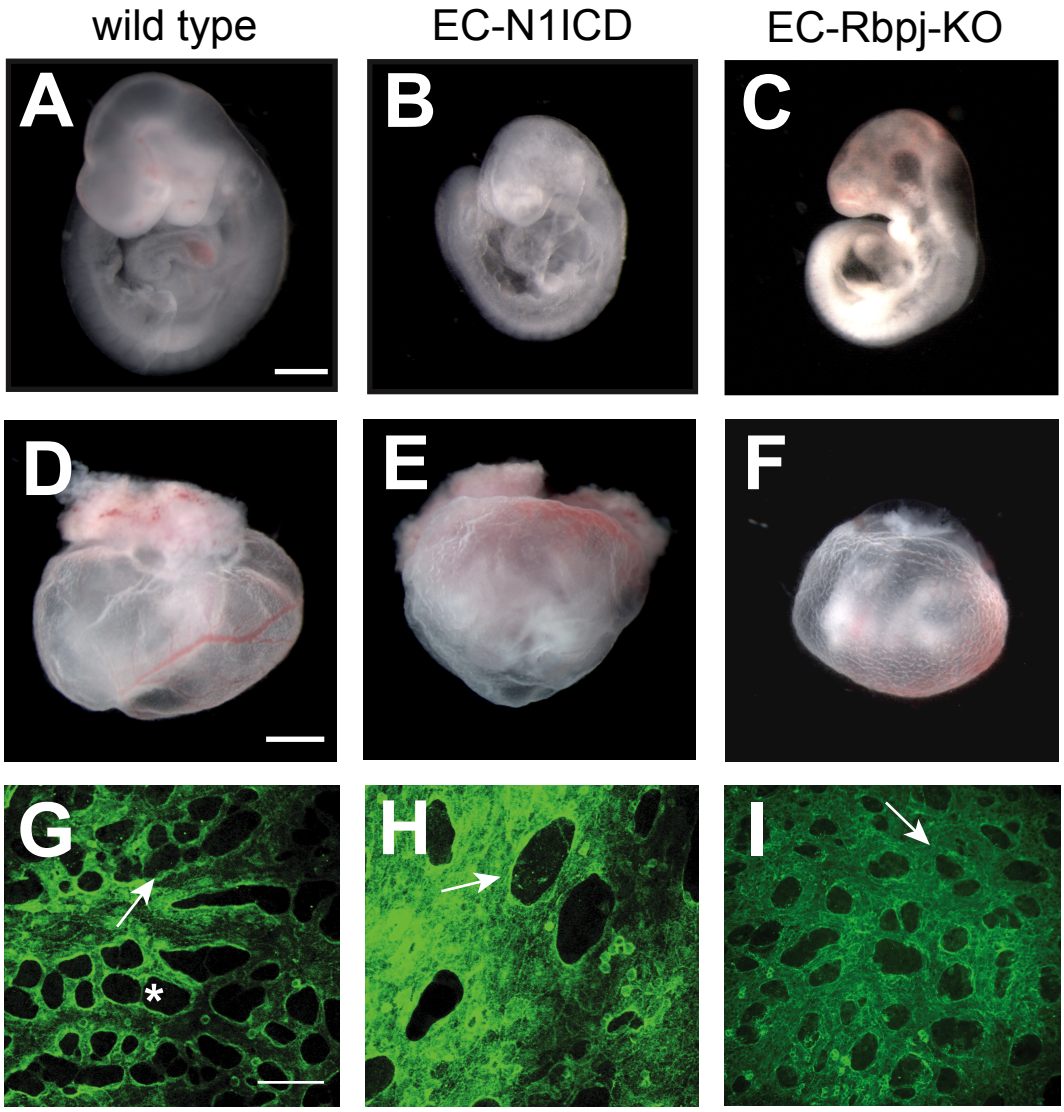

Figure 3.4. Defects in Growth and Yolk Sac Vasculature Remodeling in EC-N1ICD and EC-Rbpj-KO Embryos

(A-C) Lateral view of E9.5 wild type (A), EC-N1ICD (B), and EC-Rbpj-KO (C) embryos. EC-N1ICD and EC-Rbpj-KO embryos were smaller in size than the wild type and exhibited cardiovascular defects. (D-F) Whole mount E9.5 wild type (D), EC-N1ICD (E), and EC-Rbpj-KO (F) embryos with surrounding yolk sac. The EC-N1ICD and EC-Rbpjk-KO yolk sac lacked the large, well-defined blood vessels seen in the wild type. The blood in the EC-N1ICD yolk sac collected near the attachment to the placenta. (G-I) Immunofluorescence image of E9.5 wild type (G), EC-N1ICD (H) and EC-Rpbj-KO (I) yolk sac visualized with an antibody to PECAM. Wild type embryos showed a remodeled yolk sac vasculature, with both large and small caliber vessels. The EC-N1ICD yolk sac did not exhibit branching; all vessels were of a large caliber. The EC-Rbpj-KO yolk sac also failed to show vascular remodeling, although all vessels were of a small caliber. Scale bars are 500 μm (A-C), 1 mm (D-F) and 100 μm (G-I). Arrows (G-I), avascular inter-vessel space. Asterisk (G), capillary collapse.

the wild type yolk sac a distribution of large and small caliber vessels were present and were filled with blood cells; in striking contrast, the EC-N1ICD yolk sac contained primarily large caliber lumenized vessels that contained blood cells (Figure 3.5A-B). Both wild type and EC-N1ICD embryos had a range of yolk sac vessel diameter. However, in wild type yolk sac a majority of the vessels measured consisted of small capillaries, while in the EC-N1ICD yolk sac a larger proportion of vessels consisted of a larger cross-sectional area. In EC-N1ICD yolk sac, approximately 36% of vessels measured had an area of 16000μm^2 or greater, while in wild type yolk sac only 5% measured this size (Figure 3.5E). This enlarged vessel phenotype in response to Notch activation was observed in other sites of the vessel differentiation in the developing embryo. The dorsal aortae (DA) of EC-N1ICD embryos were approximately twice the cross-sectional area of wild type embryos (Figure 3.5C-D, asterisks). The embryo-derived vasculature of the placenta of EC-N1ICD embryos did invade into the labyrinth layer of the placenta (Figure 3.5G, arrowheads), but exhibited greatly enlarged vessel diameter (Figure 3.5G, arrows). The EC-Rbpj-KO embryos exhibited a decrease in vessel diameter, including the DA, and arteriovenous malformations (Krebs et al. 2004). EC-Rbpj-KO embryo-derived vasculature of the placenta was also reduced in size and did not invade the labyrinth layer of the placenta (Figure 3.5H, arrow). Immunostaining of E9.5 wild type and EC-N1ICD embryos using anti-SMA, indicated that the dorsal aortae of wild type are surrounded by smooth muscle cells, while the EC-N1ICD did not recruit any SMA-positive cells to the dorsal aorta (Venkatesh et al. 2008; Figure 3.5F-G).

The morphological analyses of the models of altered Notch signaling were consistent with previous analysis of Notch function in the vasculature (Krebs et al. 2000; Uyttendaele et al. 2001; Krebs et al. 2004; Krebs et al. 2010). These results point to multiple roles for Notch signaling in the formation of both the intra- and extraembryonic vasculature, including the remodeling of the yolk sac vasculature, the regulation of vessel

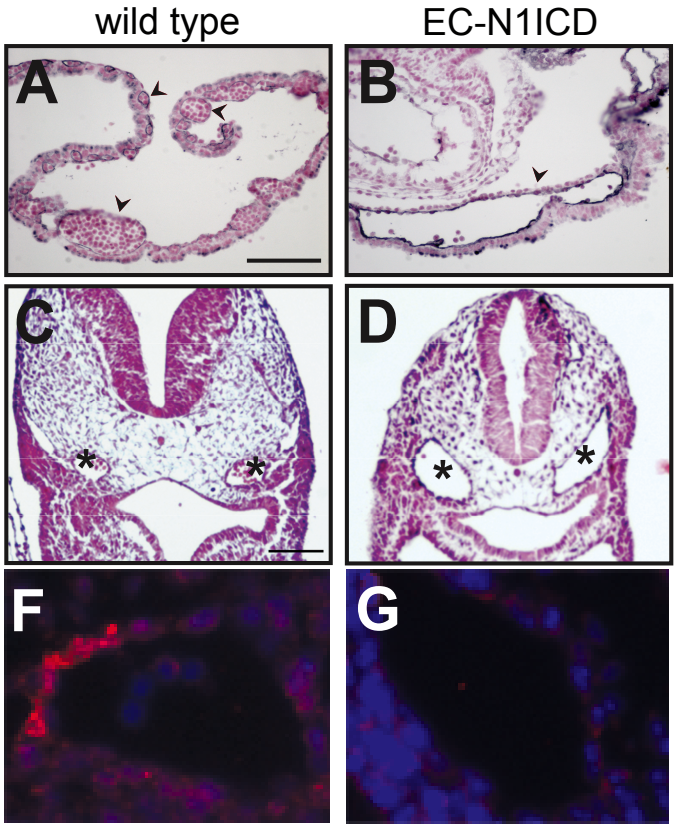
wild type
EC-N1ICD
A
B
C
D
F
G

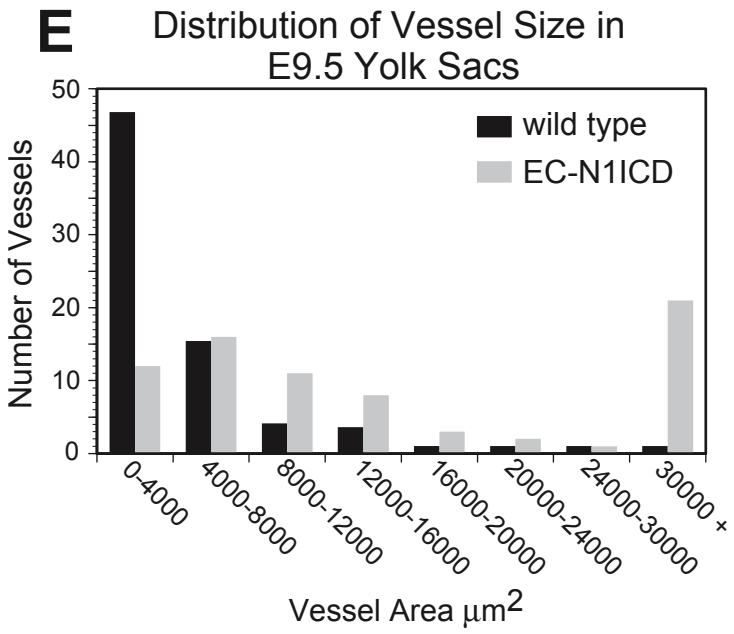
E
Distribution of Vessel Size in
E9.5 Yolk Sacs
wild type
EC-N1ICD
Number of Vessels
50
40
30
20
10
0
0-4000
4000-8000
8000-12000
12000-16000
16000-20000
20000-24000
24000-30000
30000 +
Vessel Area μm2

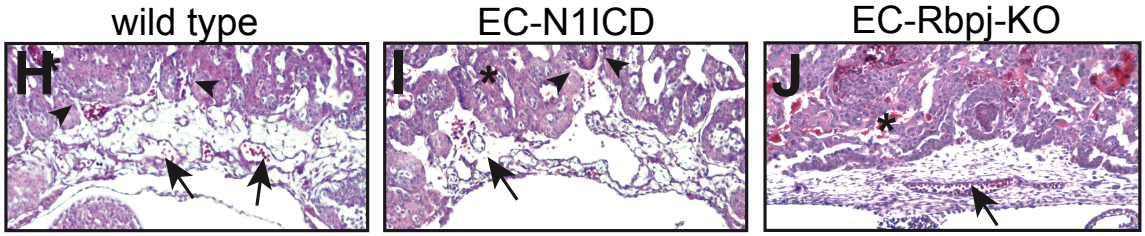
wild type
EC-N1ICD
EC-Rbpj-KO
H
I
J

Figure 3.5. Defects in Vessel Diameter in EC-N1ICD and EC-Rbpj-KO Embryos
Histological sections (lateral) of PECAM1 and NFR-stained E9.5 yolk sac (A-B) and embryos (C-D) at the level of the heart. The wild type yolk sac contained both large and small caliber vessels (A, arrowheads). The EC-N1ICD yolk sacs contained primarily large caliber vessels (B, arrowheads), however they were lumenized. The dorsal aortae of the EC-N1ICD embryos (D, asterisk) were approximately twice the area of wild type dorsal aortae (C, asterisk). (E) Distribution of vessel area in the yolk sac of wild type and EC-N1ICD embryos. Both wild type and EC-N1ICD embryos had an array of differently sized vessels. However, wild type yolk sac had a majority of vessels with an area of 0-4000μm2, while EC-N1ICD contained many vessels with an area of 30000μm2 or greater. (F-G) Histological sections of E9.5 dorsal aorta stained with an antibody to smooth muscle α-actin. The dorsal aortae of the wild type contain SMA-positive cells (F), while the EC-N1ICD dorsal aortae are SMA-negative. (H-J) Histological sections of the placental vasculature in wild type (H), EC-N1ICD (I), and EC-Rbpj-KO (J) embryos. Blood vessels containing nucleated erythrocytes in EC-N1ICD placenta (I, arrow) were of larger caliber than blood vessels in wild type placenta (H, arrow). In both, the fetal vasculature invaded into the maternal portion of the placenta. The vessels of the EC-Rbpj-KO placenta (J, arrow) were small in size and had not invaded into the labyrinthine layer. Asterisk (H-J), maternal blood. Scale bars are 100 μm (A-D).

diameter, and the invasion of the embryo-derived vasculature into the labyrinth layer of the placenta.

3.2.4 Identification of Notch regulated genes in EC-N1ICD yolk sacs and EC-Rbpj-KO yolk sacs

Gene expression defects in the Notch models were examined to determine potential molecular mechanisms of how altered Notch disrupts vascular differentiation, through altered expression of putative Notch targets. RNA from yolk sacs of E9.5 wild type, EC-N1ICD and EC-Rbpj-KO embryos (resulting from a cross with *Tie2-Cre* or *Flk1-Cre* mice) was isolated for gene expression analysis via microarray and semiquantitative RT-PCR. Whole genome microarray identified a large number of gene expression defects in these Notch models, many of which were confirmed with RT-PCR. To identify putative Notch targets, genes were categorized on the altered response in the gain-of-function and loss-of-function models (Figure 3.6). Only a relatively small set of genes displayed upregulation in the EC-N1ICD model and downregulation in the EC-Rbpj-KO model, which would be suggestive of genes that are positively regulated by the Notch1-Rbpj axis. Interestingly, no genes were identified as being downregulated in the EC-N1ICD model and upregulated in EC-Rbpj-KO (Figure 3.6).

The members of the Hairy/Enhancer of split-related (HES/HEY) family are well described Notch targets, many of which are directly regulated by Notch1 signaling via its binding to RBPJ (Maier and Gessler, 2000) to regulatory regions of these loci. The microarray datasets revealed that in yolk sacs of EC-N1ICD embryos, both *Hey1* and *Heyl* were highly induced, and expression of these genes was reduced in the EC-Rbpj-KO; these results were confirmed by semi-quantitative RT-PCR (Figure 3.7A). Expression of *Hey1* and *Heyl* was increased 4.4-fold and 20.5-fold in the EC-N1ICD model respectively, and decreased to 35% and 46% of wild type levels in the EC-Rbpj-

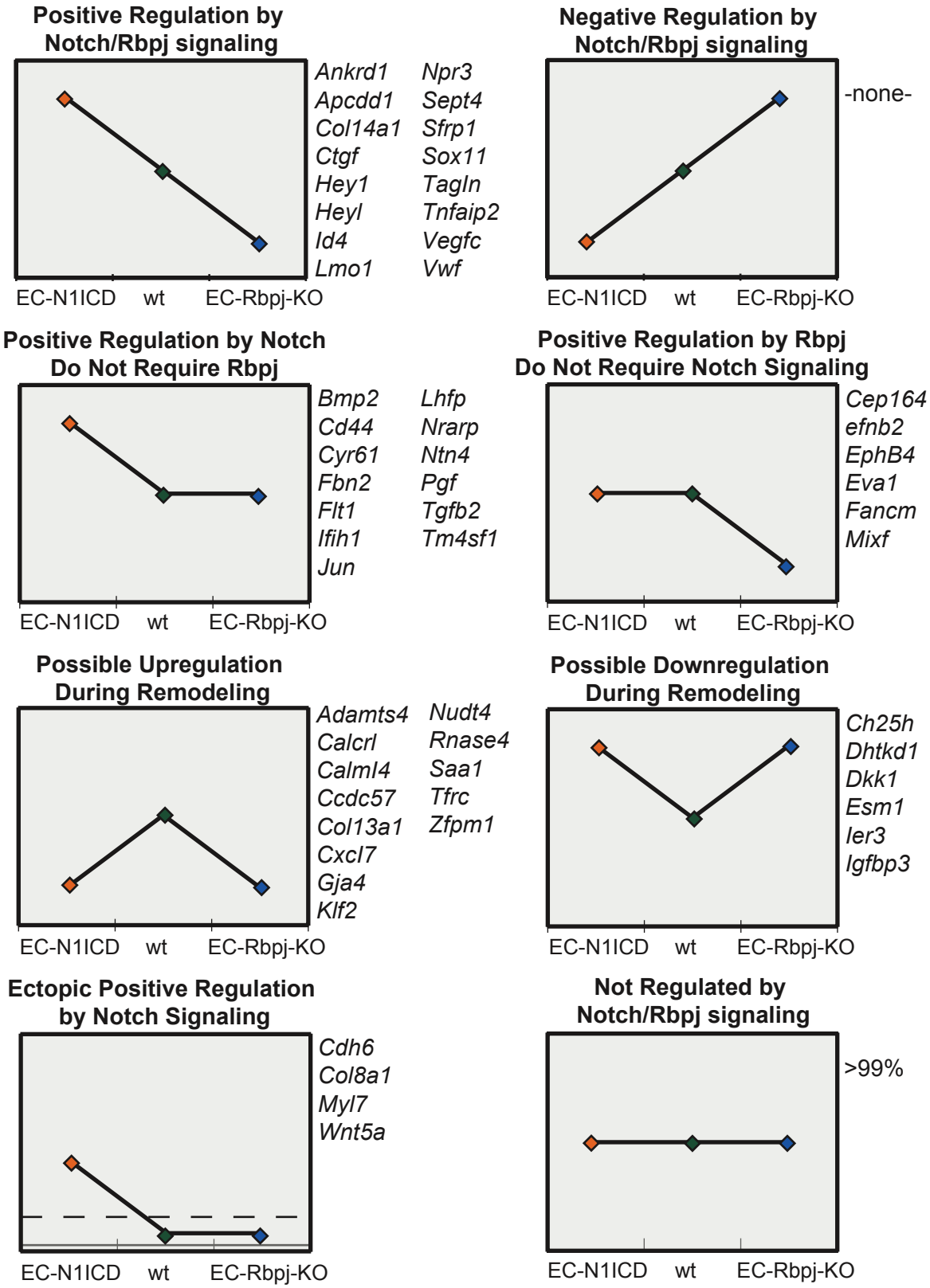

Figure 3.6. Gene Expression in EC-N1ICD and EC-Rbpj-KO Yolk Sac Tissues
A graphical representation of possible outcomes of expression data and the corresponding genes that display this type of expression.

KO yolk sac tissue, respectively. Interestingly, the expression of other HES family members, such as *Hes1* and *Hes6* was not affected in these Notch models (data not shown), consistent with a context-dependent regulation of Notch targets (Radtke and Raj 2003; Bolos et al. 2007); i.e. Notch signaling invokes distinct downstream targets depending on both the cell type and the local environment.

The expression of the endogenous Notch ligands and receptors was also examined in detail. Previous work has suggested a potential autoregulatory loop for Notch signaling in the control of ligands and receptors (Ross and Kadesh 2004; Qian et al. 2009). Although expression of the Notch family receptors was not altered in either the EC-N1ICD or EC-Rbpj-KO yolk sacs, the Notch ligands Delta-like 4 (*Dll4*) and Jagged 1 (*Jag1*) showed higher expression in EC-N1ICD (2.5-fold and 2.0-fold, respectively) with little or no change in expression in EC-Rbpj-KO yolk sac. These findings point to specific Notch pathway targets in the extraembryonic yolk sac vasculature.

3.2.5 Notch-Rbpj signaling regulates the vascular expression of key signaling molecules

Given the defects in vessel diameter and remodeling in response to altered Notch activity, we wished to focus on gene expression analysis of secreted factors. Genes encoding several known and putative secreted factors were differentially expressed in the Notch models (Table 3.1). Expression defects of a subset of these genes were confirmed via RT-PCR, with a focus on genes with putative roles in vascular differentiation and that display coordinate defects in expression in the EC-N1ICD and EC-Rbpj-KO models. Although the expression of some VEGF family members was not significantly different in yolk sac, the microarray datasets indicated that expression of the VEGF family members *Vegfc,* encoding VEGF-C, and *Pgf,* encoding placental growth factor (PlGF), were both increased in EC-N1ICD, and *Vegfc* was decreased in EC-Rbpj-KO (Table 3.1).

RT-PCR confirmed that *Vegfc* was upregulated 2.6-fold in the EC-N1ICD and decreased to 8% in the EC-Rbpj-KO compared to control yolk sac tissue; *Pgf* was upregulated 1.9-fold in the EC-N1ICD and decreased to 74% in the EC-Rbpj-KO compared to control yolk sac tissue. The secreted cytokine *Tgfb2* also exhibited increased expression in the yolk sacs of EC-N1ICD embryos (4.7-fold) and decreased expression in EC-Rbpj-KO (49% of wild type levels) (Figure 3.7B).

Given that the N1-ICD was activated specifically in the endothelia in this transgenic model, we wished to confirm that the gene expression defects in this model are confined to the endothelial lineage, to determine if the gene expression defects are intrinsic to the endothelium, or are associated with another cell type within the yolk sac. To these ends, gene expression of Notch regulated genes was examined in endothelial cells purified via flow cytometry. Via fluorescent activated cell sorting (Figure 3.8), N1ICD embryos (from a cross with *Flk1-Cre* mice) and RNA was isolated from the purified cells for gene expression analysis via real time PCR. To confirm the enrichment of sorted endothelial cells within the PECAM1+ population, expression of lineage markers were compared between RNA from purified PECAM1+ cells and from whole unsorted wild type yolk sac tissue. Endothelial specific genes such as *Cdh5* (*VE-cadherin*) and *Pecam1* exhibited significant enrichment in PECAM1+ cells (5.7-fold and 6.7-fold respectively). In contrast, the levels of the primitive visceral endodermal marker *Rhox5 (Pem,* Lin et al. 1994) were reduced to 10% in the sorted cells compared to whole wild type yolk sac tissue (Figure 3.9A), demonstrating a substantial reduction of visceral endoderm cells in the purified endothelial cells. These findings demonstrate a specific enrichment of yolk sac endothelial cells via flow sorting.

The Notch-responsive genes identified in the previous analysis of whole yolk sac tissues were then examined in the sorted yolk sac endothelial cells. The endothelial marker, *Pecam1* exhibited statistically equivalent expression between the EC-N1CD and

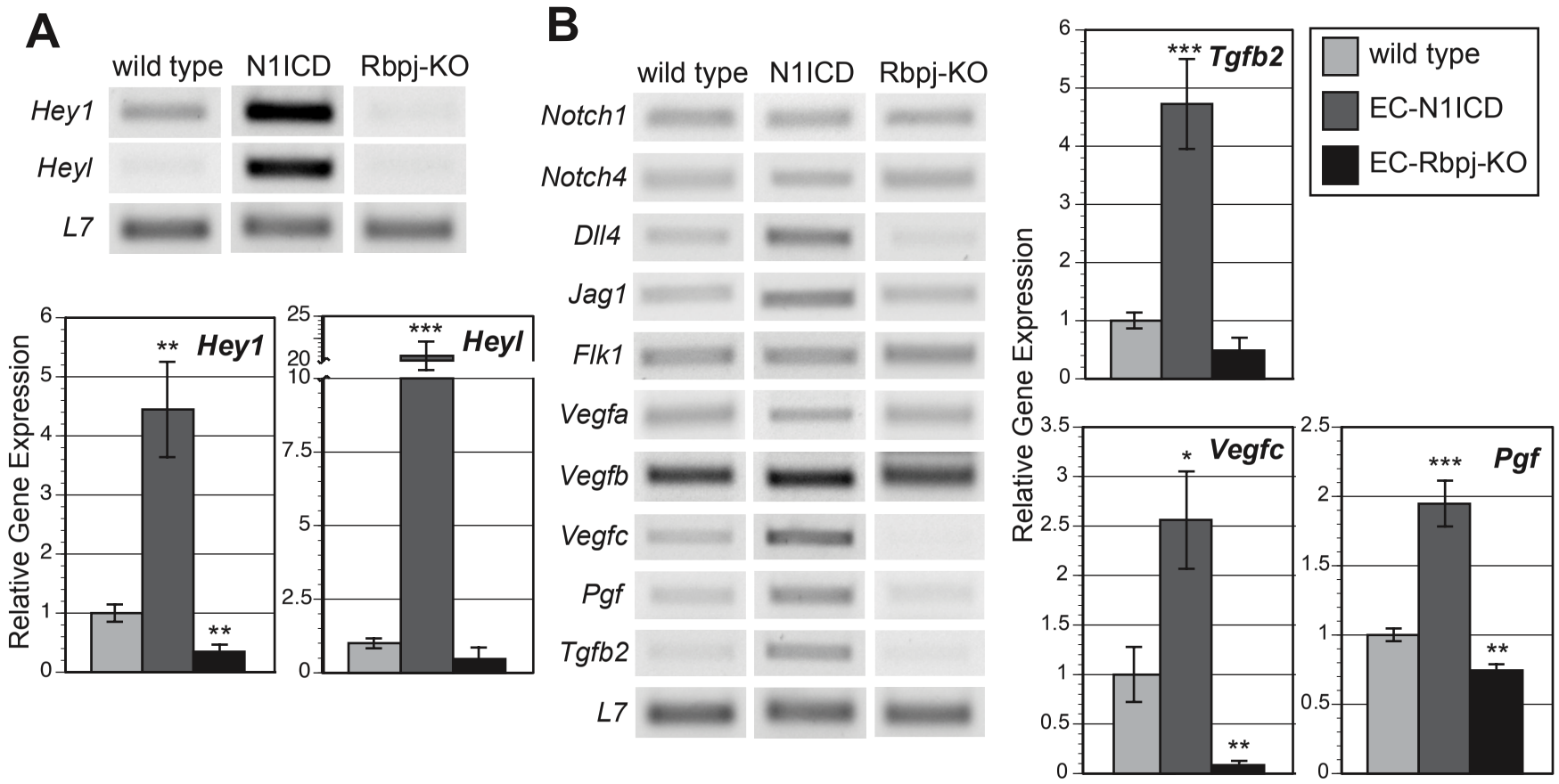

Figure 3.7. Gene Expression in Transgenic EC-N1ICD and EC-Rbpj-KO Embryo Yolk Sacs
Semiquantitative RT-PCR analysis was used to confirm gene expression differences seen in whole genome microarrays. (A) RT-PCR analysis of *Hey1* and *Heyl* in wild type, EC-N1ICD, and EC-Rbpj-KO E9.5 yolk sacs. Quantitated relative mRNA levels are shown in the lower graph. (B) RT-PCR analysis of genes critical for the formation of the early embryonic vasculature. Quantitated relative mRNA levels of select genes are shown in the graphs to the right. * p< .05, ** p< .01, *** p< .001 compared to wild type.

Table 3.1. Microarray Expression of Genes Encoding Secreted Factors in EC-N1ICD and EC-Rbpj-KO Yolk Sac Tissues

Gene Symbol	Gene Name	Fold Change EC-N1ICD	Fold Change EC-Rbpj-KO
Upregulated in EC-N1ICD			
Bmp2	bone morphogenetic protein 2	2.35	1.11
Col14a1	collagen, type XIV, alpha 1	2.29	-1.96
Col8a1	collagen, type VIII, alpha 1	4.88	1.07
Ctgf	connective tissue growth factor	2.13	1.18
Cxcl12	chemokine (C-X-C motif) ligand 12	1.94	1.29
Cyr61	cysteine rich protein 61	2.63	1.66
Esm1	endothelial cell-specific molecule 1	3.41	3.51
Flt1	FMS-like tyrosine kinase 1	1.94	1.07
Ier3	immediate early response 3	2.01	2.10
Igfbp3	insulin-like growth factor binding protein 3	3.85	4.05
Ntn4	netrin 4	5.76	1.39
Rdh5	retinol dehydrogenase 5	2.06	1.39
Snn	stannin	1.97	1.63
Tgfb2	transforming growth factor, beta 2	3.11	1.32
Vegfc	vascular endothelial growth factor C	3.65	-2.50
Vtn	vitronectin	3.34	3.15
Vwf	Von Willebrand factor homolog	2.05	-3.33
Wnt4	wingless-related MMTV integration site 4	2.09	2.45
Wnt5a	wingless-related MMTV integration site 5A	2.47	-1.12
Pgf	placental growth factor	1.93	1.43
Downregulated in EC-N1ICD			
Adamts4	a disintegrin-like and metallopeptidase with thrombospondin type 1 motif, 4	-2.12	-2.44
Cxcl4	chemokine (C-X-C motif) ligand 2	-4.22	-1.11
Hhip	Hedgehog-interacting protein	-2.33	-1.39
Oit3	oncoprotein induced transcript 3	-3.70	1.53
Rnase4	ribonuclease, RNase A family 4	-2.14	-2.04
Saa1	serum amyloid A1	-2.39	-2.44

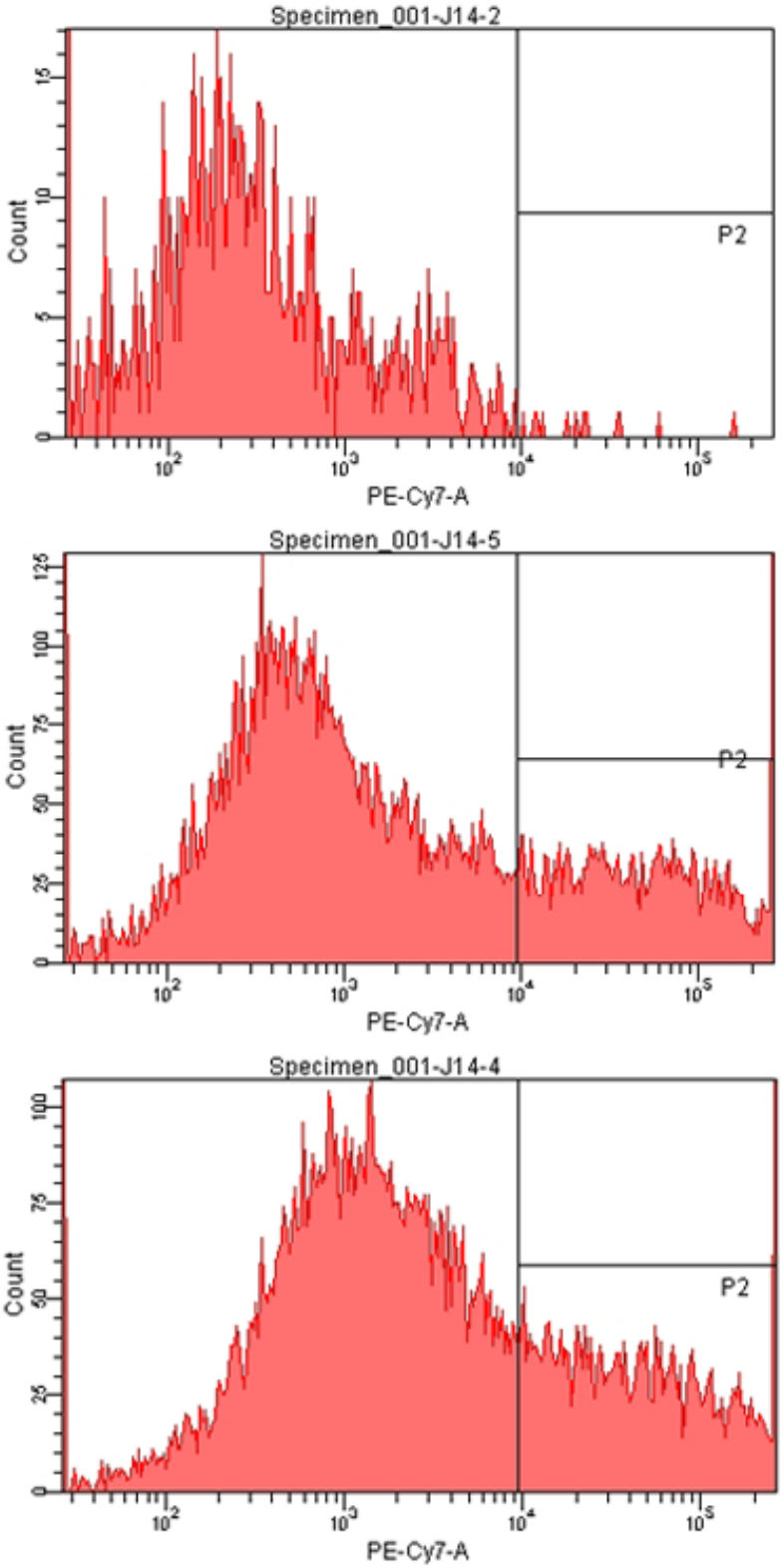

Figure 3.8. Histograms Obtained from PECAM1-PE Cy7 Fluorescent Activated Cell Sorting

Representative histograms showing the distribution of dissociated yolk sac cells for the (A) isotype control and PECAM1 staining (B) wild type yolk sac and (C) EC-N1ICD yolk sac. The gating used to purify PECAM1 cells is indicated.

wild type sorted cells, similar to that seen in whole yolk sac tissues (data not shown). However, expression of *Hey1* and *Heyl* was increased 4.4-fold and 16.7-fold in the EC-N1ICD sorted endothelial cells respectively. Similarly, the VEGF family members *Vegfc* and *Pgf* were upregulated 2.1-fold and 1.9-fold, respectively in sorted EC-N1ICD endothelial cells compared to wild type, while *Tgfb2* was increased 6.9-fold (Figure 3.9B). These results demonstrate that the expression of these genes is upregulated specifically in the endothelial lineages in EC-N1ICD yolk sac. Taken together, the gene expression defects demonstrate that Notch-Rbpj signaling acts to regulate many key genes specifically in the endothelia of the developing yolk sac. The misexpression of some of these factors may contribute to the vascular differentiation defects seen in the transgenic models.

3.2.6 Putative Notch regulated genes contain potential RBPJ binding sites in the upstream regulatory region

The in vivo studies have identified a number of putative Notch regulated genes in the developing vasculature. Many of these genes are known Notch targets, including *Hey1* and *Heyl*, with known RBPJ binding sites within regulatory elements (Maier and Gessler 2000). These studies however also identified altered expression of several genes, including *Vegfc*, *Tgfβ2*, and *Pgf*, for which their regulation by Notch signaling has not previously been described. Bioinformatic tools were used to determine if these genes are potentially direct targets of Notch signaling through RBPJ. Several RBPJ binding sites, with a core consensus binding sequence GTGGGAA (Tun et al. 1994), have been previously identified in known Notch targets such as the HES family members (Nishimura et al. 1998; Maier and Gessler 2000). The bioinformatic tool, ECR browser (Ovcharenko et al. 2004), was used to determine if canonical RBPJ binding sites were observed in the promoter proximal regions of loci encoding the secreted factors, *Vegfc*,

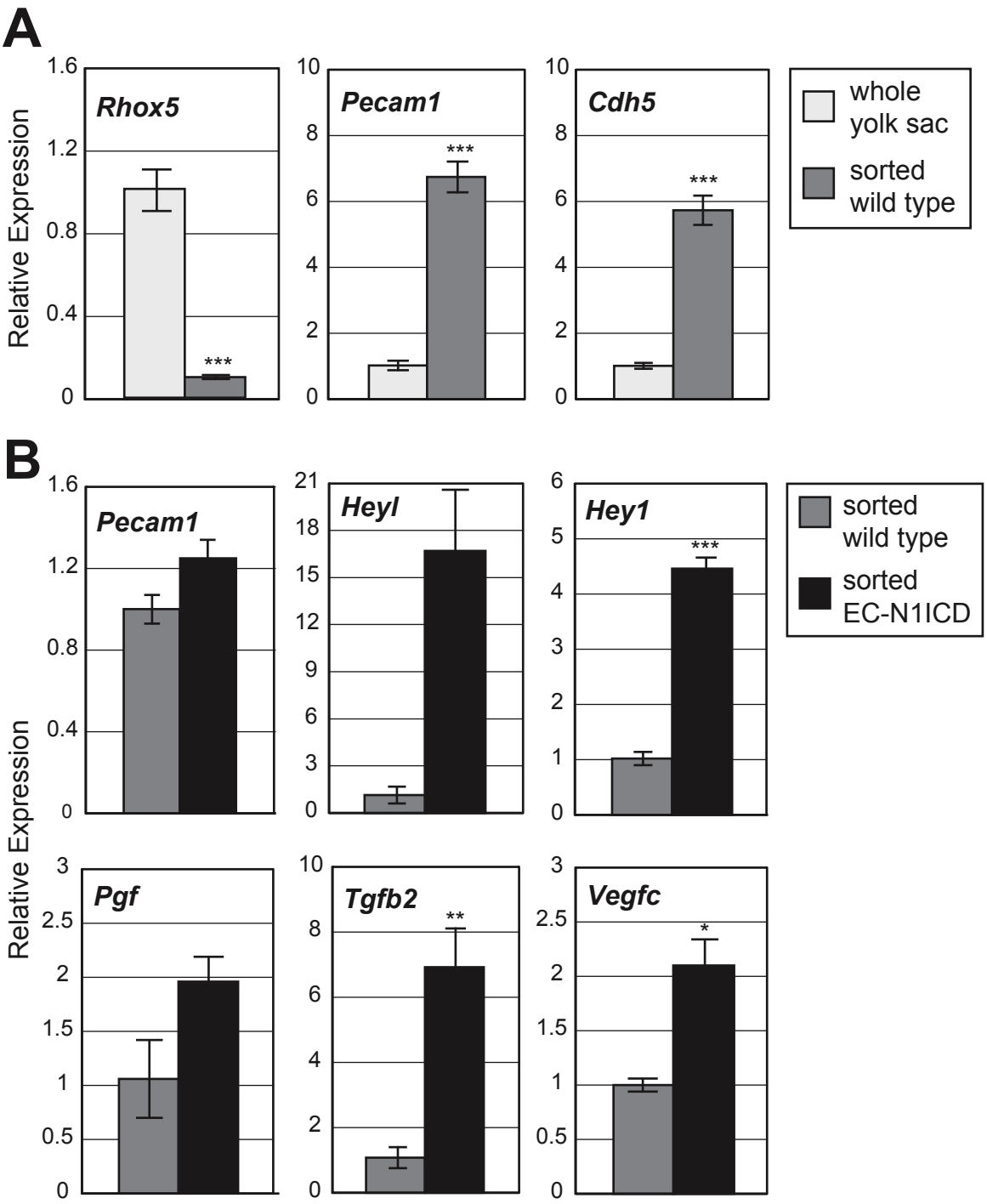

Figure 3.9. Gene Expression in Transgenic EC-N1ICD PECAM1+ Sorted Yolk Sac Tissues

Real time-PCR analysis was used to analyze gene expression differences seen in PECAM1+ sorted yolk sac cells. (A) Real time-PCR analysis of *Cdh5*, *Pecam1* and *Rhox5* in wild type E9.5 whole yolk sac tissues and sorted yolk sac endothelial cells. (B) Real time-PCR analysis of select Notch responsive genes. * p< .05, ** p< .01, *** p< .001 compared to wild type.

Pgf, and *Tgfb2*. The mouse, human, and rat genomic sequences of each of the target genes were aligned and examined for the RBPJ conserved transcription factor binding sites (TFBS) within the evolutionary conserved regions (ECRs) upstream and downstream of the start site. In each of the genes a GTGGGAA consensus sequence was found, indicating a potential RBPJ sites (Figure 3.10). In *Vegfc* locus, an RBPJ binding site is apparent approximately 7.8kb upstream of the start site, while in *Pgf* locus harbors an RBPJ binding site 4.1kb upstream and one at 3.8kb downstream of the transcriptional start site. RBPJ sites were observed at approximately 2.5kb and 5.8kb upstream of the start site of the *Tgfβ2* locus. The putative Notch binding sites in each gene suggests that these genes may be direct targets of Notch signaling.

3.3 Discussion

Numerous studies have indicated critical roles for Notch signaling in the proper formation and maintenance of the early vascular system in the mouse. However, the mechanisms by which Notch signaling regulates such diverse aspects of endothelial differentiation in its various contexts are active areas of research. Our analysis details the morphological and molecular defects associated with altered Notch signaling in vivo, with a focus on the extraembryonic vasculature of the yolk sac. This work has characterized distinct morphological defects in the early embryonic and extraembryonic vasculature associated with loss or gain of Notch activity. Substantial gene expression differences in these models point to putative Notch target genes, and suggest potential mechanisms by which Notch signaling directs endothelial cell differentiation.

Morphological analysis of both EC-N1ICD and EC-Rbpj-KO models confirmed that the regulation of Notch signaling is critical in the formation of the intra- and extraembryonic vasculature of the developing embryo. Detailed examination of the yolk sac vasculature, dorsal aortae, and fetal vasculature of the placenta revealed an enlarged

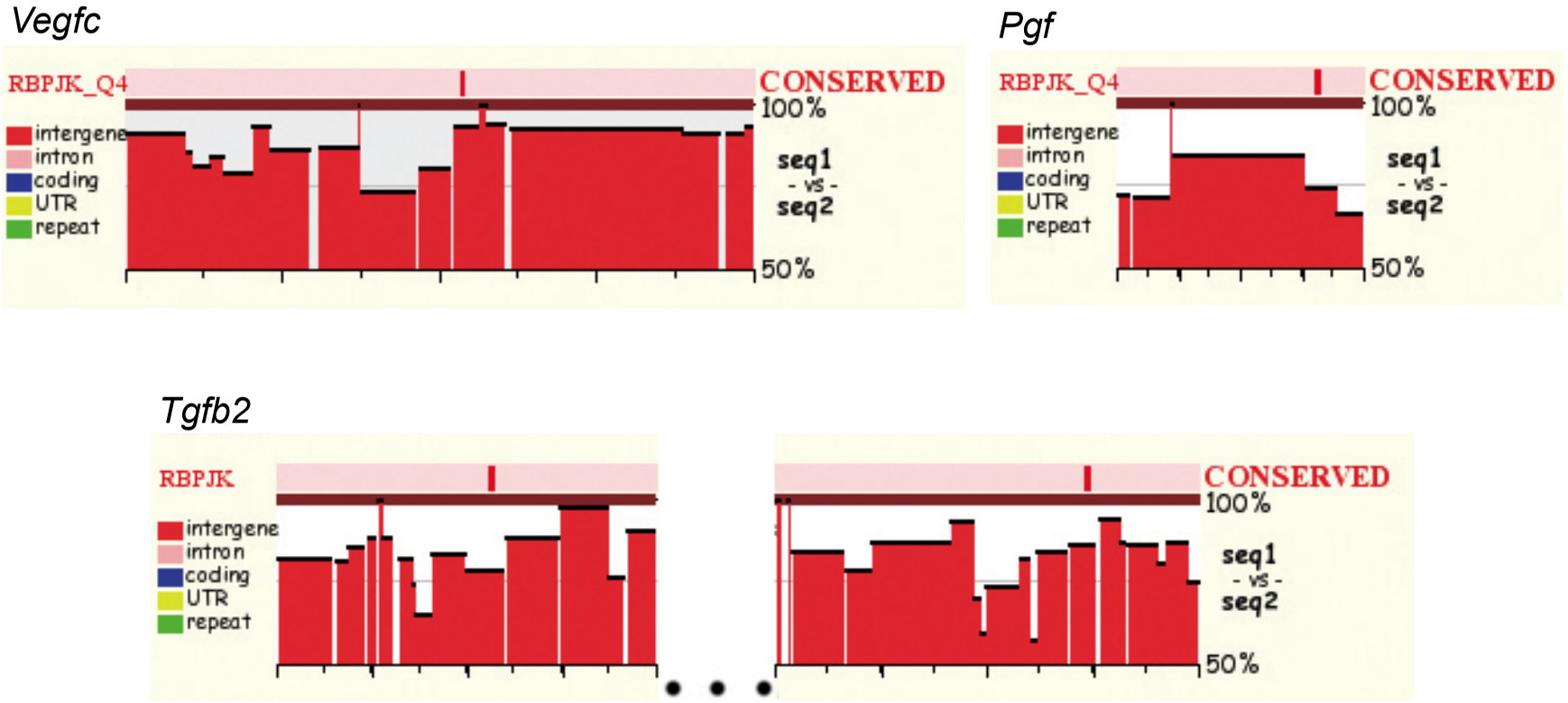

Figure 3.10. rVista Visualization of Conserved RBPJ Binding Sites
Using the ECR browser, the genomic sequence of each of the three secreted genes, *Vegfc*, *Pgf*, and *Tgfβ2* was examined for the RBPJ binding site. The red bars identify the resulting binding sites.

vessel phenotype in the EC-N1ICD, remarkably apparent within the yolk sac, in which the plexus is converted to a mass of large diameter vessels (Figure 3.11A). In contrast, small caliber non-remodeled vessels are present in the EC-Rbpj-KO yolk sac model (Figure 3.11A). Other Notch models have demonstrated malformations in vessel diameter resulting from altered Notch activity, including other models of activated Notch in vivo (Venkatesh et al. 2008; Krebs et al. 2010). *Notch1* deficient mice (Swiatek et al. 1994), mice lacking *Rbpj* in the endothelia, and *Dll4*$^{+/-}$ embryos (Krebs et al. 2004) each exhibit collapsed dorsal aortae and a lack of vascular remodeling. In contrast, embryos overexpressing either *Dll4* (Trindade et al. 2008) or *Notch4* (Uyttendaele et al. 2001) have enlarged dorsal aorta. Data indicated that the enlargement of the dorsal aorta in mice overexpressing *Dll4* was due not to a proliferation of endothelial cells, but to the improper migration of these cells (Krebs et al. 2004). These data point to an important role for Notch signaling to regulate vessel diameter.

The defects in vessel diameter and the remodeling failure in the Notch models used in this study indicate a possible defect in the reallocation of endothelial cells from capillaries into arterioles and suggest that Notch plays a significant role in this migration. The phenotype observed in the EC-N1ICD yolk sac vasculature is possibly due to increased mobilization and disorganized recruitment of capillary-derived endothelial cells, resulting in a field of enlarged vessels. Conversely the failure of the yolk sac remodeling in the EC-Rbpj-KO model is due to the abrogation of endothelial cell migration to form the larger caliber vessels. Live imaging of the behavior of endothelial yolk sac cells in the Notch models used in this study will be required to elaborate this model.

A detailed understanding of the downstream effectors of Notch signaling during vascular differentiation in vivo, particularly within the extraembryonic tissues, has been lacking. The molecular analysis of the Notch models presented here identified a variety

of gene expression defects associated with altered Notch activity. Both the gain- and loss-of- function in vivo models suggest misregulation of a number of genes. Data indicated that two of the Notch family ligands, *Dll4* and *Jag1* were upregulated in EC-N1ICD yolk sac, indicating a possible positive feedback loop for Notch signaling to direct expression of its ligands. There is some precedence for a positive regulatory loop in which Notch regulates the expression of ligands, including *Jag1* in NIH 3T3 cells (Ross and Kadesh 2004) and *Dll1* in glioma cells (Qian et al 2009).

Importantly, the gene expression analysis also identified a number of secreted factors whose expression within the endothelia is altered in the Notch models. These data suggest that the Notch signaling pathway regulates a number of secreted factors important in endothelial differentiation such as, *Pgf*, *Vegfc*, and *Tgfβ2*, either directly or indirectly. Targeted deletions of select TGFβ signaling components in mice result in the improper formation of the yolk sac vasculature, indicating the importance for TGFβ signaling in the formation of the early vascular system (Goumans and Mummery 2000). VEGF signaling has critical early roles in the formation of the blood vessels in the early embryo (Carmeliet et al. 1996; Ferrara and Davis-Smyth 1997). VEGF has also been shown to act as an upstream component of Notch in the signaling cascade directing the differentiation of the zebrafish vasculature (Lawson et al. 2002). PlGF has known roles in pathological angiogenesis (Carmeliet et al. 2001; Oura et al. 2003), and may act as a VEGF agonist by countering the effects of the VEGFA antagonist FLT1. In addition to the essential functions of VEGFC in the developmental origin of the lymphatic system (Karkkainen et al. 2004; Lohela et al. 2009), there is conflicting data to suggest it plays a broader role in angiogenesis. Although this factor has known angiogenic activities in certain assays (Cao et al. 1998), no vascular defects have been reported in mice lacking *Vegfc* (Karkkainen et al. 2004). The expression of VEGFC within the yolk sac however suggests a potential non-lymphatic function for this factor in this tissue. A putative role

for VEGFC in angiogenesis may involve the modulation of its receptors, KDR (VEGFR2) and FLT4 (VEGFR3), both of which play a critical role in early angiogenesis.

Notch signaling is essential for vessel remodeling, as our data shows that Notch regulates the expression of a variety of secreted factors. Notch signaling may play potential nonautonomous roles in the remodeling of the yolk sac capillary plexus (Figure 3.11B). Notch signaling is important for the regulation of select signaling molecules, including members of the VEGF family and TGF-β family, which would emanate from the developing arteriole where activity of Notch signaling is highest. These molecules then act in a paracrine and autocrine manner to elaborate the local arterial microenvironment about Notch expressing cells, which may potentially influence adjacent capillary endothelial cells, smooth muscle or mural cells, and hematopoietic cells. Indeed, nonautonomous functions for Notch signaling in the endothelium have been suggested, including attenuating proliferation of smooth muscle cells (Venkatesh et al. 2008). Testing of the nonautonomous functions of Notch signaling in the vasculature will require determining the roles of Notch-regulated secreted factors in vivo. These experiments may include the use of conditional transgenics and knockouts of these factors in the endothelia, and determining remodeling and endothelial differentiation defects in these models.

The transcriptional network controlled by Notch signaling during extraembryonic endothelial differentiation is largely unknown. The present data demonstrate a role for Notch signaling in the regulation of a number of key genes in the embryonic vasculature of the yolk sac, including a variety of secreted factors important for endothelial differentiation. These downstream targets suggest a mechanism for Notch regulation of vessel diameter size during the remodeling process in the yolk sac vasculature. Further work on the in vivo models will help to further define the relationship between the

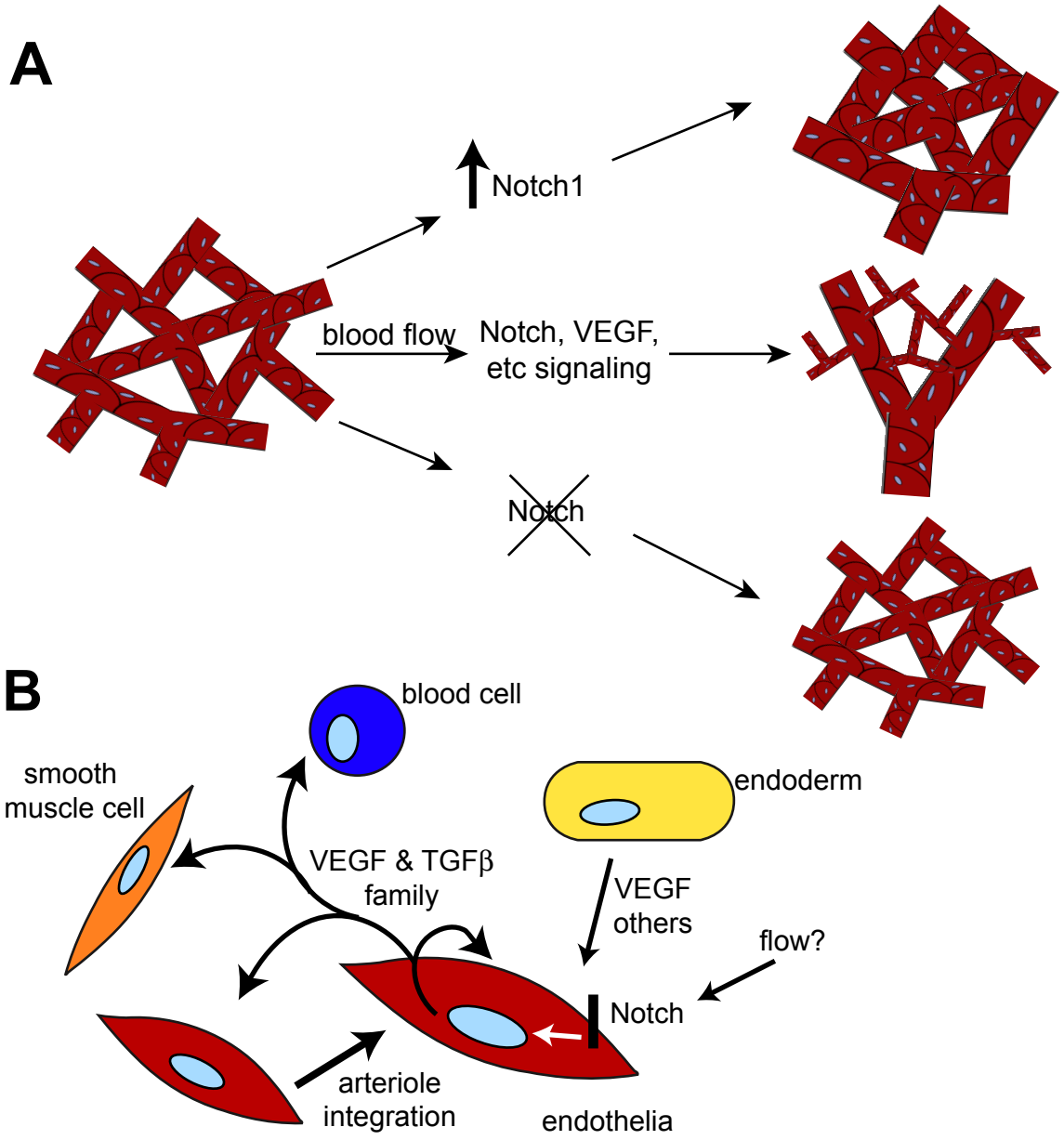

Figure 3.11. Notch Regulates the Expression of Key Genes and the Remodeling of the Yolk Sac Vasculature

(A) Proposed model depicts the Notch pathway as a key component in the regulation of the remodeling of the vasculature. In wild type yolk sac Notch acts in concert with VEGF and other signaling families to direct the integration of the endothelial cells into both large and small caliber vessels. When Notch is activated this integration is increased leading to very large caliber vessels with limited intra-vascular space. When Notch activity is abrogated the integration is limited and the vasculature retains the simple unremodeled appearance of the early vascular plexus. (B) Proposed model of signaling in the endodermal and endothelial cells of the early yolk sac. Signaling from the endoderm and regulation from blood flow activates Notch signaling in select endothelial cells. Notch activates the expression of select secreted genes that act in both a paracrine and juxtacrine manner to direct endothelial cell migration and integration within the developing vasculature.

transcriptional networks regulated by Notch to direct endothelial differentiation, and the role of these Notch downstream targets in endothelial migration and vascular remodeling. The understanding of these interaction and processes will aid in the development of treatments affecting vascular differentiation, including heart disease and tumor progression.

Chapter 4

Development of an embryonic stem cell differentiation model for Notch functions in vascular development

4.1 Introduction

In mouse studies, both loss-of-function and gain-of-function of members of the Notch family lead to abnormalities in the vasculature and embryonic lethality (Swiatek et al. 1994; Krebs et al. 2000; Uyttendaele et al. 2001; Iso et al. 2003; Krebs et al. 2010). These and other data indicate a definite role for Notch signaling in the control of endothelial differentiation in the early embryo. However, the downstream targets of this signaling systems and its interaction with other signaling families important for vascular remodeling remain largely undefined, particularly during early embryogenesis. Previous work to define Notch downstream targets in cell culture models have identified VEGFR-3 as a direct target of Notch in 3 human primary endothelial cell lines (Shawber et al. 2007) and the induced expression of both VEGFR-1 transcripts and protein as a result of Notch activation (Funahashi et al. 2010). Much work remains to establish the correct sequence of the signaling cascades involved in vascular differentiation.

Mouse embryonic stem (ES) cells are derived from the inner cell mass (ICM) of E3.5 pre-implantation embryos. ES cells are pluripotent, capable of dividing and remaining in an undifferentiated state for long periods of time, and can be induced to differentiate into specialized cells. Mouse ES cells are amenable to extensive gene targeting, allowing for the development of numerous mutant mouse models (Niwa 2010). Human and mouse ES cell models have been used to study both Notch signaling and

endothelial differentiation in both in vivo and in vitro studies. ES cell culture systems are a useful tool to study the morphological and molecular mechanisms behind ES cell differentiation. ES cells are able to maintain pluripotency in cell culture studies and with modified culture conditions or genetic manipulation can be induced to differentiate into numerous cells types including neuronal, cardiac, and epithelial (Niwa 2007). Because mouse ES cell culture models mimic the pre- and post-implantation development of embryonic cells lineages, they are useful in recapitulating in vivo differentiation and for the study of the molecular mechanisms that underlie these processes.

ES cell differentiation models have proven to be useful tools to understand endothelial differentiation, leveraging the capacity for genetic manipulation of the ES cell model, among other advantages (McCloskey et al. 2006; Ryolva et al. 2008). Endothelial cells (ECs) can be derived through in vitro differentiation of ES cells via a variety of methods. Firstly, via the aggregation of ES cells into embryoid bodies (EBs) by hanging drop culture that are then attached to a substratum resulting in a primitive vascular plexus similar to that seen in the early mouse yolk sac (Ryolva et al. 2008). Secondly, mouse ES cells can be co-cultured with a layer of OP9 stromal cells in defined media that facilitates endothelial and hematopoietic differentiation. This process limits the environment to two cell types instead of the multilineage composition of the EBs. And thirdly, mouse ES cells can be plated on an acellular matrix and supplemented with defined media to promote ES cell growth and differentiation, completely limiting the influence from other cell types (Noghero et al. 2010). The ability to analyze genetic manipulation in the ES cell-derived ECs is proving to be an important tool. These ECs express many of the same markers as in vivo and mimic mutant phenotypes seen in vivo. Previous work has

utilized this model system to investigate the role of Flt-1 isoforms in vessel formation (Kappas et al. 2008).

In this study mouse ES cells were used to study the Notch signaling pathway in vitro. A tetracycline-inducible Notch1-ICD transgenic ES cell line was generated to activate Notch signaling, while a gamma secretase inhibitor was used for the inhibition of Notch signaling. Molecular analysis of the ES cell lines showed altered gene expression of a limited subset of Notch target genes similar to that seen in the in vivo models. These results help to expand the molecular hierarchy of Notch signaling in the endothelia, however modifications to the system need to be made to recapitulate results seen in the in vivo systems analyzed and discussed in chapters 3 and 5 to fully understand the role of Notch signaling.

4.2 Results

4.2.1 Design and generation of Ainv15-N1-ICD ES cells

To further understand the role of Notch signaling during endothelial differentiation, a tetracycline-inducible Notch1-ICD transgenic ES cell line (Ainv15-N1-ICD) was generated. The ploxN1-ICD vector was made by digesting the EGFP gene, which acts as a stuffer fragment in PGK-lox-neoEGFP (Kyba et al. 2002), with XbaI and XhoI and inserting the XbaI-SalI Notch1-ICD fragment from pBS mNotchIC (Murtaugh et al, 2003) to generate ploxNotchICD. A cell line, Ainv15 (Kyba et al. 2002), which consists of the reverse tetracycline transactivator (rtTA) targeted to the *Rosa26* locus, and a doxycycline-inducible locus targeted to the *Hprt* locus, was targeted with PALP-NotchICD and pSALK-Cre by co-electroporation (Figure 4.1A).

The resulting ES cell line, Ainv15-N1-ICD, was genotyped to confirm proper Cre-mediated integration. The genotyping confirmed single-copy integration of the N1-ICD cassette into the dox-inducible locus. The cell line displayed sensitivity to induction via dox-supplemented media compared to control (untreated cells). The cell line exhibited the expression of the Notch1-ICD in both a time and concentration dependent manner with expression 80-fold higher with a 1.0μg/mL dox concentration (Figure 4.1B-C).

Importantly, the upregulation of select target genes after dox treatment was seen via semi-quantitative RT-PCR, indicating that the Ainv15-N1-ICD ES cells mimic the in vivo transgenic models (Figure 4.2). A whole genome microarray was performed to examine the gene defects imposed by the addition of dox, and subsequent activation of Notch signaling, in greater detail. RNA isolated from Ainv15-N1-ICD ES cells treated with dox for 0hrs and 20hrs was compared. Some Notch responsive genes, such as *Hes5* and *Nrarp*, showed greatly increased expression in dox treated Ainv15-N1-ICD cells, while others, including *Hey1*, *Heyl*, and *Pgf*, were either unchanged or not expressed (Table 4.1). As undifferentiated ES cells, the Ainv15-N1-ICD construct is responding to treatment as expected and appears to upregulate some Notch target genes identified in EC-N1ICD embryos.

A gamma secretase inhibitor (GSI), which inhibits the cleavage of the Notch-ICD, was also employed to inhibit Notch signaling in the ES cells. During Notch signaling, the Notch receptor is processed in three separate events. The final event, following ligand binding is cleavage of the receptor within the transmembrane domain by a γ-secretase-like protease, through to be the Presenilins, which releases the Notch-ICD. The Notch-

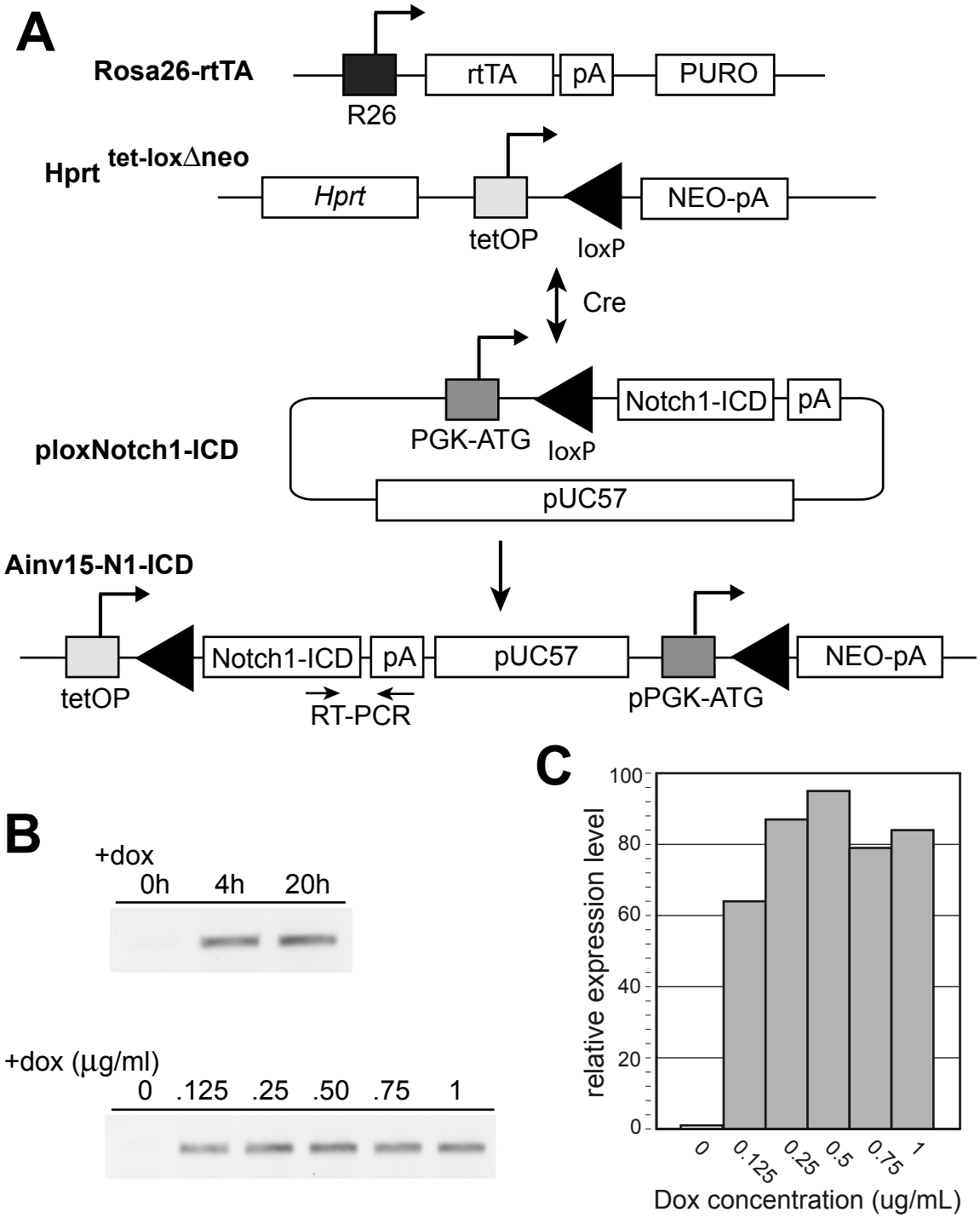

Figure 4.1. Generation of an Ainv15-N1-ICD ES Cell Line Specifying an Inducible Notch1-ICD Transgene

(A) Schematic representation of integrated expression cassettes. Co-electroporation and Cre-mediated recombination of the targeting vectors allows for the isolation of transgenic cells. The primers used for RT-PCR are indicated. (B) RT-PCR of an Ainv15-N1-ICD ES cell clone induced with doxycycline for 0, 4, and 20 hours and at different concentrations. The clones showed a strong induction of the N1-ICD at all time points and concentrations. (C) Quantitated relative mRNA levels of the concentration gradient.

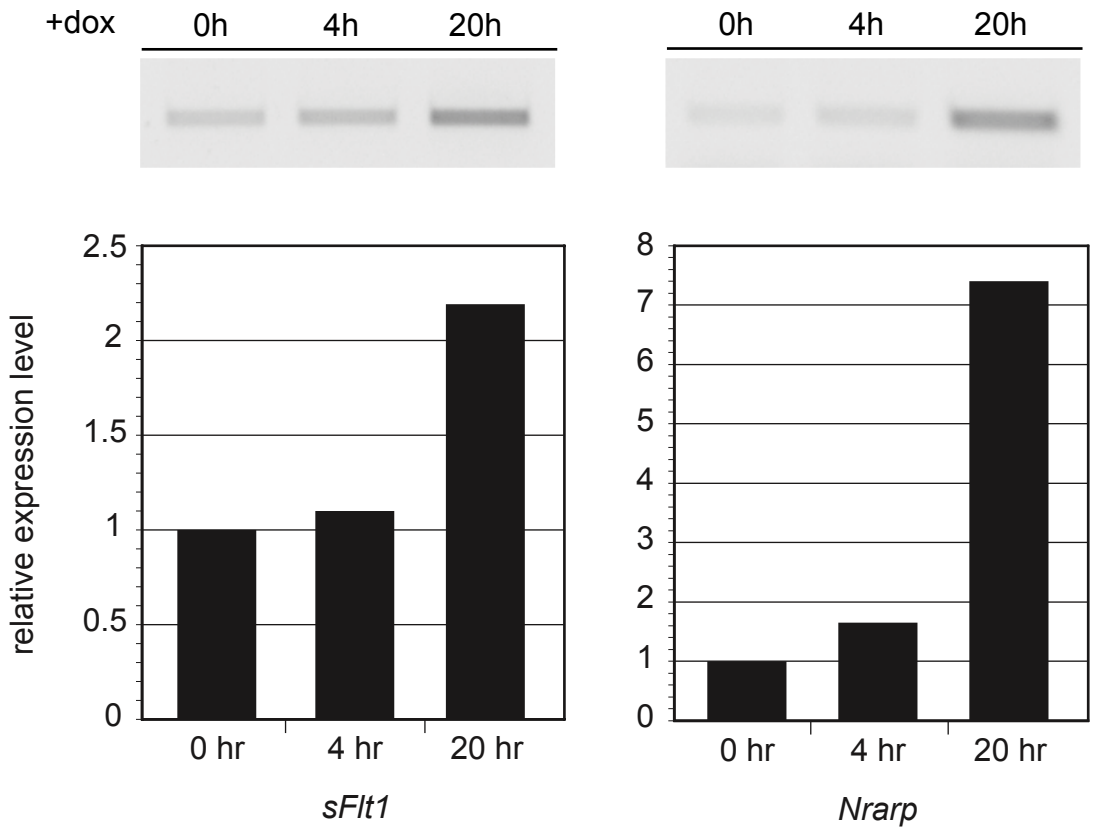

Figure 4.2. Expression Analysis of undifferentiated Ainv15-N1-ICD ES Cells after Doxycycline Treatment

RNA was isolated from Ainv15-N1-ICD ES cells treated with dox for 0, 4, and 20 hours and RT-PCR was performed to analyze the expression of select markers. The upregulation of *sFlt1* and *Nrarp* at 20 hours is similar to that seen in EC-N1ICD yolk sac.

Table 4.1. Expression Analysis of Select Genes as Analyzed by Microarray in Undifferentiated Ainv15-N1-ICD ES Cells in Response to Dox Treatment

Gene Name	Symbol	Synonyms	Fold Change
hairy and enhancer of split 5 (Drosophila)	*Hes5*	bHLHb38	22.84
Notch-regulated ankyrin repeat protein	*Nrarp*		5.09
Left-right determination factor 2	*Lefty2*	Ebaf, Leftb	3.97
soluble FMS-like tyrosine kinase 1	*sFlt1*	VEGFR1	2.35
hairy/enhancer-of-split related with YRPW motif 1	*Hey1*	Herp2, Hesr1, HRT1	1.30
hairy/enhancer-of-split related with YRPW motif-like	*Heyl*	Hesr3, Hey3, Hrt3	Not expressed
cadherin 5	*Cdh5*	CD144, VE-cadherin	Not expressed
kinase insert domain protein receptor	*Kdr*	Flk1, VEGFR2	Not expressed
CD34 antigen	*CD34*		Not expressed
delta-like 4 (Drosophila)	*Dll4*	Delta 4	Not expressed
placental growth factor	*Pgf*	PLGF	-1.06
vascular endothelial growth factor C	*Vegfc*		-1.14
lymphoid enhancer binding factor 1	*Lef1*		-4.55

ICD translocates to the nucleus where it activates transcription of target genes. By employing a GSI, this cleavage step is inhibited abrogating the translocation of the NICD and the activation of downstream targets.

4.2.2 Endothelial cells differentiated from Ainv15-N1-ICD ES cells

Two protocols were established to generate endothelial cells from differentiating ES cells (Figure 4.3). Both procedures generated endothelial cells from Ainv15-N1-ICD ES cells through the aggregation of the ES cells to form embryoid bodies (EBs) via hanging drops, in media lacking LIF and supplemented with a serum lot that enhances differentiation (EC media). Real-time PCR of RNA isolated from EBs after four days of growth and from undifferentiated ES cells was performed to analyze the gene expression of select ES and endothelial cell markers (Figure 4.4A). The decreased expression of ES cell markers (*Oct4* and *Nanog*) and the increased expression of endothelial markers (*Flk1* and *Cdh5*) indicates that cells within the EBs were trending toward an endothelial-like cell state. The low expression of the endothelial marker *CD34* indicates that they are more likely an early angioblast-like cell type.

To differentiate the EBs to endothelial cells, after four days, EBs were collected and plated on a collagen Type IV-coated plate. The growth factors VEGF and FGF2 were added to the media (ECVF media) to promote endothelial cell differentiation for 4-6 days. Marker analysis over the course of this procedure demonstrated substantial endothelial differentiation that in many ways recapitulates embryonic development. The decreased expression of *Flk1* and the increase of *CD34* and *Dll4* in the differentiated cells compared to ES cells and EBs indicates the plated cells have differentiated into an

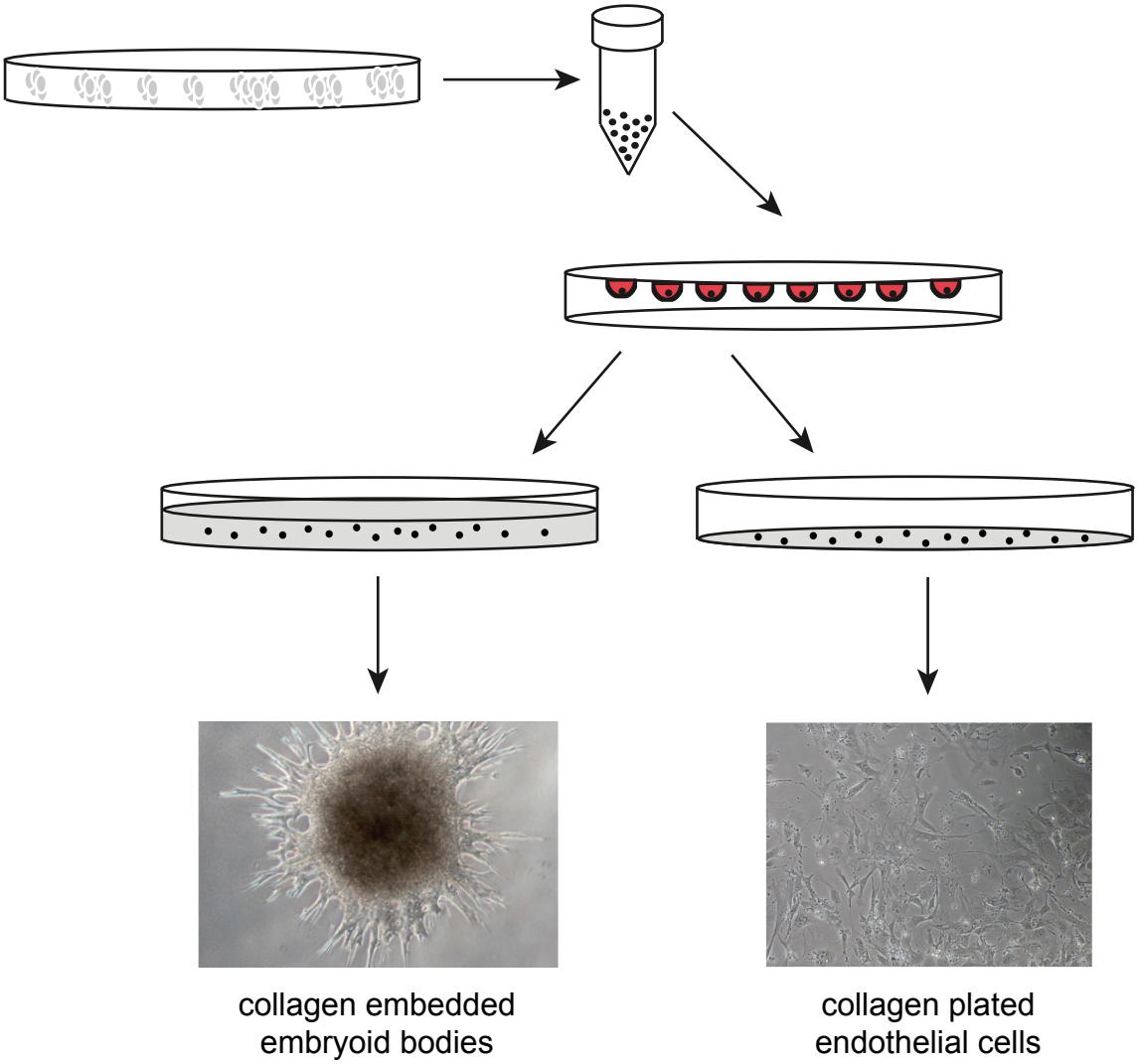

Figure 4.3. Schematic of the Differentiation Process of Ainv15-N1-ICD ES Cells into Endothelial Cells

Ainv15-N1-ICD cells are grown feeder free for two passages. Embryoid bodies (EBs) are created by allowing cells to aggregate via the hanging drop method in media supplemented with serum specified for endothelial cells (EC media). After growing for four days, the EBs are collected and plated on a collagen coated plate or they are embedded into collagen. The growth factors VEGF and FGF2 are added to the media at this stage to promote endothelial cell differentiation. Cells embedded on collagen are allowed to differentiate to obtain an endothelial-like cell population.

endothelial-like cell (Figure 4.4B). Fluorescence imaging of the collagen-plated EBs indicates a number of cells that express the endothelial cell marker *CD34* (Figures 4.4C).

A whole genome microarray was performed to examine the differences in gene expression in the differentiated endothelial cells in greater detail. RNA isolated from undifferentiated Ainv15-N1-ICD ES cells and collagen-plated EBs was compared. Endothelial markers, such as *CD34*, *Flk1*, and *Cdh5* exhibited greatly increased expression in the differentiated ES cells, while the ES cell markers *Nanog* and *Dppa3* were decreased (Table 4.2). This demonstrates that the ES cells were differentiated to a variety of cell types, including an endothelial-like cell type. These data indicate that with the addition of a specialized and supplemented media, endothelial-like cells can be generated and purified from differentiated mouse ES cells.

4.2.3 Gene regulation in differentiated Ainv15-N1-ICD ES cells

Gene expression analysis of the in vivo EC-N1ICD transgenic model has identified a set of genes with upregulated expression as a result of activated Notch signaling, most interestingly the secreted factors *Vegfc*, *Tgfb2*, and *Pgf*. To test the hypothesis that genes regulated in the endothelia by Notch in vivo are also regulated by Notch in the differentiated Ainv15-N1-NICD cell line, collagen plated EBs were allowed to differentiate in ECVF media alone, ECVF +dox to activate Notch, or with ECVF +GSI to inhibit Notch signaling for 5 days. RNA was isolated, in triplicate, from the cells and gene expression levels were examined in the cells by real-time PCR. A few genes, including *Heyl and Hey1* mimic the regulation seen in vivo, with an upregulation of the gene in response to dox treatment and a downregulation in response to GSI (Figure 4.5,

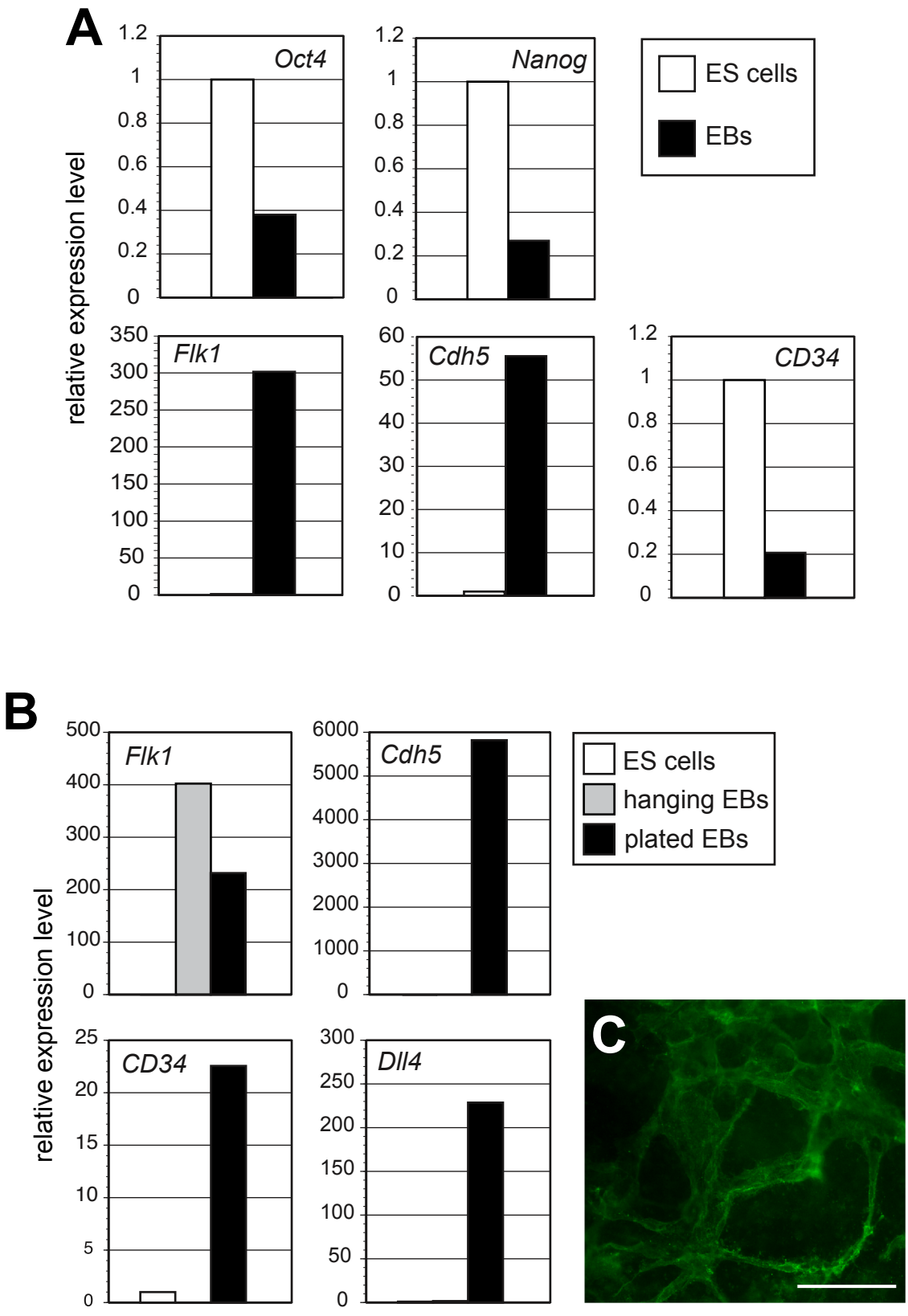
A
relative expression level
Oct4
Nanog
Flk1
Cdh5
CD34
ES cells
EBs
B
relative expression level
Flk1
Cdh5
CD34
Dll4
ES cells
hanging EBs
plated EBs
C

Figure 4.4. Expression Analysis of Ainv15-N1-ICD Embryoid Bodies and Differentiated Cells

(A) RNA was isolated from embyroid bodies formed from Ainv15-N1-ICD ES cells grown in hanging drops in EC media for four days. *Oct4* and *Nanog* expression levels were decreased indicating that the embryoid bodies were losing the ES cell genotype. The upregulation of *Flk1* and *Cdh5* and the low expression of *CD34* indicated that the embryoid bodies were tending toward an early angioblast-like cell type. (B) Ainv15-N1-ICD ES cells were aggregated into EBs in hanging drops. EBs were then collected and plated on collagen coated plates. Plated EBs were grown in ECVF media and allowed to differentiate for 5 days. RNA was isolated and real-time PCR was performed to analyze the expression of select endothelial markers in differentiated cells compared to ES cells and EBs in hanging drops. The increased expression of *CD34* and *Dll4* indicated the cells were trending toward a more endothelial-like cell type. (C) Fluorescence image of differentiated Ainv15-N1-ICD ES cells stained with an antibody to the endothelial marker *CD34*. Scale bars are 100μm (C).

Table 4.2. Expression Analysis of Select Endothelial Genes as Analyzed by Microarry in Differentiated Ainv15-N1-ICD Cells Compared to Undifferentiated ES cells

Gene Name	Symbol	Synonyms	Fold Change
CD34 antigen	*CD34*		16.20
kinase insert domain protein receptor	*Kdr*	Flk1, VEGFR2	8.90
cadherin 5	*Cdh5*	CD144, VE-cadherin	6.72
delta-like 4 (Drosophila)	*Dll4*	Delta 4	4.23
vascular endothelial growth factor C	*Vegfc*		3.96
hairy/enhancer-of-split related with YRPW motif-like	*Heyl*	Hesr3, Hey3, Hrt3	2.54
soluble FMS-like tyrosine kinase 1	*sFlt1*	VEGFR1	2.38
placental growth factor	*Pgf*	PLGF	2.28
hairy/enhancer-of-split related with YRPW motif 1	*Hey1*	Herp2, Hesr1, HRT1	2.25
Notch-regulated ankyrin repeat protein	*Nrarp*		1.84
hairy and enhancer of split 5 (Drosophila)	*Hes5*	bHLHb38	-1.11
developmental pluripotency-associated 3	*Dppa3*	PGC7, Stella	-3.22
SRY-box containing gene 2	*Sox2*	Icc, ysb	-9.09
left-right determination factor 2	*Lefty 2*	Ebaf, Leftb	-10.10
nanog homeobox	*Nanog*	ecat4, ENK	-15.87

top row). Other genes, including *Dll4*, *Pgf*, and *Vegfc*, do not appear to be regulated by Notch in vitro the same manner they were in vivo (Figure 4.5, bottom row). These data indicate that while endothelial cells can be generated from differentiated mouse ES cells with the addition of a specialized and supplemented media, gene expression of the differentiated cells shows that only a limited number of genes exhibit a similar regulation in vitro as they do in vivo, while many others do not.

4.2.4 Collagen embedded embryoid bodies mimic sprouting angiogenesis

Notch signaling has been shown to play an important role in the process of sprouting angiogenesis. Endothelial cells sprout from existing vessels in response to VEGF signaling. The leading, or tip, cell receives the signal from VEGF-A which activates the expression of *Dll4*. This in turn signals through the Notch receptor in the base, or stalk, cell, which downregulates the expression of VEGF receptors. Thus the tip cell is free to migrate in search of other sprouts while the stalk cell remains tethered to the pre-existing vessel (Siekmann et al. 2008). In addition to plating on collagen, EBs picked from hanging drops after four days were embedded into a 3D microenvironment of collagen Type IV, suspending the EBs, and facilitating the formation of sprouts from the pre-existing vascular bed (Noghero et al. 2010).

To study this process, embedded EBs were grown for 6 days in the presence of ECVF media. A time course of embryoid body growth showed that the EBs quickly grew greatly in both size and in number of sprouts (Figure 4.6A). Immunochemistry with an antibody to PECAM of an embedded EB at day 5 showed that many of the cells

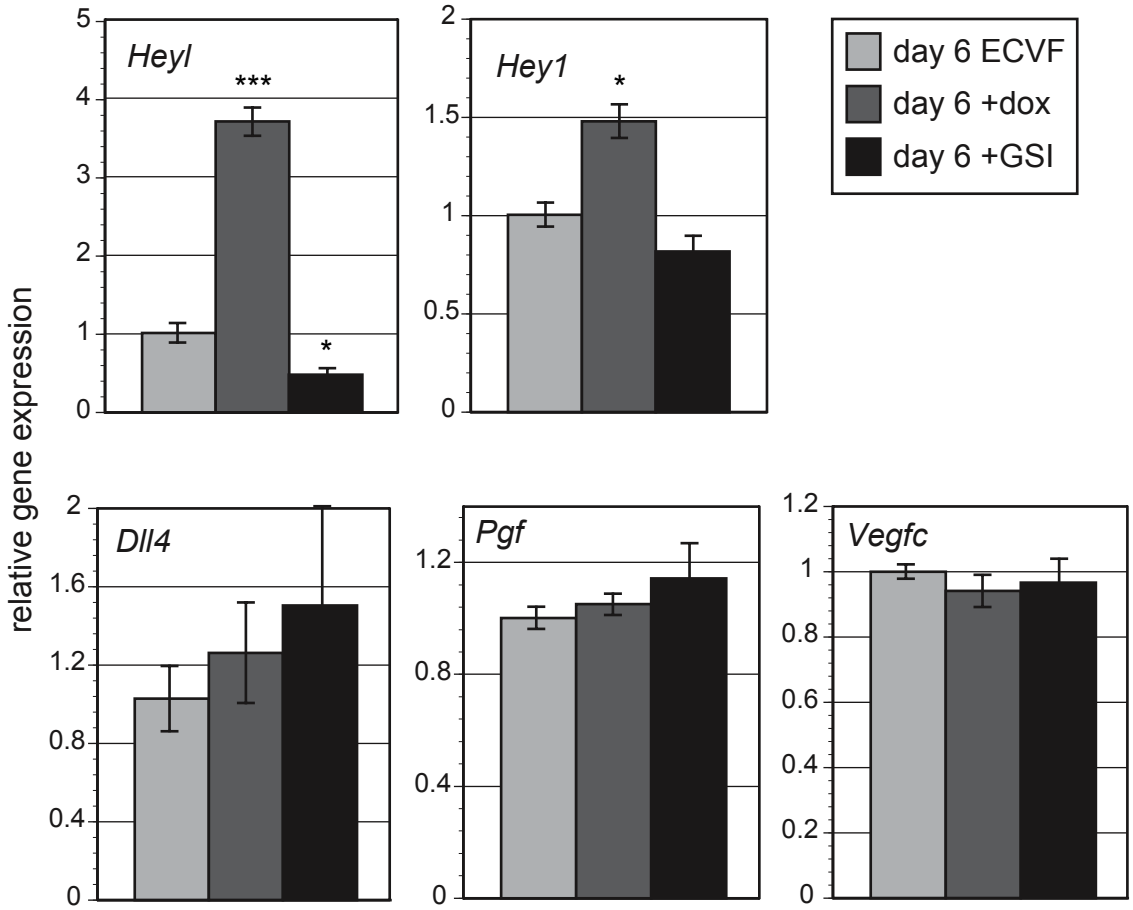

Figure 4.5. Expression Analysis of Select Genes in Differentiated Ainv15-N1-ICD ES Cells as Analyzed by Real-time PCR

Collagen plated EBs were allowed to differentiate for 5 days in ECVF media supplemented with dox to activate Notch signaling or with GSI to inhibit Notch signaling. Gene expression levels were examined in the cells by real-time PCR. * $p < .05$, *** $p < .001$.

associated with the sprouts were early endothelial cells (Figure 4.6B). At day 6, CD34 immunofluorescence indicated that the sprouts consisted of mature endothelial cells, primarily at the base of the sprout. Cells at the tip of the sprout were likely an earlier endothelial-like cell type (Figure 4.6C-D). To examine the effects of Notch signaling on the endothelial sprouts, EBs embedded in collagen were allowed to grow for 6 days in collagen supplemented with either ECVF media, ECVF + Dox, or ECVF +GSI. Based on previous data documenting the role of Notch signaling in the formation of sprouts, a decrease in migrating tip cells was expected with activated Notch signaling and an increase in the number of sprouts was expected with Notch inhibition. These EBs were isolated and visualized by staining with an antibody to CD34. The endothelial outgrowth of the EBs formed a vascular plexus similar to that seen in the early embryo, however the treated EBs did not mimic results seen in the in vivo Notch gain and loss of function. Neither addition of Dox to activate Notch signaling, or GSI to inhibit Notch signaling had any visible effects on the formation of the endothelial sprouts (Figures 4.6E-G).

As with the plated EBs, the in vitro model system of embedding the EBs in collagen will help to further understand the formation of the early vascular system and the process of sprouting angiogenesis. However, like the plated EBs, the embedded EBs, do not exactly mimic the results seen in either of the models presented in Chapter 3 or in previously reported studies.

4.3 Discussion

Notch signaling has been studied extensively both in vitro and in vivo and has been shown to play an important role in the formation of the early vascular system.

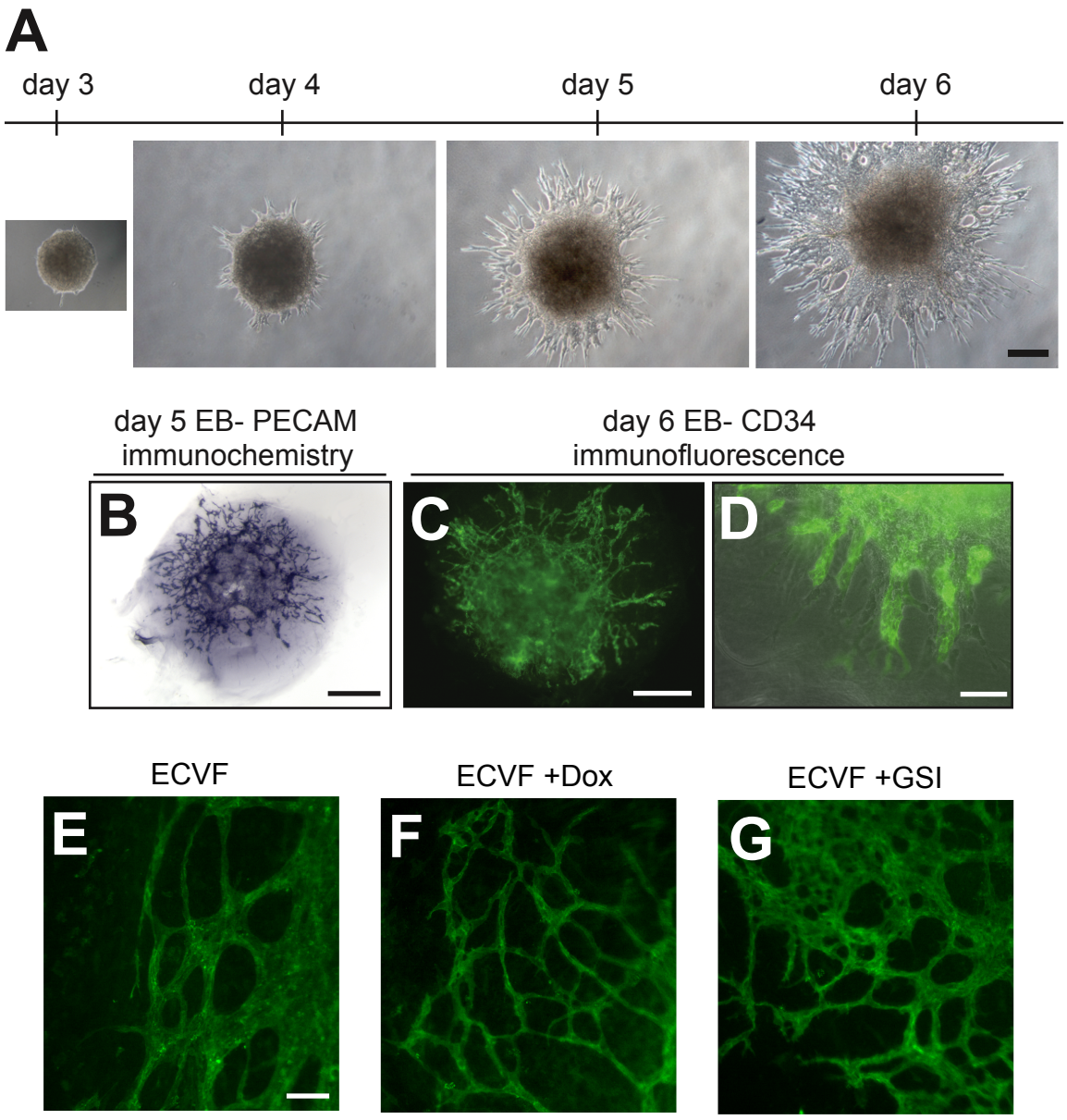

Figure 4.6. Collagen Embedded EBs Mimic Sprouting Angiogenesis but are Unresponsive to Treatment

(A) Time course of embryoid body growth shows that the EBs quickly grew greatly in both size and number of sprouts. (B-D) At day 5, an immunochemical PECAM stain was done that showed that many of the cells associated with the sprouts were early endothelial cells (B). At day 6, an immunofluorescence stain was done which showed that the sprouts are endothelial cells (C-D). The fluorescent and light overlap image showed that the endothelial cells were matured near the base of the sprout and were either an earlier endothelial-like cell or a different cell type at the tip (D). (E-G) Fluorescence image of collagen embedded EBs stained with an antibody to the endothelial marker CD34. EBs were grown in ECVF alone (E), ECVF supplemented with doxycycline (dox) (F), or ECVF supplemented with gamma secretase inhibitors (GSI) (G). Scale bars are 500 µm (A-C), 100 µm (D-G).

Previous work in our lab has demonstrated that both the gain and loss of function of Notch signaling in vivo result in vascular differentiation and gene expression defects. Gene expression analysis of the in vivo transgenic model has identified a set of genes with upregulated expression as a result of activated Notch signaling, most interestingly the secreted factors *Vegfc*, *Tgfβ2*, and *Pgf*. Our analysis employed an in vitro ES cell model system to examine whether or not the results seen in vivo were replicated in vitro and to further determine the mechanisms of Notch regulated gene expression in vascular endothelial cells. Although some important similarities were noted, the in vitro ES cell systems of altered Notch signaling used here did not completely mimic the in vivo results. Steps will need to be taken to modify the ES cells system to better reproduce an in vivo like environment.

ES cell differentiation models have proven to be useful tools to understand endothelial differentiation (McCloskey et al. 2006; Hermant et al. 2007; Ryolva et al. 2008). The differentiated ES cells in our model, and in others, expressed endothelial markers seen in vivo, including CD31, CD34, PECAM, and VE-cadherin, (McCloskey et al. 2006; Ryolva et al. 2008) indicating the cells are differentiating from an ES cell to an endothelial-like cell population. In depth studies comparing ES cell derived endothelial cells to mature mouse aortic endothelial cells (MAEC) showed that while the in vitro differentiated cells express endothelial markers they are not as mature as the MAEC (McCloskey et al. 2006). This finding may, in part, explain the differences between the in vivo and in vitro Notch models.

Previous work analyzing genetic manipulations has shown that differentiated *Flt1*$^{-/-}$ mutant ES cells (Kearney et al. 2004) and differentiated ES cells lacking one or

both VEGF-A alleles (Bautch et al. 2000) display morphological defects similar to those seen in their in vivo counterparts. Although Notch regulation has been examined in human endothelial cell lines (Shawber et al. 2007; Funahashi et al. 2010), little has been done using mouse endothelial cells in vitro. Additionally, an extensive genetic analysis of any transgenic differentiated ES cell models has yet to be done. Our work focused on both the morphological and molecular analysis of a gain and loss of function Notch transgenic ES cell differentiation model.

The molecular analysis of differentiated ES cells in our studies indicated that some genes are regulated by Notch signaling in a similar manner as in vivo, including *Hey1* and *Heyl*; other genes, including *Vegfc*, *Tgfb2*, and *Pgf* were not. The differences in Notch targets between the in vivo, ES cell differentiation, and the primary endothelial cell models suggest complex, highly regulated, and context-dependent functions for Notch signaling in endothelial differentiation. Importantly, morphological analysis of the collagen embedded EBs showed that vessel diameter defects were not observed in the altered Notch signaling model, in striking contrast to the in vivo results. The vascular plexus formed from the differentiating embedded EBs was unaffected by the addition of either dox or GSI. Modifications will have to be made to this system as well in order to fully understand these processes.

Modifications of the differentiation protocol may help elaborate the basis of these differences. In the in vitro ES cell protocols used, the EBs and differentiated endothelial cells were grown in or on collagen in media supplemented with growth factors. In vivo, endothelial cells neighbor, and are influenced by, primitive endoderm and are acted upon by the shear stress of blood flow. If a protocol was designed in which the EBs were

grown with endodermal cells and something to reproduce blood flow, this model system might better mimic the in vivo results. Because the EBs from which the ECs differentiate consist of many different lineages, purification of the ECs with an endothelial cell specific antibody via flow cytometry would also allow for a cleaner analysis of the gene expression differences within the EC lineage.

As for the collagen embedded protocol to study sprouting angiogenesis, a recent study also examining the role of Notch signaling in sprouting angiogenesis did result in increased sprouting with the addition of the gamma-secretase inhibitor, DAPT. In this model the EBs were grown and embedded following a protocol similar to ours, the only differences were in the length of time the embedded EBs were grown and the concentration of the γ-secretase inhibitor (Jakobsson et al. 2010). Simple modifications such as these could be implemented in our model to better replicate previous results seen in vitro and in vivo.

The ES cell differentiation model will prove to be useful for certain studies for which the early embryo is not amenable, including epigenetic changes associated with Notch activity. It is currently unknown whether the affected genes in the in vivo Notch models are direct targets of Notch signaling through RBPJk. Chromatin Immunoprecipitation (ChIP) and luciferase assays could be utilized in the ES cell differentiation model to find genes that are directly regulated by Notch signaling through RBPJ and the chromatin changes associated with Notch activity.

This in vitro model system, developed in our lab, is a useful tool for the differentiation of endothelial cells from ES cells. It will aid in the determination of the mechanisms of Notch regulated gene expression in vascular endothelial cells in at least a

subset of the Notch regulated genes observed in vivo. However, modifications to the system need to be made in order to utilize the in vitro model as a companion to the in vivo Notch models. With further modification to the system and additional assays this model system will further define the role of Notch in the formation of the vascular system, specifically the differentiation and migration of the early endothelial cells, and the relationship between the various signaling families important for vascular differentiation. These findings will advance treatments for vascular abnormalities, including heart disease and cancer.

Chapter 5

Overexpression of placental growth factor in the early embryo disrupts vascular differentiation

5.1 Introduction

The processes involved in the formation of the early vasculature are tightly regulated by a number of signaling cascades, including the angiopoietin/Tie receptor pathway, the Notch pathway, the transforming growth factor-β (TGF-β) pathway, and the vascular endothelial growth factor (VEGF) pathway, among others (Carmeliet 2000; Dumont et al. 1994; Krebs et al. 2000; Suri et al. 1996; Tallquist et al. 1999; Yancopoulos et al. 2000). VEGF has been shown to be an endothelial cell-specific mitogen, an inducer of angiogenesis, and a mediator of vascular permeability (Park et al. 1994). The VEGF family includes VEGF-A (VEGF), VEGF-B, VEGF-C, VEGF-D, and placental growth factor (PlGF). VEGF binds to two transmembrane receptor tyrosine kinases, FLT1 (VEGFR-1) (Shibuya et al. 1990) and KDR (VEGFR-2, FLK1) (Quinn et al. 1993), both of which are expressed in the endothelia of the developing vessels. FLT1 also exists as a truncated, soluble form containing only the extracellular region (Kendall and Thomas 1993). Although VEGF binds with higher affinity to FLT1, the angiogenic signal is thought to result from the binding of VEGF-A to KDR (Neufeld et al. 1999; Tjwa et al. 2003).

The VEGF family homolog, PlGF, is also believed to be an inducer of angiogenesis. PlGF binds with high affinity to FLT1 (Park et al. 1994). PlGF is thought to stimulate vascular formation in two ways, by signaling through FLT1 (Neufeld et al.

1999) or by acting as a 'decoy'; limiting VEGF-A binding to FLT1 thereby increasing the amount of VEGF-A available to activate KDR (Park et al. 1994). Previous work has revealed a significant increase in the expression of *Pgf* in the yolk sac of embryos with an activated Notch1 intracellular domain (N1ICD) in the endothelia compared to wild type (Copeland et al. 2011). Although PlGF has been shown to play a role in pathological angiogenesis in the adult (Carmeliet et al. 2001; Lutton et al. 2002 Odorisio et al. 2002; Oura et al. 2003), there has been little analysis of PlGF expression and activity in the early embryo. It is still unclear what the role of PlGF is in the signaling pathways controlling vascular differentiation in the embryo, specifically how it interacts with the Notch pathway and what downstream genes PlGF affects to initiate cell specification.

To better understand the activity of PlGF in the formation and remodeling of the early vascular system, a gain-of-function conditional PlGF transgenic mouse model was generated, and detailed morphological and molecular analyses were performed. Embryos with activated *Pgf* in the endothelia displayed two distinct phenotypes, which have been classified moderate and severe. Moderate embryos exhibited growth and cardiovascular defects, improper remodeling of the yolk sac, increased expression of key genes important in vascular differentiation, and subsequent embryonic lethality. Severe embryos had extensive morphological defects and an even greater increase in gene expression than the moderate embryos. Molecular analysis of the yolk sacs of moderate embryos indicated increased expression in Notch family members. Our data provides an in-depth analysis of PlGF signaling in the early embryo, its effects on vascular differentiation and the relative importance of *Pgf* overexpression in the activated N1ICD embryos. Taken together the upregulation of *Pgf* expression by Notch signaling

(Copeland et al. 2011) and the subsequent upregulation of both Notch ligands and receptors by PlGF, indicates a possible feedback loop between the Notch and VEGF pathways in the regulation of vascular remodeling in the early embryo.

5.2 Results

5.2.1 Design and generation of a transgene to conditionally modulate the expression of placental growth factor in the endothelia

To expand expression of *Pgf*, a conditional transgene was generated. Initially the Z/EG expression vector (Novak et al. 2000) was modified via the addition of AscI and PacI restriction sites between the BglII and XhoI sites of the Z/EG vector. Using TOPO cloning an AscI site was added to the 5' end and a PacI site to the 3' end of the *Pgf* CDS. The Z/EG-Pgf construct was made by digesting the Z/EG vector with AscI and PacI and inserting the AscI-PacI *Pgf* CDS fragment. The resulting vector was linearized with the StuI and ScaI restriction enzymes. The resulting Z/EG-Pgf transgene contained a β-geo cassette flanked by *loxP* sites under the control of the β-actin promoter, followed by the *Pgf* cDNA and an EGFP cassette. Removal of the β-geo cassette and 3 polyA sequences through *loxP*-mediated recombination, via a CRE expressing transgene, results in the expression of *Pgf* and EGFP (Figure 5.1). The transgene was introduced into E14 embryonic stem (ES) cells (in the 129P2 genetic background) via electroporation and clones that carried the transgene were selected through G418 resistance. The G418-resistant clones were screened for a high level of *lacZ* expression conferred by the β−geo fusion gene. Additionally the clones were lysed for DNA and analyzed via PCR for the expression of the transgene. As a final test, four clones displaying high levels of *lacZ* and

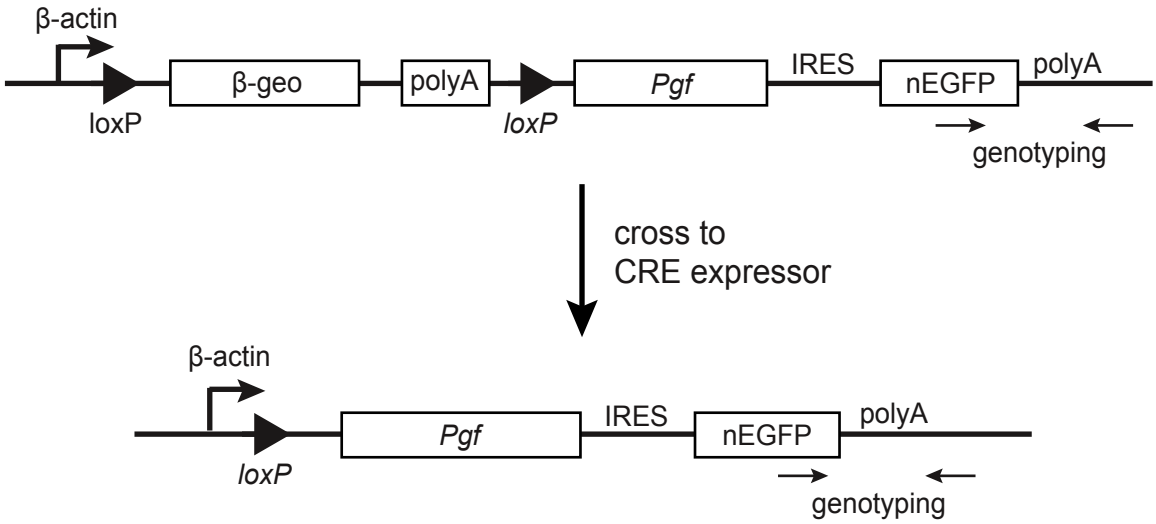

Figure 5.1. Conditional Mouse Z/EG-Pgf Transgene Construct
The Z/EG-Pgf construct conists of a β-actin promoter directing expression of the *loxP*-flanked β-geo cassette and 3 polyA sequences which is upstream of the *Pgf* coding sequence, an EGFP coding sequene and a polyA sequence. Upon crossing mice that carry the Z/EG-Pgf transgene to a mouse that expresses Cre in the endothelia, recombination will remove the neomycin cassette and induce expression of *Pgf*. Locations of the primer pairs used for genotyping are indicated.

genomic expression of the transgene were selected and further screened by karyotyping. The B1 clone was used to generate chimeric mice by injection into C57Bl/6 host blastocysts. The resulting male chimeras were bred to wild type C57Bl/6 females, and the resulting pups were assessed for germline transmission of the ES cell-derived cells by coat color (agouti pups indicated germline transmission). Agouti pups were genotyped to identify those that carried the transgene. The embryonic and adult expression pattern of this transgene has been characterized by staining embryos and Z/EG-Pgf adult male tissues with X-gal to visualize the level and location of *lacZ* expression. The results demonstrate that this transgene will provide appropriate spatial expression in the early embryonic endothelia and will be useful for many analyses in the adult (Figure 5.2).

5.2.2 Regulated placental growth factor expression is essential for the growth and development of the early embryo

In studies overexpressing Notch1 in the endothelia, *Pgf* expression was increased approximately 2-fold, specifically in endothelial cells (Figures 3.7B and 3.8). To examine the functions of PlGF activity in the early embryo, female mice heterozygous for the Z/EG-Pgf transgene were crossed with male mice hemizygous for the *Tie2-Cre* transgene (Koni et al. 2001), and the resulting embryos were analyzed. In addition to normal wild type embryos, two mutant phenotypes were observed, termed Z/EG-Pgf moderate and severe. The Z/EG-Pgf moderate embryos, when compared to stage-matched wild type embryos at E9.5, exhibited a reduction in overall size and obvious developmental defects (Figure 5.3A-B). Z/EG-Pgf severe embryos displayed extreme developmental defects; embryonic structures were indistinguishable (Figure 5.3C). The

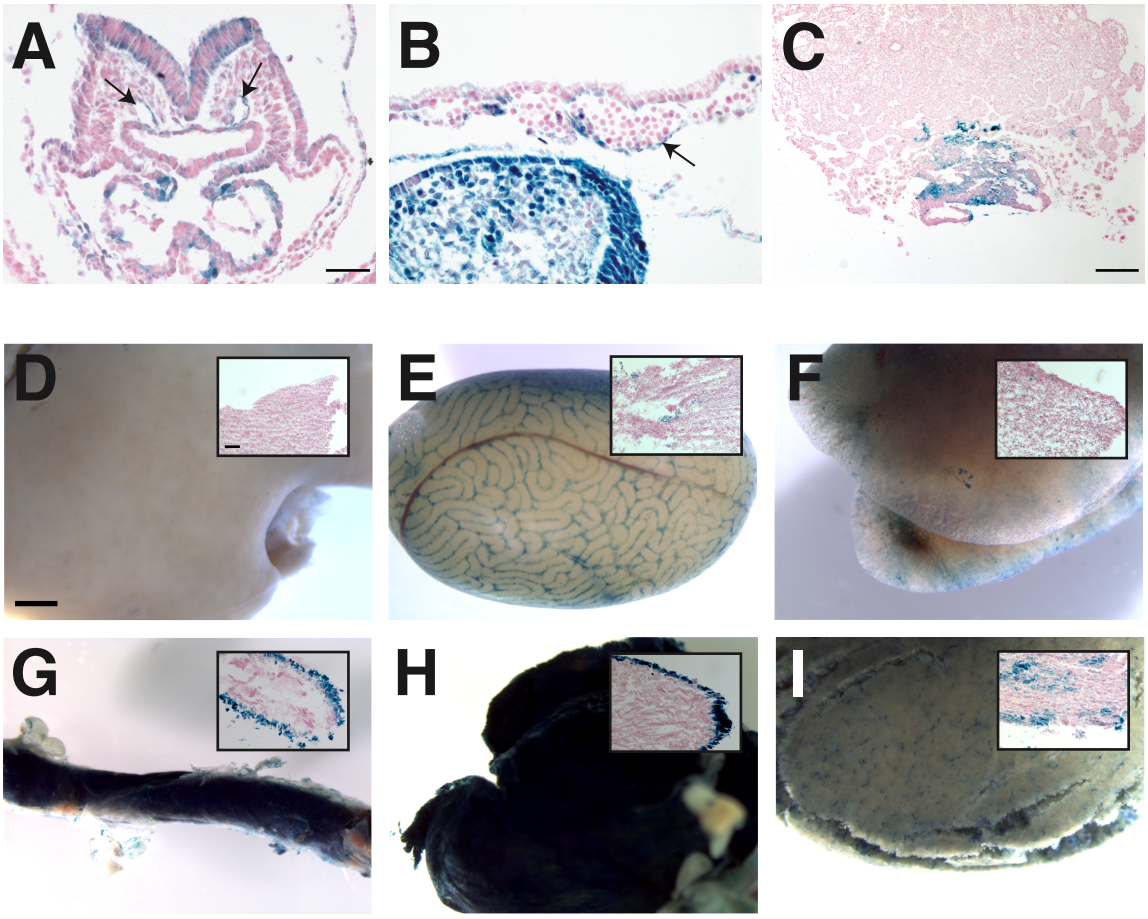

Figure 5.2. *LacZ* Expression in Embryonic and Adult Tissues in the Z/EG-Pgf Transgene

(A-B) Embryo at E8.5. Note the expression in many tissues, specifically in the endothelial cells of the dorsal aorta (A, arrows) and yolk sac (B, arrow). (C) Placenta at E8.5. (D-I) *lacZ* expression in adult male tissues. Note the expression in the esophagus (D), heart (E), testes (F), lung (G), and kidney (H). No expression was seen in the liver (I). Scale bars are 50 µm (A, B), 250 µm (C), 1mm (D-I), and 100 µm (D-I, inset).

intact yolk sac of the moderate and severe embryos was comparable in size to the wild type, but had a wrinkled appearance and lacked any discernable blood vessels (Figure 5.3E-F). The morphological defects in the Z/EG-Pgf moderate embryos were similar to those seen EC-N1ICD embryos, indicating that this model will prove to be very useful to define the importance of *Pgf* overexpression in the phenotypes observed in the EC-N1ICD embryos, and that the expression level of *Pgf* must be properly regulated.

5.2.3 Expression of PlGF via GFP after CRE excision

As two distinct phenotypes are seen as a result of a cross with *Tie2-Cre*, PlGF expression in the early embryo and the placenta was localized via the expression of EGFP. Immunostaining of E9.5 wild type and Z/EG-Pgf moderate embryos using an anti-GFP antibody indicated the expression of PlGF in the developing vasculature of the Z/EG-Pgf moderate embryo, including the dorsal aortae, cardinal veins, and the vasculature surrounding the head and heart (Figure 5.4B, arrows and arrowhead). As expected, the wild type embryo was negative for GFP expression, aside from limited autofluorescence of the blood cells (Figure 5.4A). Immunostaining was also performed in the placenta of E9.5 wild type and Z/EG-Pgf moderate and severe embryos using an anti-GFP antibody. Again, the wild type was negative for EGFP expression, however the Z/EG-Pgf moderate embryos expressed GFP in the embryo-derived vasculature and very slightly in the trophoblast cells (Figure 5.4C-D, arrow). The Z/EG-Pgf severe embryos exhibited a lack of embryo-derived vasculature and a great missexpression of GFP in the trophoblast cells of the placenta (Figure 5.4E). Based on these results, the expression level of total *Pgf* (endogenous and transgenic *Pgf*) in wild type and Z/EG-Pgf moderate and severe yolk sac tissues was compared to the level in wild type placenta via real-time PCR. *Pgf* is normally expressed at low levels in the yolk sac. The Z/EG-Pgf moderate

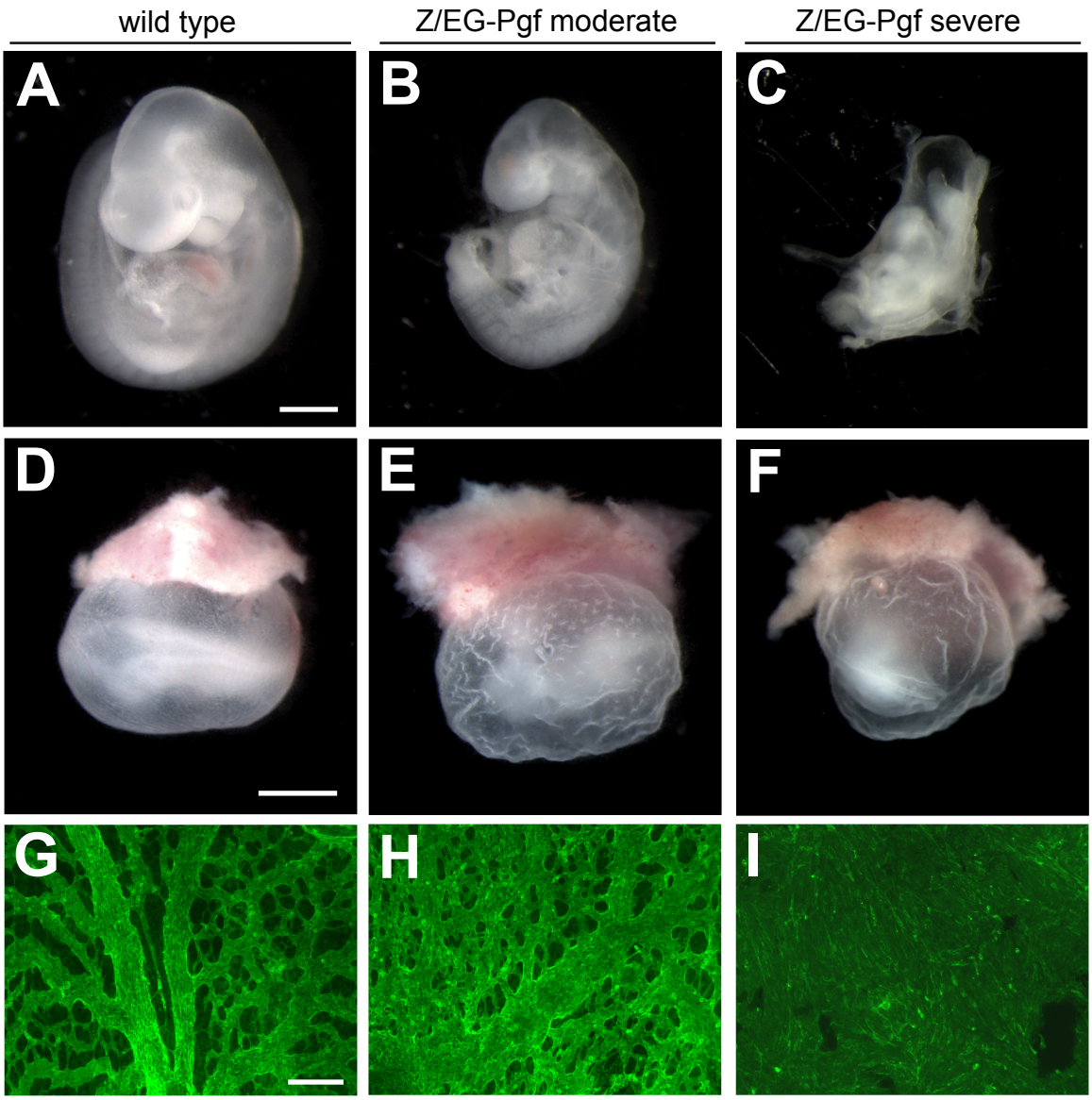

Figure 5.3. Defects in Growth and Vascular Remodeling in Z/EG-Pgf Embryos.
(A-C) Lateral view of E9.5 wild type (A), Z/EG-Pgf moderate (B), and Z/EG-Pgf severe (C) embryos. Z/EG-Pgf moderate embryos were smaller in size than the wild type and exhibited cardiovascular defects (B). Z/EG-Pgf severe embryos displayed extreme cardiac distress; embryonic structures were indistinguishable (C). (D-F) Whole mount E9.5 wild type (D), Z/EG-Pgf moderate (E), and Z/EG-Pgf severe (F) embryos with surrounding yolk sac. The Z/EG-Pgf moderate and severe yolk sac were similar in size to the wild type, however they had a wrinkled appearance and lacked the large, well-defined blood vessels. (G-I) Immunofluorescence image of E9.5 wild type (G), Z/EG-Pgf moderate (H), and Z/EG-Pgf severe (I) yolk sac visualized with an antibody to PECAM1. Wild type embryos showed a remodeled yolk sac vasculature, with both large and small caliber vessels. The Z/EG-Pgf moderate yolk sac exhibited limited branching; many of the vessels were of similar size. The Z/EG-Pgf severe yolk sac lacked any vascular remodeling. Scale bars are 500µm (A-C), 1mm (D-F), and 200 µm (G-I).

embryos expressed *Pgf* in the yolk sac at similar levels to those seen in wild type placenta, approximately 40-fold higher than in wild type yolk sac. The Z/EG-Pgf severe embryos expressed *Pgf* at even higher levels (approximately 130-fold higher) (Figure 5.4F). These results indicate acceptable levels of expression of *Pgf* in the vasculature of the Z/EG-Pgf moderate embryos, although not in the Z/EG-Pgf severe embryos. As a result of these findings all remaining analyses were done using Z/EG-Pgf moderate embryos, except for the analyses of the placenta.

5.2.4 Vascular defects in Z/EG-Pgf embryos

A detailed comparison of the vasculature was performed to define the vascular defects in the embryonic and extraembryonic vasculature of the Z/EG-Pgf moderate embryos. Severe defects in the formation of the vasculature were seen in the yolk sac of the developing embryo beginning at approximately E9.5. Immunofluorescence of PECAM1 stained E9.5 yolk sac allowed for the visualization of the defects in vascular remodeling in greater detail. In the Z/EG-Pgf moderate embryos, the vasculature had begun to remodel into the large and small caliber vessels seen in the stage-matched wild type yolk sac, however there was limited branching; many of the vessels were of similar size (Figure 5.3G-H). In contrast, the Z/EG-Pgf severe yolk sac lacked any vascular remodeling or any discernable lumenized vessels (Figure 5.3I).

Histological sectioning of embryonic and yolk sac tissues was performed to visualize the vasculature in cross-section via hematoxylin and eosin staining. The dorsal aortae of the Z/EG-Pgf moderate embryos were approximately twice the cross-sectional area of wild type embryos, however they were functional, lumenized, blood-filled vessels (Figure 5.5A-B, asterisks). This enlargement did not affect nearby vessels; the Z/EG-Pgf

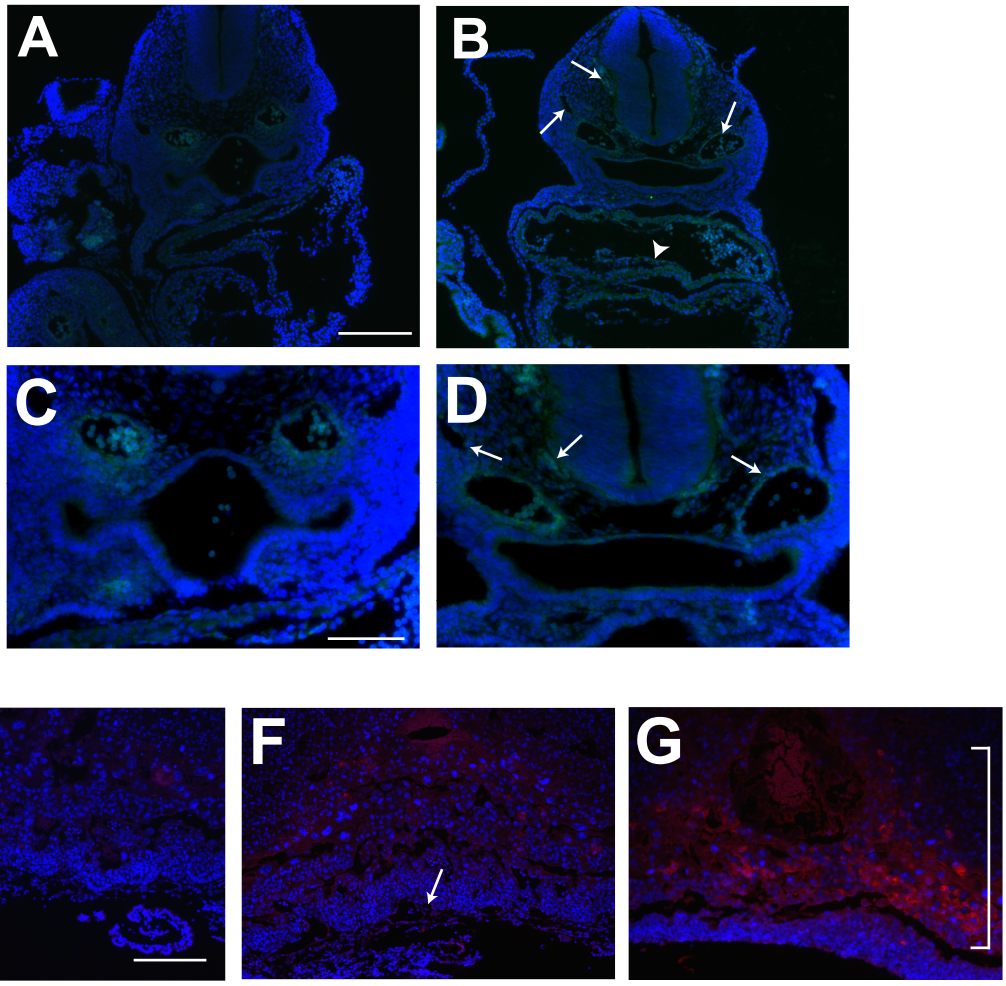
A
B
C
D
E
F
G
H
Relative gene expression
200
180
160
140
120
100
80
60
40
20
0
*
*
*
wt ys
Z/EG-Pgf moderate ys
Z/EG-Pgf severe ys
wt placenta

Figure 5.4. Resulting PlGF Expression in the Early Embryo and Placenta after *Tie2-Cre* Mice were Crossed with Z/EG-Pgf Mice

(A-D) Localization of PlGF via expression of GFP in the embryo at E9.5. Note the expression of PlGF in the dorsal aorta, cardinal vein, and veins around the neural tube (B, D, arrows) and in the vasculature of the heart (B, arrowhead) of the Z/EG-Pgf moderate. The blood cells in both the wild type (A, C) and Z/EG-Pgf moderate (B, D) exhibit auto-fluorescence. (E-G) Localization of PlGF via expression of GFP in placenta at E9.5. Note the expression of GFP in the embryonic-derived vasculature of the placenta of the Z/EG-Pgf moderate (F, arrow). In the Z/EG-Pgf severe there is a lack of embryonic-derived vessels and the missexpression of PlGF in the trophoblast (G, brackets). (H) Real time-PCR analysis of total *Pgf* expression (Z/EG-Pgf and endogenous *Pgf*) in wild type yolk sac, Z/EG-Pgf moderate and severe yolk sac, and wild type placenta at E9.5. *Pgf* expression in the Z/EG-Pgf moderate yolk sac is comparable to that in wild type placenta. Scale bars are 200 μm (A, B), 100 μm (C, D) and 250 μm (E-G). * $p < .05$.

moderate embryos contained lumenized cardinal veins (Figure 5.5B, arrow). In the wild type yolk sac a distribution of large and small caliber vessels were present and were filled with blood cells; in contrast, the Z/EG-Pgf moderate yolk sac contained primarily large caliber lumenized vessels that contained blood cells (Figure 5.5C-D, arrows and arrowheads). Both wild type and Z/EG-Pgf moderate embryos had a range of yolk sac vessel diameter. However, in wild type yolk sac a greater number of the vessels measured consisted of small capillaries compared to Z/EG-Pgf moderate yolk sac in which a larger proportion of vessels consisted of a larger cross-sectional area. In Z/EG-Pgf moderate yolk sac, approximately 24% of vessels measured had an area of 3000μm^2 or greater, while in wild type yolk sac only 2% measured this size. Conversely, only 9% of vessels measured were smaller than 500μm^2 in the Z/EG-Pgf moderate yolk sac, while in the wild type yolk sac this number was 49% (Figure 5.5E).

5.2.5 Defects in embryo-derived vasculature and gene expression in Z/EG-Pgf transgenic placenta

Upon examination of PlGF expression in the placenta, it was discovered that in the Z/EG-Pgf moderate placenta PlGF was expressed in the embryo-derived vasculature and to a small extent the trophoblast cells. The Z/EG-Pgf severe placenta, however, did not have any embryo-derived vasculature and greatly expressed PlGF in the trophoblast cells. To examine these results in greater detail histological sectioning of placental tissues was performed with H&E staining. In cross-section the embryo-derived vasculature of the placenta of Z/EG-Pgf embryos appeared normal and did invade into the labyrinth layer of the placenta, although to a lesser extent than in the wild type (Figure 5.6B, arrows and arrowheads). The Z/EG-Pgf severe placenta lacked any embryo-derived vasculature or nucleated erythrocytes (Figure 5.6C). To confirm these findings, immunostaining of E9.5 wild type, Z/EG-Pgf moderate and Z/EG-Pgf severe

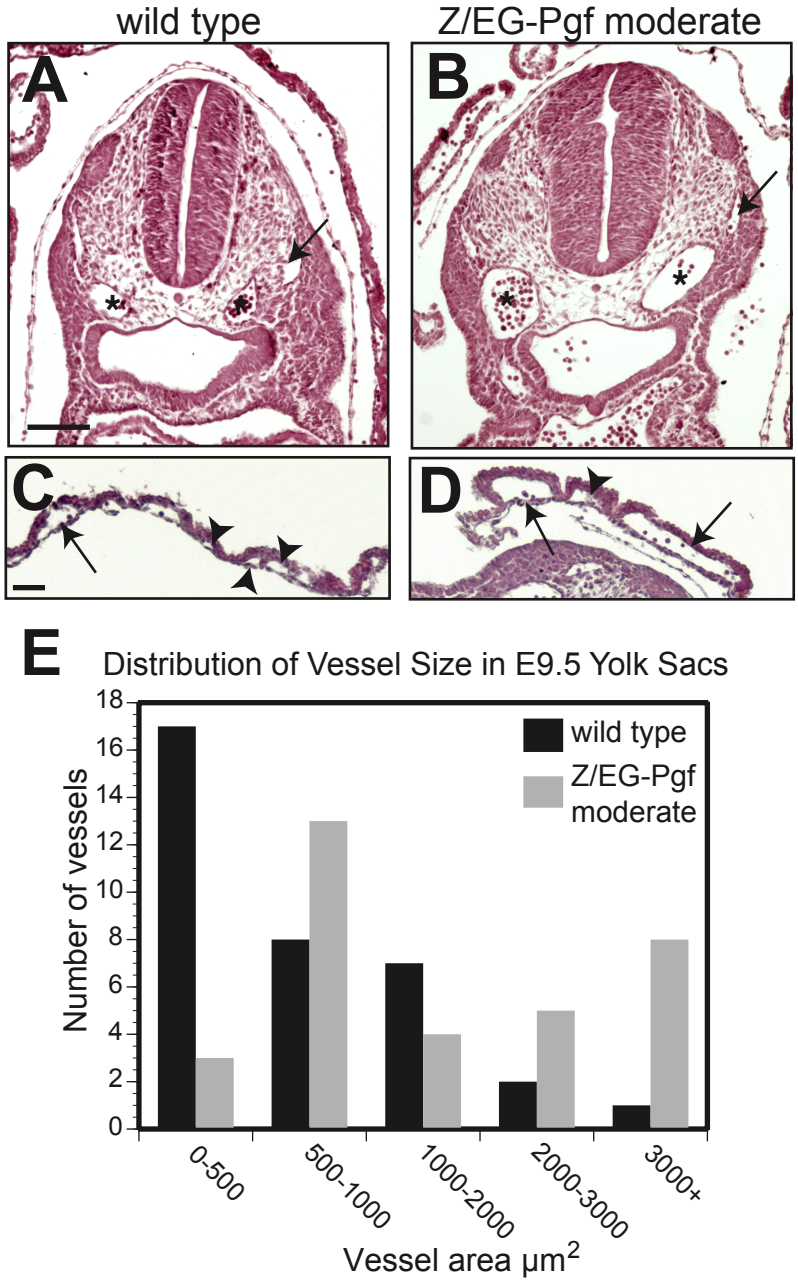

Figure 5.5. Defects in Vessel Diameter in Z/EG-Pgf Embryos

(A-D) Histological sections (lateral) of H&E-stained E9.5 embryos (A, B) and yolk sac (C, D) at the level of the heart. The dorsal aortae of the Z/EG-Pgf embryos (B, asterisk) were approximately twice the area of wild type dorsal aortae (A, asterisk). Both contained lumenized cardinal veins (A, B, arrows). The wild type yolk sac contained an array of different caliber vessels, some larger (A, arrows) and some quite small (A, arrowheads). The Z/EG-Pgf yolk sacs also contained large and small vessels, however there were primarily large caliber vessels (B, arrows). (E) Distribution of vessel area in the yolk sac of wild type and Z/EG-Pgf embryos. Both wild type and Z/EG-Pgf embryos had an array of differently sized vessels. However, wild type yolk sac had a greater number of vessels with an area of 0-500µm^2, while Z/EG-Pgf contained more vessels with an area of 3000 µm^2 or greater. Scale bars are 100 µm (A, B) and 50 µm (C, D).

placenta was performed using anti-PECAM1 antibody to visualize the vasculature. As expected, the embryo-derived vasculature of the wild type and Z/EG-Pgf moderate placenta was positive for PECAM1 staining, and still no vessels were seen in Z/EG-Pgf severe placentas (Figure 5.6D-F, arrows). Interestingly, expression levels of PECAM1 were elevated slightly in Z/EG-Pgf moderate trophoblast cells and to a greater extent in Z/EG-Pgf severe trophoblast cells (Figure 5.6E-F, brackets). These results indicate multiple functions for PlGF activity in the early embryo, including the remodeling of the yolk sac vasculature, the regulation of vessel diameter, and formation of the embryo-derived vasculature of the placenta and its invasion into the labyrinth layer.

5.2.6 Overexpression of *Pgf* in the endothelia induces the expression of Notch signaling family members

Gene expression defects in Z/EG-Pgf moderate yolk sac were examined to determine a potential molecular mechanism of how altered PlGF affects vascular differentiation and how it interacts with the Notch signaling pathway. Based on earlier results from Notch models, a subset of genes were analyzed in RNA from yolk sacs of E9.5 wild type and Z/EG-Pgf embryos via real-time PCR. Of the genes examined only Notch family members and targets exhibited significant increased expression. The endothelial expressed Notch ligands *Notch1* and *Notch4* were both upregulated in Z/EG-Pgf moderate yolk sac (approximately 2-fold and 3-fold, respectively), as was the ligand *Dll4* (approximately 2.5-fold). Interestingly, the Notch ligand *Jag1* was unaffected (Table 5.1). The well characterized members of the Hairy/Enhancer of split-related (HES/HEY) family, which are directly regulated by Notch1 signaling via its binding to RBPJ to regulatory regions of these loci (Maier and Gessler, 2000), also exhibited increased expression in Z/EG-Pgf moderate yolk sac. Real-time PCR revealed that expression of

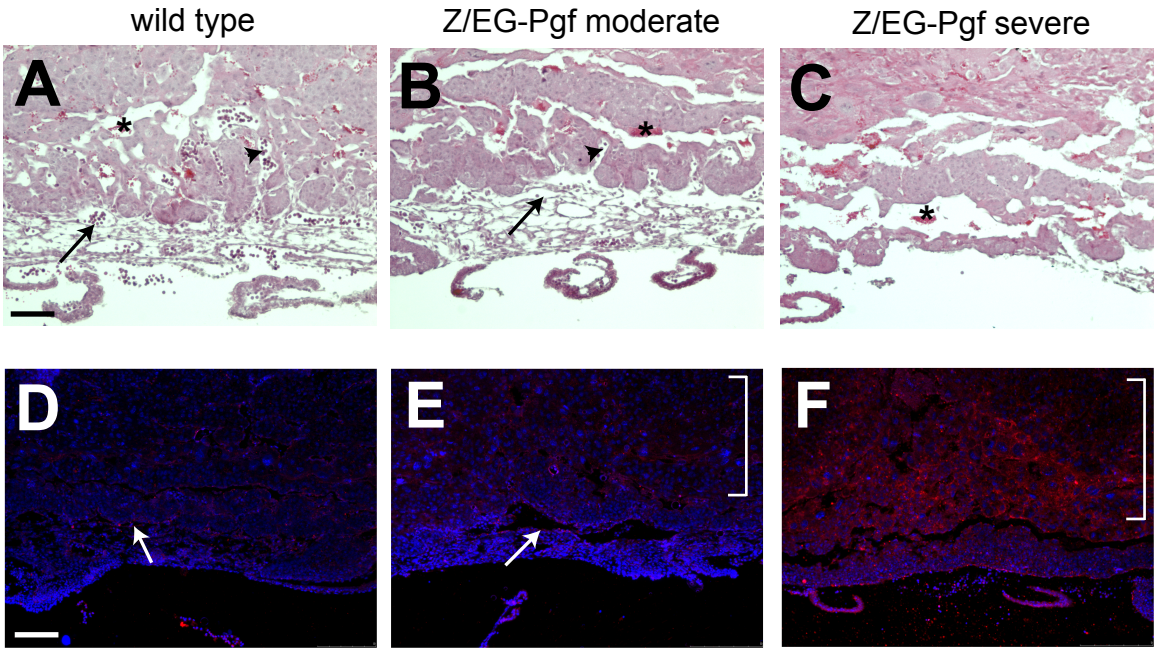

Figure 5.6. Defects in Embryonic-Derived Vasculature and Gene Expression in Z/EG-Pgf Moderate and Severe Placentas

(A-C) Histological sections of E9.5 H&E-stained placenta in wild type (A), Z/EG-Pgf moderate (B), and Z/EG-Pgf severe (C) embryos. Blood vessels containing nucleated erythrocytes were present in wild type (A, arrow) and Z/EG-Pgf moderate placenta (B, arrow), and in both the fetal vasculature invaded into the maternal portion of the placenta (A, B arrowheads). The Z/EG-Pgf severe placenta (C) lacked any fetal vasculature or nucleated erythrocytes. (D-F) Histological sections of E9.5 placenta stained with an antibody to PECAM1. The fetal vessels of the wild type and Z/EG-Pgf moderate placenta contain PECAM1-positive cells (D, E, arrows), while fetal vessels were undistinguishable in Z/EG-Pgf severe placenta. Expression of PECAM1 was increased slightly in Z/EG-Pgf trophoblast cells (E, bracket) and to a much greater degree in Z/EG-Pgf severe trophoblast cells (F, bracket). Asterisk (A-C), maternal blood. Scale bars are 100 μm (A-F).

Hey1 and *Heyl* was increased 2-fold and 2.5-fold in the Z/EG-Pgf moderate yolk sac respectively (Figure 5.7). The Notch regulated gene *Nrarp* (Krebs et al. 2001) was also upregulated, 1.98-fold in response to PlGF activation. The expression of members of the VEGF family, the endothelial marker *Cd34*, and *Tgfb2* was also examined (Table 5.1). Although the expression differences were slight for these genes, specifically *Vegfa* and *Tgfb2*, the proper level of expression is critical in the development of the embryo. These results, specifically the upregulation of the Notch receptors and ligand, corroborate findings that VEGF signaling can act as an upstream component of Notch (Lawson et al. 2002), and that PlGF plays an important role in this regulation.

5.3 Discussion

The members of the VEGF signaling family have been shown to play specific and important roles in the formation of the early vasculature and lymphatic systems and in the regulation of pathological angiogenesis. PlGF in particular has been shown to regulate pathological angiogenesis, vascularization, inflammation, and edema formation (Luttun et al. 2002; Odorisio et al. 2002; Oura et al. 2003). To date all studies of PlGF activity have been performed in the adult, its role in the early embryo is still largely unknown. Previous work in our lab demonstrated that the gain-of-function of Notch signaling resulted in the increased gene expression of *Pgf*, specifically in the endothelia of the early embryo (Copeland et al. 2011). Our current analysis employed a similar conditional transgenic model to overexpress *Pgf* in the endothelia under the control of *Tie2-Cre*, allowing for the in depth analysis of PlGF activity in the early embryo. Our analysis concentrated on the morphological and molecular abnormalities associated with this increased expression, specifically in the extraembryonic vasculature of the yolk sac and

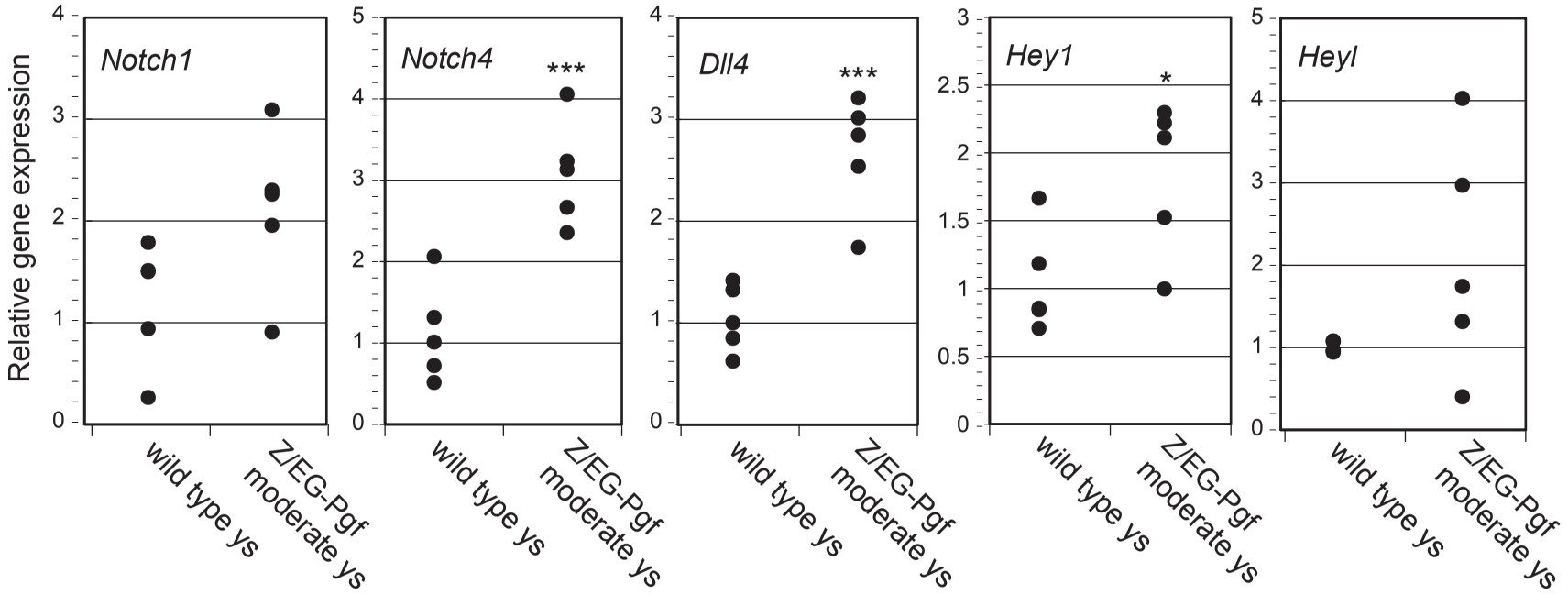

Figure 5.7. Gene Expression in Z/EG-Pgf Moderate Yolk Sac Tissues
Real time-PCR analysis was used to analyze gene expression differences seen in Z/EG-Pgf yolk sac tissues. Real time-PCR analysis of the Notch family members *Notch1*, *Notch4, Dll4, Hey1,* and *Heyl* in wild type E9.5 whole yolk sac tissues and Z/EG-Pgf moderate yolk sac tissues. * p< .05, ** p< .01, *** p< .001 compared to wild type.

Table 5.1. Expression of Select Genes in Z/EG-Pgf Moderate Yolk Sac Tissues

Gene Symbol	Gene Name	Fold Change Z/EG-Pgf
Jag1	jagged 1	1.13
Nrarp	Notch-regulated ankyrin repeat protein	1.98 *
Pgf (endogenous)	placental growth factor	0.99
Vegfa	vascular endothelial growth factor A	0.82 *
Vegfc	vascular endothelial growth factor C	1.56
Flt1	FMS-like tyrosine kinase 1	1.53
Kdr	kinase insert domain protein receptor	1.35
CD34	CD34 antigen	1.61 *
Tgfb2	transforming growth factor, beta 2	1.68 *

* $p < .05$

placenta. Substantial defects in the formation of the vasculature in the embryo, yolk sac, and placenta were observed, mimicking some of the vascular defects seen in the gain-of-function Notch model. Gene expression defects were also seen as a result of increased PlGF expression, specifically in Notch family members. This, taken with data from the gain-of-function Notch studies, indicates a potential regulatory loop between the Notch and VEGF signaling families to direct the formation and remodeling of the vasculature in the developing embryo.

Defects in the placenta, both morphological and molecular, were also observed in Z/EG-Pgf transgenic embryos. In the developing placenta the fusion of the allantois to the chorion leads to the invasion of embryo-derived vessels into the trophoblast, while maternal vessels enter the placenta and are invaded by trophoblast cells. Maternal blood bathes the trophoblast cells facilitating the exchange of nutrients and waste with the embryo (Coultas et al. 2005; Huppertz and Peeters 2005). Mutations in many signaling pathways that have vascular abnormalities in the embryo also exhibit defects in placenta development, including the Notch pathway (Gasperowicz and Otto 2008). In our model, Z/EG-Pgf moderate embryos exhibited decreased invasion of embryo-derived vessels into the labyrinth zone and Z/EG-Pgf severe embryos lack embryo-derived vessels entirely, likely due to a failure of allantois-chorion fusion. PlGF is endogenously expressed at its highest level in the trophoblast cells of the placenta, as well as endothelial cells (Park et al. 1994). Our transgene exhibited increased expression of PlGF in the trophoblast cells, slightly in Z/EG-Pgf moderate placenta and to a greater extent in Z/EG-Pgf severe placenta. This increased expression and the resulting vascular abnormalities likely contribute to the morphological defects in the embryo and yolk sac, due to a failure

in the maternal-embryonic interaction in the placenta. At approximately E8.5 the allantois makes contact with the chorion. Blood vessels from the allantois grow into the labyrinth of the placenta. There the embryo-derived vessels facilitate the exchange of materials and waste with the maternal blood system. Cells of the placenta, such as the giant and spongiotrophoblast cells, also produce molecules, including VEGF and others, that are important for embryonic development. A failure or defect in this formation leads to defects in the growth and development of the embryo.

Morphological analysis of Z/EG-Pgf transgenic mice further confirmed that VEGF signaling, specifically the regulation of PlGF expression levels, is critical for embryonic vascularization. Similar to the EC-N1ICD model, resulting Z/EG-Pgf moderate embryos exhibited growth defects at E9.5 and early lethality, while Z/EG-Pgf severe embryos were grossly disfigured. Examination of the vasculature of the early embryo revealed abnormalities in the dorsal aortae, yolk sac vasculature, and embryonic-derived vasculature of the placenta. These defects were much more severe in the Z/EG-Pgf severe embryos, which had no apparent remodeling in the yolk sac and no embryonic-derived vessels in the placenta, further confirming the need for proper regulation of PlGF expression. Other VEGF models demonstrated defects in vessel formation in the early embryo from altered expression of VEGF family members. Mutation of *Vegfa* leads to a decrease in the size and caliber of the blood vessels (Carmeliet et al. 1996; Ferrara et al. 1995), *Flt1* null mice form abnormal blood vessels (Fong et al. 1995) and mice overexpressing *Pgf* in the skin displayed an increase in blood vessel number, branching, and size (Odorisio et al. 2006). These data stress the

importance for VEGF signaling in the formation of the early embryonic vasculature and subsequent development of the embryo.

Previous studies of *Pgf* knockout mice indicated that PlGF plays a limited role in the development of the vasculature of the early embryo and instead its activity is restricted to pathological angiogenesis in the adult (Carmeliet et al. 2001). However, our studies and data from mice overexpressing *Pgf* in the skin indicates that while PlGF activity may not be critical for vascular development, it does act to stimulate it (Odorisio et al. 2002). Likely the limited requirement for PlGF in the early embryo is due to its low expression levels, its lower affinity for FLT1, or the increase of VEGF-A as compensation (Carmeliet et al. 2001). PlGF may act in a number of ways in our model to stimulate vascular formation. First, PlGF may act directly to activate FLT1, transmitting the angiogenic signals (Carmeliet et al. 2001). Secondly, PlGF may form PlGF/VEGF heterodimers, which enhances the angiogenic response (Cao et al. 1996). And finally, PlGF may displace VEGF-A from the FLT1 'sink', making more VEGF-A available to signal through KDR (Park et al. 1994) (Figure 5.8A). Further analysis of the Z/EG-Pgf model is needed to determine the correct function of PlGF activity in the early embryo. An extensive examination of the gene expression defects in the Z/EG-Pgf moderates could be done, via microarray, to identify novel genes regulated by PlGF activity. Comparing resulting data with the EC-N1ICD microarray data set could identify possible genes involved specifically in this model of Notch/VEGF interaction. Analysis of the level of phosphorylation of the VEGF receptors, via Western blot or immunofluorescence, could help identify the function of PlGF in the VEGF signaling pathway during the regulation of vascular development.

To further examine PlGFs activity in the early embryo a molecular analysis of the Z/EG-Pgf moderate embryo was performed. While no misregulation was apparent in many of the genes examined, including members of the VEGF family and *Tgfb2*, members of the Notch signaling pathway showed increased expression in the yolk sac of the Z/EG-Pgf moderate embryos. These included the Notch receptors *Notch1* and *Notch2*, the ligand *Dll4*, and the downstream target genes *Hey1* and *Heyl*. Interestingly the Notch ligand *Jag1* was unaffected. It has been demonstrated that a complex hierarchy of signaling involving VEGF and Notch is required for the patterning of the vasculature in both the early embryo and the adult during neoangiogenesis. Epistasis experiments in zebrafish indicated that Notch signaling is downstream of VEGF signaling in arterial specification (Lawson et al. 2002). In vitro it was shown that upregulation of VEGF-A can increase expression of Notch members in human arterial endothelial cells (Liu et al. 2003). This interaction is also seen in the process of sprouting angiogenesis, where the interaction between the Notch and VEGF pathways regulates the formation of the endothelial sprouts (Siekmann et al. 2008). This model is a perfect example of the feedback loop between Notch and VEGF signaling. Based on these previous studies and results from our molecular analysis, PlGF activity may act, in one way or another, to regulate Notch signaling in the remodeling of the yolk sac vascular plexus. PlGF may regulate the Notch signaling pathway by displacing VEGF from the FLT1 receptor, increasing the amount of VEGF signaling through KDR. This signaling then induces the expression of the Notch ligand *Dll4,* which interacts with a receptor on a neighboring endothelial cell thus activating the Notch signaling pathway and subsequently increasing the expression of the target genes *Hey1* and *Heyl* (Figure 5.8B). PlGF could also act, in a

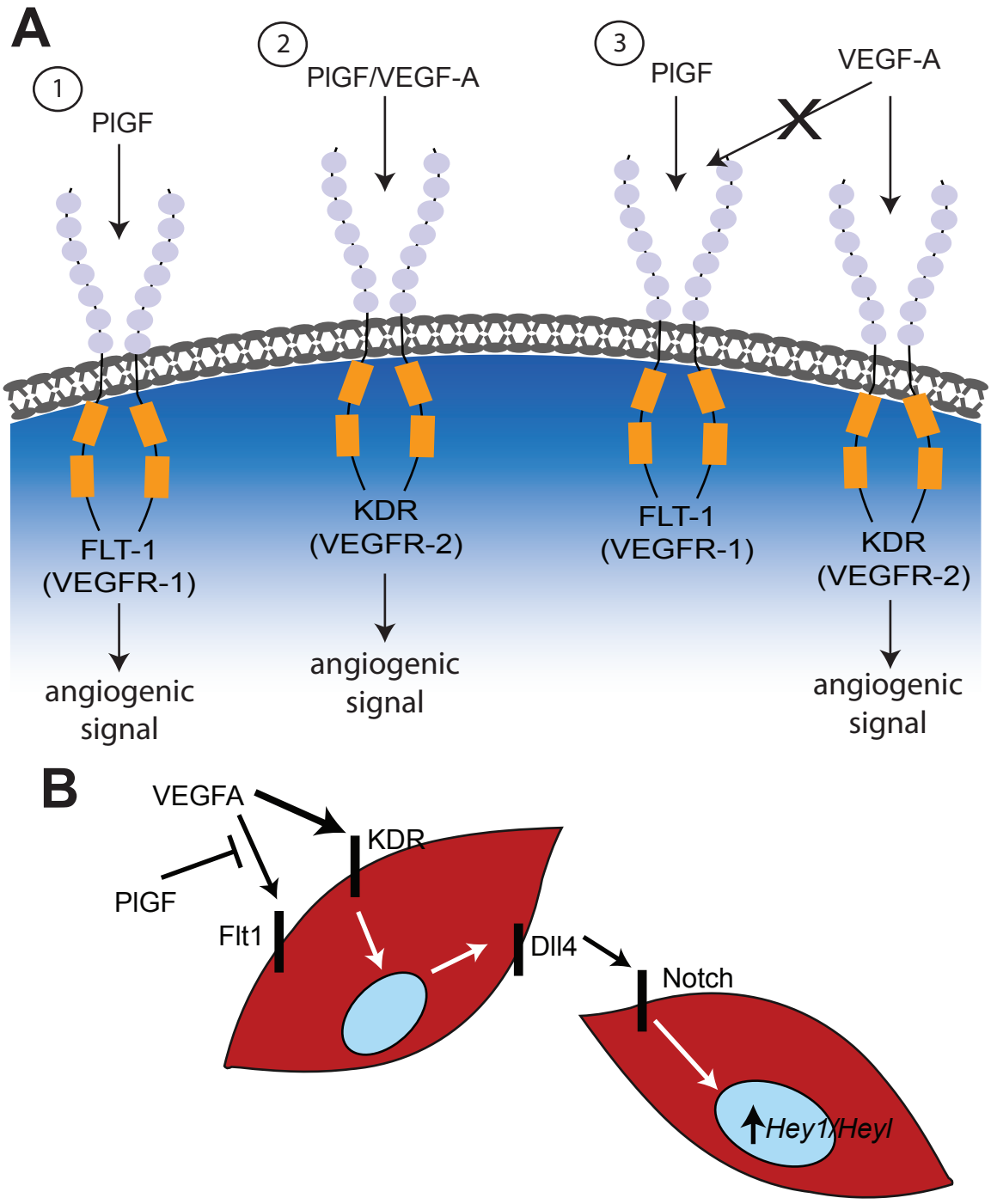

Figure 5.8. PlGF modulates the VEGF-response and regulates the expression of Notch family members

(A) Schematic model of the role of PlGF, VEGF-A, KDR, and FLT1 in the modulation of the angiogenic signal. 1. PlGF activates signaling through FLT1. 2. PlGF forms heterodimers with VEGF to signaling through KDR. 3. PlGF displaces VEGF-A from FLT1, increasing its activity through KDR. (B) Proposed model of signaling in the endothelial cells of the early yolk sac. PlGF signaling increases the expression of the Notch ligand *Dll4* which binds to Notch receptors in adjacent cells. Notch signaling is activated increasing the expression of the target genes, *Hey1* and *Heyl*, among others.

similar fashion, to increase the expression of the Notch receptors in the endothelial cells, also resulting in increased Notch signaling.

Interaction between the Notch and VEGF signaling pathways has been examined but the specifics are still largely unknown. The Z/EG-Pgf model further demonstrates a role for PlGF in regulating vascular differentiation and in the regulation of Notch family members. Notch signaling in the endothelia is also important for vascular remodeling and embryonic development, as well as the regulation of key genes. Taken together the data expands on the idea of a complex hierarchy of signaling in the regulation of vascular differentiation in both the embryo and the adult. Additional work in these in vivo models will help to further define the exact interaction between the pathways and how this interaction leads to proper formation of the vasculature.

Chapter 6

General Discussion and Prospectus

In this dissertation I focus on the role of Notch signaling in the formation and remodeling of the vasculature in the early embryo. Previous studies found that Notch family members are expressed in the endothelia of the early vessels (Uyttendaele et al. 1996; Villa et al. 2001) and that mutations in Notch family ligands, receptors, and targets result in defects in the vasculature and embryonic lethality (Xue et al. 1999; Krebs et al. 2000; Uyttendaele et al. 2001; Iso et al. 2003; Gale et al. 2004; Krebs et al. 2010). It had also been shown that the Notch signaling pathway interacts with the VEGF and TGFβ pathways to control this process (Lawson et al. 2002; Lobov et al. 2007; Holderfield and Hughes 2008). However, an in depth analysis of the key genes involved in this complex hierarchy was lacking. To study Notch function in vivo, I employed a gain-of-function conditional Notch transgenic system and a tissue-specific loss of RBPJ mutation. Both models exhibited growth retardation and defects in the remodeling of the vasculature, particularly in the caliber of the vessels. Gene expression analysis in the yolk sacs of these models indicated defects in a number of genes, specifically the secreted ligands *Tgfb2*, *Vegfc* and *Pgf* (Chapter 3). Furthermore, I employed a doxycycline-inducible Notch1-ICD transgenic ES cell line and small molecule inhibitor γ-secretase to study the effects of Notch activation and inhibition in vitro. Molecular analysis showed altered gene expression with results differing from results seen in vivo (Chapter 4). To better understand the activity of placental growth factor in the formation of the vasculature and its relation to Notch signaling, a gain-of-function PlGF transgenic mouse model was generated. Resulting embryos displayed two distinct phenotypes with defects in growth and vascular development and gene expression analysis indicated an increase in the expression of Notch family members (Chapter 5). Taken together, the data help to

further define the role of both Notch and VEGF signaling in the regulation of vascular development in the early embryo. Specifically, the in depth molecular analysis introduces novel gene and pathway interactions critical for this process.

6.1 Insights into vascular remodeling

The EC-N1ICD, EC-Rbpj-KO, and Z/EG-Pgf models each exhibited defects in the formation of the vasculature. Detailed examination of the yolk sac vasculature, dorsal aortae, and fetal vasculature of the placenta revealed an enlarged vessel phenotype in the EC-N1ICD, remarkably apparent within the yolk sac, in which the plexus is converted to a mass of large diameter vessels. In contrast, small caliber non-remodeled vessels are present in the EC-Rbpj-KO yolk sac model. Similar to the EC-N1ICD model, the vasculature in the Z/EG-Pgf moderate embryo revealed abnormalities in the dorsal aortae, yolk sac vasculature, and embryonic-derived vasculature of the placenta. The aortae and vessels of the yolk sac were enlarged. These vascular defects were much more severe in the Z/EG-Pgf severe embryos, which had no apparent remodeling in the yolk sac and no embryonic-derived vessels in the placenta. These data stress the importance for Notch and VEGF signaling in the formation and remodeling of the early embryonic vasculature.

Given that Notch signaling is associated with arterial identity (Uyttendaele et al. 1996; Villa et al. 2001), the function of Notch signaling to control vessel size may represent an aspect of Notch function in the definition of the arteriole. The mechanisms of how the Notch, VEGF, and other signaling pathways control vessel size in the various regions of the developing embryo are not well defined, and are likely context dependent. Some models suggest that directional cell division is important to dictate whether endothelial cell proliferation within a patent vessel results in an increase in luminal diameter (Zeng et al. 2007). Other models suggest the recruitment of endothelial or

angioblast cells into existing vessels as an important mechanism to increase vessel diameter (Schmidt et al. 2007). The remodeling process of the yolk sac makes extensive use of reallocation of cells during remodeling (discussed below), suggesting complex roles for Notch signaling in controlling endothelial cell behavior during remodeling.

The yolk sac vasculature represents a genetically tractable model to study endothelial differentiation, and the work presented here has made extensive analysis of this tissue. Endothelial differentiation within the yolk sac is initiated as groups of cells from the proximally situated extraembryonic mesoderm condense into blood islands by approximately embryonic day 7.0, which subsequently migrate toward the distal region of the yolk sac. The peripheral cells will differentiate to the endothelial cells lining the vasculature, whereas the inner cells become blood cells. The endothelial cells expand and fuse to form the vascular plexus, which is contiguous with the embryonic vasculature at the onset of blood flow (Lucitti et al. 2007). The capillaries are then remodeled into the hierarchical vascular network of vitelline artery, capillaries, and vitelline vein. Observations of vessel remodeling in the yolk sac, particularly in the chick embryo, suggest that the formation of large diameter vessels is from pre-existing capillary-derived endothelial cells, via the process of intussusceptive angiogenesis. This process is readily perceived by examination of the avascular space ('pillars'), in which adjacent pillars 'fuse' during this remodeling process. This process involves the collapse of some capillary microvessels, and the endothelial cells from the capillary are then recruited into the nascent vessels to result in a larger diameter vessel (Figure 3.4G, asterisk). This mode of remodeling has been suggested to be an efficient and rapid mode of angiogenesis in a variety of sites (Djonov et al. 2000). Although Notch signaling does play a significant role in sprouting angiogenesis (Siekmann et al. 2007) in many other contexts, the remodeling of the yolk sac in the early embryo may not utilize a sprouting angiogenesis method. Based on the current model of endothelial remodeling within the

yolk sac plexus, the defects in vessel diameter and the remodeling failure in the Notch models used in this study indicate a possible defect in the reallocation of endothelial cells from capillaries into arterioles during intussusceptive arborization, suggesting that Notch plays a significant role in this migration. The phenotype observed in the EC-N1ICD yolk sac vasculature is possibly due to the increased mobilization and disorganized recruitment of capillary-derived endothelial cells, resulting in a field of enlarged vessels. Conversely the failure of yolk sac remodeling in the EC-Rbpj-KO model is due to the abrogation of endothelial cell migration to form the larger caliber vessels. Indeed, this early vascular remodeling is a rather distinct vascular mechanism that is not entirely clear and remains to be studied in detail.

Yolk sac vessel remodeling occurs after the initiation of blood flow, which initiates at approximately E8.5 in the mouse (Lucitti et al. 2007), and this flow is essential for the remodeling process. It is formally possible that the enlarged luminal diameter of the dorsal aorta in the Notch gain-of-function model could give rise to a secondary failure of yolk sac remodeling solely due to reduced flow and associated shear stress. However, the vessel architecture reported in mouse models with remodeling defects solely due to altered blood flow (Lucitti et al. 2007) display very different phenotypes from those observed in the N1ICD model. This comparison suggests that the remodeling defects and some of the associated gene expression defects in the yolk sac in this Notch1 gain-of-function model are not secondary to embryonic vessel defects or defects in blood flow. The cellular and subsequent molecular response to the shear stress associated with blood flow is not completely understood, but may involve complex cell surface signaling molecules including VEGFR2, PECAM1, and VE-cadherin (Tzima et al. 2005). Shear stress thus initiates a molecular cascade in endothelial cells to direct further morphological changes to direct remodeling. An important question is what is the link

between blood flow and Notch signaling, both of which are essential for vessel remodeling. During remodeling, an arteriole rudiment is first observed at the site of yolk sac vasculature contact with the omphalomesentric artery. Early *Dll4* expression is observed at this arteriole rudiment within the yolk sac (Duarte et al. 2004), indicating it is likely the Notch ligand that initiates Notch activity within this restricted region of the yolk sac vasculature. It remains to be seen the extent to which fluid dynamics control the expression of Notch signaling components and the subsequent remodeling process.

6.2 Model of role of Notch and VEGF pathways in vascular remodeling

Based on data from this dissertation, I propose a model for the role of Notch-VEGF signaling interactions in the regulation of the development of the vasculature, specifically in the remodeling of the vessels in to the large and small caliber vessels via the reallocation of endothelial cells. In the developing yolk sac endothelial cells are acted upon by factors from the adjacent endoderm and flow-induced shear stress. These in turn induce activation of the Notch signaling pathway in the endothelial cells. In particular, in my model, VEGF from the endoderm signals through its receptor, KDR, under the regulation of the secreted factor PlGF. This in turn induces the expression of the notch receptor, which translocates to the cell surface. Interaction between the Notch receptor and a Notch ligand on an adjacent endothelial cell is important for the regulation of select secreted factors, including *Tgfb2*, *Vegfc*, and *Pgf* among others. These molecules then act in a paracrine and autocrine manner to elaborate the local arterial microenvironment about the cell, including adjacent endothelial cells, smooth muscle cells and hematopoietic cells. Specifically PlGF acts to regulate VEGF signaling through KDR, which then activates Notch signaling by inducing the expression of both Notch ligands and receptors indicating a positive regulatory loop between the Notch and VEGF pathways in vascular development. This interaction directs endothelial cell migration and integration within the developing vasculature (Figure 6.1).

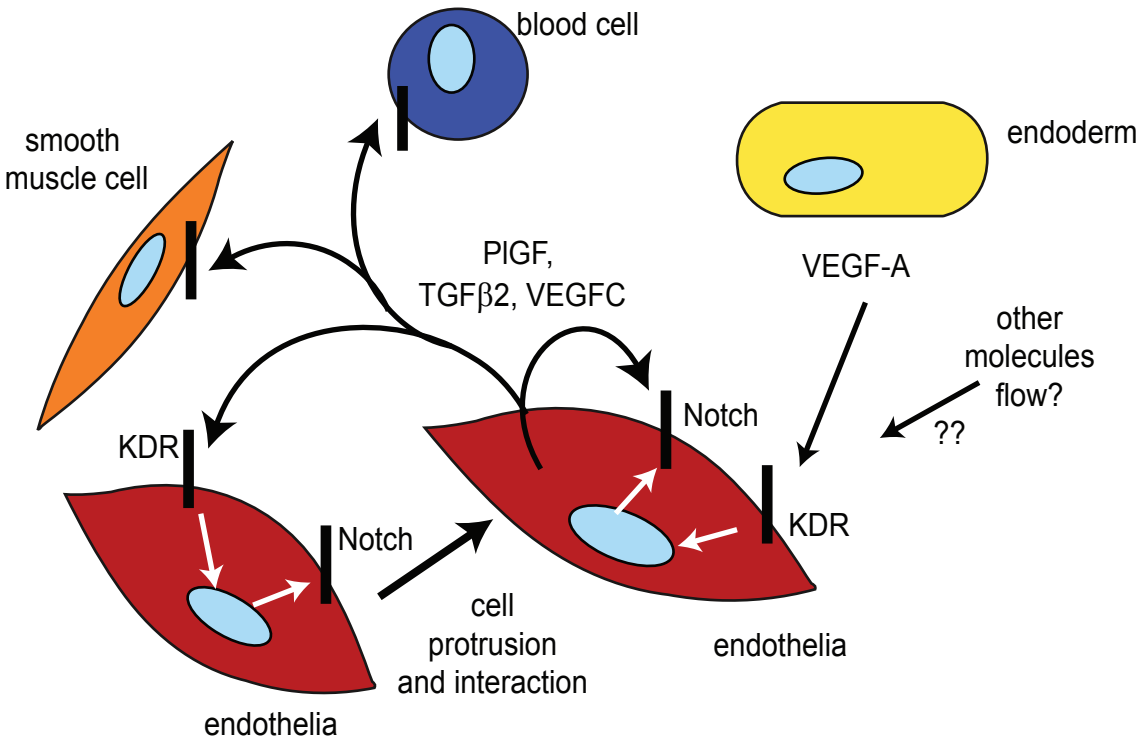

Figure 6.1. Model of Role of Notch and VEGF Pathways in Vascular Remodeling
Proposed model of signaling in the endodermal and endothelial cells of the early yolk sac. Signaling from the endoderm and regulation from blood flow activates Notch signaling in select endothelial cells. Notch activates the expression of secreted molecules, including PlGF, TGFβ2, and VEGFC, that in turn act in both a paracrine and juxtacrine manner to activate the Notch signaling pathway directing endothelial cell migration and integration within the developing vasculature.

6.2.1 Implications of model

6.2.1.1 Notch/VEGF interaction in embryonic vascular development

The data in this dissertation implicate Notch-VEGF signaling interactions as a key component in the regulation of vascular development. Previous work revealed genetic interaction between these pathways during arterial endothelial cell differentiation and sprouting angiogenesis (Siekmann et al. 2008). Non-endothelial cell studies indicate PTEN as a direct Notch target, resulting in the promotion of VEGF signaling through the MAPK pathway leading to arterial differentiation (Whelan et al. 2007). In mouse studies, Notch and VEGF interact to modulate endothelial cell identity during sprouting angiogenesis (Lobov et al. 2007). Recent in vitro studies indicate that Notch may function in these processes by directly regulating the expression of the VEGF receptors (Harrington et al. 2007; Taylor et al. 2002; Shawber et al. 2007). Gene expression analysis of the gain- and loss-of-function Notch models and the Z/EG-Pgf model showed only a little change in the expression of the VEGF receptors; aside from FLT1, which is increased approximately 2 fold in EC-N1ICD yolk sac (Table 3.1). Instead, Notch appears to regulate VEGF signaling through the regulation of ligand expression, namely PlGF and VEGFC, which in turn could increase the angiogenic signal through VEGF. VEGF signaling then acts to regulate expression of Notch ligands and receptors, forming a feedback loop between the two pathways similar to that seen in tumor angiogenesis.

It is hypothesized that in the early embryo, particularly in the yolk sac, the remodeling of the early vascular plexus occurs through the process of intussusceptive angiogenesis. As reviewed in Chapter 1, this process occurs via the insertion of 'pillars', which form from the protrusion, interaction, and perforation of endothelial cells from

opposing walls of a capillary. Data show that Notch signaling can regulate the expression of secreted factors that can then act to influence adjacent cells. Specifically, during the process of intussusceptive angiogenesis, Notch on one endothelial cell could act in both a paracrine and autocrine manner, via the secretion of VEGF and TGFβ molecules, to induce migration of itself and an endothelial cell on the opposing capillary wall, thus creating a 'pillar'. Overexpression of Notch, as in the gain-of-function model, increases the level of these secreted genes and in 'pillar' formation, resulting in a decrease in capillaries and vessel enlargement. A decrease in Notch signaling, like that in the loss-of-function model, results in a decrease of 'pillar' formation. The resulting vasculature is not remodeled and retains the immature polygon-shaped plexus.

6.2.1.2 Notch/VEGF interaction in pathological angiogenesis

As stated previously, Notch and VEGF signaling both play a role in the regulation of vascular formation in pathological conditions. Mutations in the *Notch3* gene lead to cerebral autosomal dominant arteriopathy with subcortical infarct and leukoencephalopathy (CADASIL) (Tang et al. 2009). Mutations in *Jag1* or in *Notch2* lead to Alagille Syndrome (AGS) (Kamath et al. 2004; Niessen and Karsan 2007). VEGF-A induces vascular permeability via activation of KDR and subsequent signaling involving Src-kinases (Eliceiri et al. 1999). PlGF has been shown to stimulate vascular leakage, likely by attenuating the response to VEGF-A (Park et al. 1994; Luttun et al. 2002). PlGF has also been shown to regulate inflammation and edema formation in adult mice (Oura et al. 2003).

Notch signaling and VEGF are both important for tumor angiogenesis, where they have been shown to interact. The ligand *Dll4* is strongly expressed in tumor vessels (Mailhos et al. 2001). VEGF-A and KDR are inducers of tumor angiogenesis (Kim et al. 1993; Carmeliet et al. 2001). PlGF is upregulated during tumor angiogenesis enhancing the angiogenic activity of VEGF-A (Carmeliet et al. 2001). In *Pgf*-deficient mice, tumor angiogenesis and growth are reduced (Carmeliet et al. 2001), while mice overexpressing *Pgf* in the skin exhibit increased melanoma growth (Marcellini et al. 2006). In tumors VEGF-A induces *Dll4* expression in sprouting endothelial cells, which in turn signals through Notch repressing the activation of VEGF receptors acting as a negative regulator of growth. Inhibition of Dll4/Notch signaling resulted in increased vessel density, but decreased vessel function (Noguera-Troise et al. 2006).

In the Notch1 gain-of-function model, the VEGF genes, *Vegfc* and *Pgf* were upregulated; while in the PlGF gain-of-function model the Notch genes, *Notch1*, *Notch4*, and *Dll4* had increased expression. These data further support the interaction between the Notch and VEGF signaling pathways observed in the regulation of tumor angiogenesis. However, in sprouting angiogenesis Notch acts to inhibit VEGF signaling by regulating VEGF receptors in the stalk cells, while in the proposed model Notch stimulates VEGF signaling through regulated expression of the VEGF ligands. This difference highlights contrasting roles for Notch in the regulation of vessel remodeling in the early embryonic yolk sac and sprouting angiogenesis in the adult and tumors. Further examination of these processes and development of therapies to regulate this interaction in tumor formation could be a successful treatment of cancer.

6.3 Future directions

Extensive analysis by others and myself has demonstrated an important role for both the Notch and VEGF pathways in physiological and pathological vascular formation. These pathways have also been shown to interact in a number of models, which has been corroborated in this dissertation in the remodeling of the yolk sac vasculature. However, there is much that remains unknown about this interaction and how it acts to regulate these processes. Although an extensive analysis of the Notch and Z/EG-Pgf models revealed significant morphological and molecular anomalies, further examination of the models is needed to refine the proposed model.

Specifically, the precise role of PlGF and its interaction with VEGF in the early embryo remains unknown. Further examination of its activity in both the Z/EG-Pgf and Notch models would add greatly to the current knowledge. Additionally, in respect to the in vitro Notch model, modifications to the system to better replicate in vivo results would be beneficial and would allow for additional type of experiments to be performed. A number of other, specific, experiments remain which would enhance the current knowledge of Notch and VEGF signaling and their role in the formation of the vascular system. These experiments are outlined in the following pages.

6.3.1 Notch signaling in vascular remodeling

Although there has been extensive analysis of the morphological defects resulting from mutations of the Notch signaling pathway and our lab has demonstrated altered patterns of gene expression in a number of genes in the gain-of-function Notch model, questions still remain. Additional experiments could expand on the exact mechanism of

vascular remodeling and the role of Notch in this process. Defects in the formation of the vasculature, particularly in the remodeling, are seen in both the gain-of-function and loss-of-function Notch models. Live imaging of the yolk sac in both Notch models used in this study would help to elaborate the behavior of the endothelial cells in the remodeling process.

Additionally, in this dissertation I initially examined gene expression via microarray and subsequently confirmed misexpression of only a subset of genes via RT-PCR. Numerous other genes were also upregulated and downregulated in these models, opening the door to a plethora of genes regulated directly or indirectly by Notch signaling, particularly secreted factors. The use of conditional transgenics and knockouts of these factors in the endothelia will be required to determine the roles of these factors in vivo in the remodeling process. Gene expression of the VEGF family members *Vegfc* and *Pgf* was however observed and confirmed in both whole yolk sac and isolated endothelial cells. Although *Vegf* and *Kdr* expression was not increased, it would be important to examine whether or not VEGF signaling through KDR was increased due to the increase in *Pgf* and/or *Vegfc*. Protein from EC-N1ICD yolk sac tissues could be analyzed via Western blot with antibodies to the phosphorylated form of KDR and compared to wild type tissues. These experiments could show an increase in the angiogenic signal through KDR resulting from the activation of the Notch pathway. This would be interesting, as it would further confirm the role of Notch in the modulation of the VEGF pathway.

6.3.2 Transgenic ES cell model

Our lab successfully generated an inducible ES cell line to examine Notch

signaling in vitro and optimized a protocol to differentiate ES cells to an endothelial cell type via ES cell aggregation. However, molecular analysis of the collagen-plated cells showed only limited similarity to in vivo models. Modifications to the system could help utilize the in vitro model as a companion to the in vivo Notch models. In vivo the endothelial cells of the developing vasculature of the yolk sac neighbor primitive endodermal cells from which signals arise and can influence the endothelial cells. These cells are also acted upon by the shear stress of blood flow, which is essential for vascular remodeling (Lucitti et al. 2007). If a protocol was established in which the plated EBs were co-cultured with an extraembryonic endoderm (XEN) cell line (Kunath et al. 2005) or with supplemented growth factors to better replicate those found in vivo and/or the flow-induced shear stress was replicated, the gene expression may better mimic the in vivo results. Furthermore, the growth factors present in the culture can influence the morphology of the vascular plexus and the expression patterns (Jakobsson et al. 2007). Although VEGF and FGF have been established as important growth factors for the differentiation of endothelial cells in culture, adjustments could improve the model system. Alternatively, this model of ES cell differentiation requires the formation of EBs, which consist of many different lineages. Purification of the differentiated ECs with an endothelial cell specific antibody, like PECAM1, via flow cytometry would also allow for a cleaner analysis of the gene expression differences within the EC lineage.

This study also utilized a collagen embedding protocol to study sprouting angiogenesis. Previous work by others following a protocol similar to ours saw an increase in sprouting with the addition of a gamma-secretase inhibitor visualized by immunofluorescence after treatment with a CD31 antibody (Jakobsson et al. 2010).

However, we saw no difference in the formation of the sprouts with either the activation or the abrogation of Notch signaling. The only differences between the two protocols were in the concentration of the gamma-secretase inhibitor and the length of time the embedded EBs were grown and visualized (6 days in our protocol compared to 10 days). Simple modifications to the system such as these could lead to the expected results and further elucidate the role of Notch signaling in sprouting angiogenesis.

6.3.3 Placental growth factor activity in vivo

In this dissertation I successfully designed and generated a conditional transgenic mouse model to overexpress PlGF in the endothelia. Although resulting embryos were characterized and extensive morphological and molecular analyses were performed, there is still much to understand. Additional experiments to further characterize this model could expand on the role of PlGF in vascular remodeling. Gene expression analysis was performed via real time-PCR on a subset of genes known to be critical for vascular development. Additionally, a microarray could be done to compare with genes seen in the EC-N1ICD microarray data set to identify novel genes involved in this process. While data indicated an increase in Notch family members, the exact role of PlGF in this regulation remains unknown. Since PlGF likely transmits the angiogenic signals through FLT1 or KDR (Park et al. 1994; Carmeliet et al. 2001), yolk sac protein could be analyzed via Western blot with antibodies to the phosphorylated forms of FLT1 and KDR and compared to wild type yolk sac. Because PlGF is a secreted factor, and the yolk sac consists of more than one cell type, gene expression could be analyzed in isolated endothelial cells as was done in the EC-N1ICD studies. Taken together, data from these

studies could provide additional evidence as to the factors involved in the complex hierarchy of signals in the regulation of vascular development.

I also characterized placental defects with respect to both the formation of the embryo-derived vasculature and the gene expression in the trophoblast lineages. The morphological defects could be further analyzed via histological and immunofluorescence assays and a molecular analysis of the placenta via real-time PCR could be done to examine what other factors are involved in this process.

6.3.4 Future transgenic studies

As a result of activation of Notch signaling a number of secreted factors exhibited increased gene expression. This being an important component of our proposed model of the role of Notch pathway in vascular remodeling, I chose to further examine this regulation by designing a conditional transgenic system to overexpress PlGF. Since little was known about PlGF activity in the early embryo it seemed an ideal choice. Additionally, conditional transgenic mice could be made to examine any of the other secreted molecules. Targeted deletions of members of the TGF-β pathway result in the improper formation of the vasculature, indicating the importance for TGF-β signaling during vascular development (Goumans and Mummery 2000). VEGFC is required for the formation of the lymphatic system and there are data supporting activities in angiogenesis, however there are no vascular defects in *Vegfc* null mice (Karkkainen et al. 2004; Cao et al. 1998). Neither TGFβ2 nor VEGFC activity has been examined in detail in the extraembryonic tissue of the early embryo, though the expression of *Vegfc* and *Tgfβ2* within the yolk sac suggests a potential function in this tissue. The development

and study of conditional transgenes to overexpress these factors in the endothelia of the early embryo could expand on their function in vascular remodeling and their relation to the Notch pathway.

6.4 Concluding remarks

In this dissertation I demonstrated the role for Notch and VEGF activity in the remodeling of the vasculature and the regulation of key genes in the embryonic vasculature. These pathways must be tightly regulated as unregulated expression leads to vascular deformity and embryonic lethality. The morphological and molecular data indicate a mechanism for Notch regulation, in concert with VEGF signaling, of vessel calibre in early vasculature remodeling, likely through the regulation of intussusceptive angiogenesis. Further work on the in vivo models will help to further define the relationship between the transcriptional networks regulated by Notch to direct endothelial differentiation, and the role of these Notch downstream targets in endothelial migration and vascular remodeling. The understanding of these interactions and processes will aid in the development of treatments affecting vascular differentiation, including heart disease and tumor progression.

References

Achen MG, Stacker SA. 1998. The vascular endothelial growth factor family: proteins which guide the development of the vasculature. *Int J Exp Pathol* **79**: 255-265.

Artavanis-Tsakonas S, Rand MD, Lake RJ. 1999. Notch signaling: cell fate control and signal integration in development. *Science* **284**: 770-776.

Bautch VL, Redick SD, Scalia A, Harmaty M, Carmeliet P, Rapoport R. 2000. Characterization of the vasculogenic block in the absence of vascular endothelial growth factor-A. *Blood* **95**: 1979-1987.

Bolos V, Grego-Bessa, J, de la Pompa, JL. 2007. Notch signaling in development and cancer. *Endocrine Rev* **28**: 339-363.

Burri PH, Hlushchuk R, Djonov V. 2004. Intussusceptive angiogenesis: its emergence, its characteristics, and its significance. *Dev Dyn* 231: 474-488.

Cao Y, Linden P, Shima D, Browne F, Folkman J. 1996. In vivo angiogenic activity and hypoxia induction of heterodimers of placenta growth factor/vascular endothelial growth factor. *J Clin Invest* **98**: 2507-2511.

Cao Y, Linden P, Farnebo J, Cao R, Eriksson A, Kumar V, Qi JH, Claesson-Welsh L, Alitalo K. 1998. Vascular endothelial growth factor C induces angiogenesis in vivo. *Proc Natl Acad Sci USA* **95**: 14389-14394.

Carlson TR, Yan Y, Wu X, Lam MT, Tang GL, Beverly LJ, Messina LM, Capobianco AJ, Werb Z, Wang R. 2005. Endothelial expression of constitutively active Notch4 elicits reversible arteriovenous malformations in adult mice. *Proc Natl Acad Sci USA* **102**: 9884-9889.

Carmeliet P, Ferreira V, Breier G, Pollefeyt S, Kieckens L, Gertsenstein M, Fahrig M, Vandenhoeck A, Harpal K, Eberhardt C, Declercq C, Pawling J, Moons L, Collen D, Risau W, Nagy A. 1996. Abnormal blood vessel development and lethality in embryos lacking a single VEGF allele. *Nature* **380**: 435-439.

Carmeliet P. 2000. Mechanisms of angiogenesis and arteriogenesis. *Nat Med* **6**: 389-395.

Carmeliet P, Moons L, Luttun A, Vincenti V, Compernolle V, De Mol M, Wu Y, Bono F, Devy L, Beck H, Scholz D, Acker T, DiPalma T, Dewerchin M, Noel A, Stalmans I, Barra A, Blacher S, Vandendriessche T, Ponten A, Eriksson U, Plate KH, Foidart JM, Schaper W, Charnock-Jones DS, Hicklin DJ, Herbert JM, Collen D, Persico MG. 2001. Synergism between vascular endothelial growth factor and placental growth factor contributes to angiogenesis and plasma extravasation in pathological conditions. *Nat Med* **7**: 575-583.

Choi K, Kennedy M, Kazarov A, Papadimitriou J, Keller G. 1998. A common precursor for hematopoietic and endothelial cells. *Dev* **125**: 725-732.

Copeland JN, Feng Y, Neradugomma NK, Fields PE, Vivian JL. 2011. Notch signaling regulates remodeling and vessel diameter in the extraembryonic yolk sac. *BMC Dev Biol* In Press.

Cormier S, Vandormael-Pournin S, Babinet C, Cohen-Tannoudji M. 2004. Developmental expression of the Notch signalling pathway genes during mouse preimplantation development. *Gene Expr Patterns* **4**:713-717.

Coultas L, Chawengsaksophak K, Rossant J. 2005. Endothelial cells and VEGF in vascular development. *Nature* **438**: 937-945.

Deshpande N, Pysz MA, Willmann JK. 2010. Molecular ultrasound assessment of tumor angiogenesis. *Angiogenesis* **13**: 175-188.

Djonov V, Schmid M, Tschanz SA, Burri PH. 2000. Intussusceptive Angiogenesis: its role in embryonic vascular network formation. *Circ Res* **86:** 286.

Djonov V, Andres AC, Ziemiecki A. 2001. Vascular remodelling during the normal and malignant life cycle of the mammary gland. *Microsc Res Tech* **52**: 182-189.

Djonov V, Baum O, Burri PH. 2003. Vascular remodeling by intussusceptive angiogenesis. *Cell Tissue Res* **314**: 107-117.

Drake CJ, Fleming PA. 2000. Vasculogenesis in the day 6.5 to 9.6 mouse embryo. *Blood* **95**: 1671-1679.

Drake CJ. 2003. Embryonic and adult vasculogenesis. *Birth Defects Res C Embryo Today* **69**: 73-82.

D'souza B, Miyamoto A, Weinmaster G. 2008. The many facets of Notch ligands. *Oncogene* **27**: 5148-5167.

Duarte A, Hirashima M, Benedito R, Trindade A, Diniz P, Bekman E, Costa L, Henrique D, Rossant J 2004. Dosage-sensitive requirement for mouse Dll4 in artery development. *Genes Dev* **18:** 2474-2478.

Dumont DJ, Gradwohl G, Fong GH, Puri MC, Gertsenstein M, Auerback A, Breitman ML. 1994. Dominant-negative and targeted null mutations in the endothelial receptor tyrosine kinase, tek, reveal a critical role in vasculogenesis of the embryo. *Genes Dev* **8**: 1897–1909.

Eliceiri BP, Paul R, Schwartzberg PL, Hood JD, Leng J, Cheresh DA. 1999. Selective requirement for Src kinases during VEGF-induced angiogenesis and vascular permeability. *Mol Cell* **4**: 915-924.

Ferrara N, Carver-Moore K, Chen H, Dowd M, Lu L, O'Shea KS, Powell-Braxton L, Hillan KJ, Moore MW. 1996. Heterozygous embryonic lethality induced by targeted inactivation of the VEGF gene. *Nature* **380**: 439-442.

Ferrara N, Davis-Smyth T. 1997. The biology of vascular endothelial growth factor. *Endocrine Rev* **18**: 4-25.

Fischer A, Schumacher N, Maier M, Sendtner M, Gessler M. 2004. The Notch target genes Hey1 and Hey2 are required for embryonic vascular development. *Genes Dev* **18**: 901-911.

Fong GH, Rossant J, Gertsenstein M, Breitman ML. 1995. Role of the Flt-1 receptor tyrosine kinase in regulating the assembly of vascular endothelium. *Nature* **376**: 66-70.

Funahashi Y, Shawber CJ, Vorontchikhina M, Sharma A, Outtz HH, Kitajewski J. 2010. Notch regulates the angiogenic response via induction of VEGFR-1. *J Angiogenes Res* **2**: 3.

Gale NW, Dominguez MG, Noguera I, Pan L, Hughes V, Valenzuela DM, Murphy AJ, Adams NC, Lin HC, Holash J, Thurston G, Yancopoulos GD. 2004. Haploinsufficiency of delta-like 4 ligand results in embryonic lethality due to major defects in arterial and vascular development. *Proc Natl Acad Sci USA* **101**: 15949-15954.

Gasperowicz M, Otto F. 2008. The Notch Signalling Pathway in the Development of the Mouse Placenta. *Placenta* **29**: 651-659.

Goumans MJ, Mummery C. 2000. Functional analysis of the TGF receptor/Smad pathway through gene ablation in mice. *Int J Dev Biol* **44**: 253–265.

Harrington LS, Sainson RC, Williams CK, Taylow JM, Shi W, Li JL, Harris AL. 2008. Regulation of multiple angiogenic pathways by Dll4 and Notch in human umbilical vein endothelial cells. *Microvasc Res* **75**: 144-154.

Hellstrom M, Kalen M, Lindahl P, Abramsson A, Betsholtz C. 1999. Role of PDGF-B and PDGFR-beta in recruitment of vascular smooth muscle cells and pericytes during embryonic blood vessel formation in the mouse. *Dev* **126**: 3047-3055.

Hermant B, Desroches-Castan A, Dubessay ML, Prandini MH, Huber P, Vittet D. 2007. Development of a one-step embryonic stem cell-based assay for the screening of sprouting angiogenesis. *BMC Biotechnol* **7**: 20.

Hillen F, Griffioen AW. 2007. Tumour vascularization: sprouting angiogenesis and beyond. *Cancer Metastasis Rev* **26**: 489-502.

Hlushchuk R, Riesterer O, Baum O, Wood J, Gruber G, Pruschy M, Djonov V. 2008. Tumor recovery by angiogenic switch from sprouting to intussusceptive angiogenesis after treatment with PTK787/ZK222584 or ionizing radiation. *Am J Pathol* **173**: 1173–1185.

Holderfield MT, Hughes CC. 2008. Crosstalk between vascular endothelial growth factor, notch, and transforming growth factor-beta in vascular morphogenesis. *Circ Res* **102**: 637-652.

Huppertz B, Peeters LL. 2005. Vascular biology in implantation and placentation. *Angiogenesis* **8**: 157-167.

Hurwitz H, Fehrenbacher L, Novotny W, Cartwright T, Hainsworth J, Heim W, Berlin J, Baron A, Griffing S, Holmgren E, Ferrara N, Fyfe G, Rogers B, Ross R, Kabbinavar F. 2004. Bevacizumab plus irinotecan, fluorouracil, and leucovorin for metastatic colorectal cancer. *N Engl J Med* **250**: 2335-2342.

Iso T, Kedes L, Hamamori Y. 2003. HES and HERP families: multiple effectors of the Notch signaling pathway. *J Cell Physiol* **194**: 237-255.

Iso T, Hamamori Y, Kedes L. 2003. Notch signaling in vascular development. *Arterioscler Thromb Vasc Biol* **23**: 543-553.

Jain RK. 2003. Molecular regulation of vessel maturation. *Nat Med.* **9**: 685-693.

Jakobsson L, Kreuger J, Claesson-Welsh L. 2007. Building blood vessels—stem cell models in vascular biology. *J Cell Biol* **177**: 751-755.

Jakobsson L, Franco CA, Bentley K, Collins RT, Ponsioen B, Aspalter IM, Rosewell I, Busse M, Thurston F, Medvinsky A, Schulte-Merker S, Gerhardt H. 2010. Endothelial cells dynamically compete for the tip cell position during angiogenic sprouting. *Nat Cell Biol* **12**: 943-953.

Jarriault S, Brou C, Logeat F, Schroeter EH, Kopan R, Israel A. 1995. Signalling downstream of activated mammalian Notch. *Nature* **377**: 355-358.

Ji RP, Phoon CK, Aristizabal O, McGrath KE, Pali J, Turnbull D. 2003. Onset of cardiac function during early mouse embryogenesis coincides with entry of primitive erythroblasts into the embryo proper. *Circ Res* **92**: 133-135.

Jones EAV, le Noble F, Eichmann A. 2006. What determines blood vessel structure? Genetic prespecification vs. hemodynamics. *Physiology* **21**: 388-395.

Kageyama R, Ohtsuka T. 1999. The Notch-Hes pathway in mammalian neural development. *Cell Res* **9**: 179-188.

Kamath BM, Spinner NB, Emerick KM, Chudley AE, Booth C, Piccoli DA, Krantz ID. 2004. Vascular anomalies in Alagille syndrome: a significant cause of morbidity and mortality. *Circulation* **109**: 1354-1358.

Kappas NC, Zeng G, Chappell JC, Kearney JB, Hazarika S, Kallianos KG, Patterson C, Annex BH, Bautch VL. 2008. The VEGF receptor Flt-1 spatially modulates Flk-1 signaling and blood vessel branching. *J Cell Bio* **181**: 847-858.

Karkkainen MJ, Haiko P, Sainio K, Partanen J, Taipale J, Petrova TV, Jeltsch M, Jackson DG, Talikka M, Rauvala H, Betsholtz C, Alitalo K. 2004. Vascular endothelial growth factor C is required for sprouting of the first lymphatic vessels from embryonic veins. *Nat Immunol* **5**: 74-80.

Karsan A. 2005. The role of notch in modeling and maintaining the vasculature. *Can J Pysiol Pharmacol* **83**: 14-23.

Kearney JB, Kappas NC, Ellerstrom C, DiPaola FW, Bautch VL. 2004. The VEGF receptor flt-1 (VEGFR-1) is a positive modulator of vascular sprout formation and branching morphogenesis. *Blood* **103**: 4527-4535.

Kendall RL, Thomas KA. 1993. Inhibition of vascular endothelial cell growth factor activity by an endogenously encoded soluble receptor. *Proc Natl Acad Sci USA* **90**: 10705-10709.

Kerbel RS. 2008. Tumor angiogenesis. *N Engl J Med* **358**: 2039-2049.

Kim KJ, Li B, Winer J, Armanini M, Gillett N, Phillips HS, Ferrara N. 1993. Inhibition of vascular endothelial growth factor-induced angiogenesis suppresses tumour growth in vivo. *Nature* **362**: 841-844.

Koni PA, Joshi SK, Temann UA, Olson D, Burkly L, Flavell RA. 2001. Conditional vascular cell adhesion molecule 1 deletion in mice: impaired lymphocyte migration to bone marrow. *J Exp Med* **193**: 741-754.

Kovall RA. 2007. Structures of CSL, Notch and Mastermind proteins: piecing together an active transcription complex. *Curr Opin Struct Biol* **17**: 117-127.

Krebs LT, Xue Y, Norton CR, Shutter JR, Maguire M, Sundberg JP, Gallahan D, Closson V, Kitajewski J, Callahan R, Smith GH, Stark KL, Gridley T. 2000. Notch signaling is essential for vascular morphogenesis in mice. *Genes Dev* **14**: 1343-1352.

Krebs LT, Deftos ML, Bevan MJ, Gridley T. 2001. The nrarp gene encodes an ankyrin-repeat protein that is transcriptionally regulated by the notch signaling pathway. *Dev Biol* **238**: 110-119.

Krebs LT, Xue Y, Norton CR, Sundberg JP, Beatus P, Lendahl U, Joutel A, Gridley T. 2003. Characterization of Notch3-deficient mice: normal embryonic development and absence of genetic interactions with a Notch1 mutation. *Genesis* **37**: 139-143.

Krebs LT, Shutter JR, Tanigaki K, Honjo T, Stark KL, Gridley T. 2004. Haploinsufficient lethality and formation of arteriovenous malformations in Notch pathway mutants. *Genes Dev* **18**: 2469-2473.

Krebs LT, Starling C, Chervonsky AV, Gridley T. 2010. *Notch1* activation in mice causes arteriovenous malformations phenocopied by ephrinB2 and EphB4 mutants. *Genesis* **48**: 146-150.

Kunath T, Arnaud D, Uy GD, Okamoto I, Chureau C, Yamanaka Y, Heard E, Gardner RL, Avner P, Rossant J. 2005. Imprinted X-inactivation in extra-embryonic endoderm cell lines from mouse blastocysts. *Dev* **132**: 1649-1661.

Kyba M, Perlingeiro RCR, Daley GQ. 2002. HoxB4 Confers Definitive Lymphoid-Myeloid Engraftment Potential on Embryonic Stem Cell and Yolk Sac Hematopoietic Progenitors. *Cell* **109**: 29-37.

Lawson ND, Vogel AM, Weinstein BM. 2002. Sonic hedgehog and vascular endothelial growth factor act upstream of the Notch pathway during arterial endothelial differentiation. *Dev Cell* **3**: 127-136.

Leimeister C, Externbrink A, Klamt B, Gessler M. 1999. Hey genes: a novel subfamily of hairy- and Enhancer of split related genes specifically expressed during mouse embryogenesis. *Mech Dev* **85**: 173-177.

Leimeister C, Schumacher N, Steidl C, Gessler M. 2000. Analysis of HeyL expression in wild-type and Notch pathway mutant mouse embryos. *Mech Dev* **98**:175-178.

Li S, Wang DZ, Wang A, Richardson JA, Olson EN. 2003. The serum response factor coactivator myocardin is required for vascular smooth muscle development. *Proc Natl Acad Sci USA* **100**: 9366-9370.

Limbourg FP, Takeshita K, Radtke R, Bronson RT, Chin MT, Liao JK. 2005. Essential role of endothelial Notch1 in angiogenesis. *Circulation* **111**: 1826-1832.

Lin TP, Labosky PA, Grabel LB, Kozak CA, Pitman JL, Kleeman J, MacLeod CL. 1994. The Pem homeobox gene is X-linked and exclusively expressed in extraembryonic tissues during early murine development. *Dev Biol* **166**: 170-179.

Liu ZJ, Shirakawa T, Li Y, Soma A, Oka M, Dotto GP, Fairman RM, Velazquez OC, Herlyn M. 2003. Regulation of Notch1 and Dll4 by vascular endothelial growth factor in arterial endothelial cells: implications for modulating arteriogenesis and angiogenesis. *Mol Cell Biol* **23**: 14-25.

Lobov IB, Renard RA, Papdopoulos N, Gale NW, Thurston G, Yancopoulos GD, Wiegand SJ. 2007. Delta-like ligand 4 (Dll4) is induced by VEGF as a negative regulator of angiogenic sprouting. *Proc Natl Acad Sci USA* **104**: 3219-3224.

Lohela M, Bry M, Tammela T, Alitalo K. 2009. VEGFs and receptors involved in angiogenesis versus lymphangiogenesis. *Curr Opin Cell Biol* **21**: 154-165.

Lucitti JL, Jones EAV, Huang C, Chen J, Fraser SE, Dickinson ME. 2007. Vascular remodeling of the mouse yolk sac requires hemodynamic force. *Dev* **134**: 3317-3326.

Luttun A, Brusselmans K, Fukao H, Tjwa M, Ueshima S, Herbert JM, Matsuo O, Collen D, Carmeliet P, Moons L. 2002. Loss of placental growth factor protects mice against vascular permeability in pathological conditions. *Biochem Biophys Res Commun* **295**: 428-434.

Maier MM, Gessler M. 2000. Comparative analysis of the human and mouse Hey1 promoter: Hey genes are new Notch target genes. *Biochem Biophys Res Commun* **275**: 652-660.

Mailhos C, Modlich U, Lewis J, Harris A, Bicknell R, Ish-Horowicz D. 2001. Delta4, an endothelial specific notch ligand expressed at sites of physiological and tumor angiogenesis. *Differentiation* **69**: 135-144.

Makanya AN, Hlushchuk R, Djonov VG. 2009. Intussusceptive angiogenesis and its role in vascular morphogenesis, patterning, and remodeling. *Angiogenesis* **12**: 113-123.

Marcellini M, De Luca N, Riccioni T, Ciucci A, Orecchia A, Lacal PM, Ruffini F, Pesce M, Cianfarani F, Zambruno G, Orlandi A, Failla CM. 2006. Increased melanoma growth and metastasis spreading in mice overexpressing placenta growth factor. *Am J Pathol* **169**: 643-654.

Matsumoto T, Claesson-Welsh L. 2001. VEGF receptor signal transduction. *Sci STKE* **2001**: re21.

McCloskey KE, Smith DA, Jo H, Nerem RM. 2006. Embryonic stem cell-derived endothelial cells may lack complete functional maturation in vitro. *J Vasc Res* **43**: 411-421.

Millauer B, Shawver LK, Plate JH, Risau W, Ullrich A. 1994. Glioblastoma growth inhibited in vivo by a dominant negative Flk-1 mutant. *Nature* **367**: 576-579.

Miquerol L, Gertsenstein M Harpal K, Rossant J, Nagy A. 1999. Multiple developmental roles of VEGF suggested by a LacZ-tagged allele. *Dev Biol* **212**: 307-322.

Mohr OL. 1919. Character changes caused by mutation of an entire region of a chromosome in drosophila. *Genetics* **4**: 275-282.

Motoike T, Markham DW, Rossant J, Sato TN. 2003. Evidence for novel fate of $Flk1^{+}$ progenitor: Contribution to muscle lineage**.** *Genesis* **35**: 153-159.

Mumm JS, Kopan R. 2000. Notch signaling: from the outside in. *Dev Biol* **228**: 151-165.

Murtaugh LC, Stanger BZ, Kwan KM, Melton DA. 2003. Notch signaling controls multiple steps of pancreatic differentiation. *Proc Natl Acad Sci USA* **100**: 14920-14925.

Neufeld G, Cohen T, Gengrinovitch S, Poltorak Z. 1999. Vascular endothelial growth factor (VEGF) and its receptors. *Faseb J* **13**: 9-22.

Niessen K, Karsan A. 2007. Notch signaling in the developing cardiovascular system. *Am J Physiol Cell Physiol* **293**: C1-11.

Nishimura M, Fumiaki I, Makoto I, Tomita K, Tsuda H, Nakanishi S, Kageyama R. 1998. Structure, chromosomal locus, and promoter of mouse Hes2 gene, a homologue of Drosophila hairy and Enhancer of split. *Genomics* **49**: 69-75.

Niwa H. 2007. How is pluripotency determined and maintained? *Dev* **134**: 635-646.

Niwa H. 2010. Mouse ES cell culture system as a model of development. *Dev Growth Differ* **52**: 275-283.

Noghero A, Bussolino F, Gualandris A. 2010. Role of the microenvironment in the specification of endothelial progenitors derived from embryonic stem cells. *Microvasc Res* **79**: 178-183.

Noguera-Troise I, Daly C, Papdopoulos NJ, Coetzee S, Boland P, Gale NW, Lin HC, Yancopoulos GD, Thurston G. 2006. Blockade of Dll4 inhibits tumor growth by promoting non-productive angiogenesis. *Nature* **444**: 1032-1037.

Novak A, Guo C, Yang W, Nagy A, Lobe CG. 2000. Z/EG, a double reporter mouse line that expresses enhanced green fluorescent protein upon Cre-mediated excision. *Genesis* **28**: 147-155.

Nyberg P, Salo T, Kalluri R. 2008. Tumor microenvironment and angiogenesis. *Front Biosci* **13**: 6527-6553.

Odorisio T, Schietroma C, Zaccaria ML, Cianfarani F, Tiveron C, Tatangelo L, Failla CM, Zambruno G. 2002. Mice overexpressing placenta growth factor exhibit increased vascularization and vessel permeability. *J Cell Sci* **115**: 2559-2567.

Oura H, Bertoncini J, Velasco P, Brown LF, Carmeliet P, Detmar M. 2003. A critical role of placental growth factor in the induction of inflammation and edema formation. *Blood* **101**: 560-567.

Ovcharenko I, Nobrega MA, Loots GG, Stubbs L. 2004. ECR browser: a tool for visualizing and accessing data from comparisons of multiple vertebrate genomes. *Nucleic Acids Res* **32**: W280-286.

Park JE, Chen HH, Winer J, Houck KA, Ferrara N. 1994. Placenta growth factor. Potentiation of vascular endothelial growth factor bioactivity, in vitro and in vivo, and high affinity binding to Flt-1 but not to Flk-1/KDR. *J Biol Chem* **269**: 25646-25654.

Patan S. 2000. Vasculogenesis and angiogenesis as mechanisms of vascular network formation, growth and remodeling. *J Neurooncol* **50**: 1-15.

Qian C, Yan W, Zhang J, Shi L, Qian J, Fu Z, Kang C, Liu N, You Y. 2009. Notch1 induces enhanced expression of D-like-1 in the U251MG glioma cell line. *Int J Mol Med* **24**: 445-451.

Quinn TP, Peters KG, De Vries C, Ferrara N, Williams LT. 1993. Fetal liver kinase 1 is a receptor for vascular endothelial growth factor and is selectively expressed in vascular endothelium. *Proc Natl Acad Sci USA* **90**: 7533-7537.

Radtke, F, Raj, K. 2003. The role of Notch in tumorigenesis: oncogene or tumour suppressor? *Nat Rev Cancer* **3**: 756-767.

Reedijk M, Odorcic S, Chang L, Zhang H, Miller N, McCready DR, Lockwood G, Egan SE. 2005. High-level coexpression of JAG1 and NOTCH1 is observed in human breast cancer and is associated with poor overall survival. *Cancer Res* **65**: 8530-8537.

Risau W, Flamme I. 1995. Vasculogenesis. *Annu Rev Cell Dev Biol* **11**: 73-91.

Risau W. 1997. Mechanisms of angiogenesis. *Nature* **386**: 671-674.

Ross DA, Kadesh T. 2004. Consequences of Notch-mediated induction of Jagged1. *Exp Cell Res* **296**: 173-182.

Rossant J, Howard L. 2002. Signaling pathways in vascular development. *Annu Rev Cell Dev Biol* **18**: 541-573

Ryolva SN, Randhawa PK, Bautch VL. 2008. In vitro differentiation of mouse embryonic stem cells into primitive blood vessels. *Methods Enzymol* **443**: 103-117.

Saleh M, Stacker SA, Wilkes AF. 1996. Inhibition of growth of C6 glioma cells in vivo by expression of antisense vascular endothelial growth factor sequence. *Cancer Res* **56**: 393-401.

Santagata S, Demichelis F, Riva A, Varambally S, Hofer MD, Kutok JL, Kim R, Tang J, Montie JE, Chinnaiyan AM, Rubin MA, Aster JC. 2004. JAGGED1 expression is associated with prostate cancer metastasis and recurrence. *Cancer Res* **64**: 6854-6857.

Schlatter P, Konig MF, Karlsson LM, Burri PH. 1997. Quantitative study of intussusceptive capillary growth in the chorioallantoic membrane (CAM) of the chicken embryo. *Microvasc Res* **54**: 65-73.

Schmidt A, Brixius K, Bloch W. 2007. Endothelial precursor cell migration during vasculogenesis. *Circ Res* **101:** 125-136.

Shalaby F, Rossant J, Yamaguchi TP, Gertsenstein M, Wu XF, Breitman ML, Schuh AC. 1995. Failure of blood-island formation and vasculogenesis in Flk-1-deficient mice. *Nature* **376**: 62-66.

Shawber CJ, Funahashi Y, Francisco E, Vorontchikhina M, Kitamura Y, Stowell SA, Borisenko V, Feirt N, Podgrabinska S, Shiraishi K, Chawengsaksophak K, Rossant J, Accili D, Skobe M, Kitajewski J. 2007. Notch alters VEGF responsiveness in human and murine endothelial cells by direct regulation of VEGFR-3 expression. *J Clin Invest* **117**: 3369-3382.

Shibuya M, Yamaguchi S, Yamane A, Ikeda T, Tojo A, Matsushime H, Sato M. 1990. Nucleotide sequence and expression of a novel human receptor-type tyrosine kinase gene (flt) closely related to the fms family. *Oncogene* **5**: 519-524.

Siekmann AF, Lawson ND. 2007. Notch signaling and the regulation of angiogenesis. *Cell Adh Migr* **1**: 104-106.

Siekmann AF, Covassin L, Lawson ND. 2008. Modulation of VEGF signalling output by the Notch pathway. *BioEssays* **30**: 303-313.

Soriano P. 1999. Generalized lacZ expression with the ROSA26 Cre reporter strain. *Nat Genet* **21**: 70-71.

Souilhol C, Cormier S, Tanigaki K, Babinet C, Cohen-Tannoudji M. 2006. RBP-Jkappa-dependent notch signaling is dispensable for mouse early embryonic development**.** *Mol Cell Biol* **26**: 4769-4774.

Steenhard BM, Isom K, Stroganova L, St John PL, Freeburg PB, Holzman LB, Abrahamson DR. 2010. Deletion of Von Hippel-Lindau in glomerular podocytes results in glomerular basement membrane thickening, ectopic subepithelial deposition of

collagen α1α2α1(IV), expression of neuroglobin, and proteinuria. *Am J Pathol* **177**: 84-96.

Suri C, Jones PF, Patan S, Bartunkova S, Maisonpierre PC, Davis S, Sato TN, Yancopoulos GD. 1996. Requisite role of angiopoietin-1, a ligand for the TIE2 receptor, during embryonic angiogenesis. *Cell* **87**: 1171–1180.

Swiatek PJ, Lindsell CE, del Amo FF, Weinmaster G, Gridley T. 1994. Notch1 is essential for postimplantation development in mice. *Genes Dev* **8**: 707-719.

Tallquist M, Soriano P, Klinghoffer RA. 1999. Growth factor signaling pathways in vascular development. *Oncogene* **18**: 7917-7932.

Tang SC, Jeng JS, Lee MJ, Yip PK. 2009. Notch signaling and CADASIL. *Acta Neurol Taiwan* **18**: 81-90.

Tanigaki K, Han H, Yamamoto N, Tashiro K, Ikegawa M, Kuroda K, Suzuki A, Nakano T, Honjo T. 2002. Notch-RBP-J signaling is involved in cell fate determination of marginal zone B cells. *Nat Immunol* **3**: 443-450.

Taylor KL, Henderson AM, Hughes CC. 2002. Notch activation during endothelial cell network formation in vitro targets the basic HLH transcription factor HESR-1 and downregulates VEGFR-2/KDR expression. *Microvasc Res* **64**: 372-2823.

Tjwa M, Lutton A, Autiero M, Carmeliet P. 2003. VEGF and PlGF: two pleiotropic growth factors with distinct roles in development and homeostasis. *Cell Tissue Res* **314**: 5-14.

Trindade A, Kumar SR, Scehnet JS, Lopes-da-Costa L, Becker J, Jiang W, Liu R, Gill PS, Duarte A. 2008. Overexpression of delta-like 4 induces arterialization and attenuates vessel formation in developing mouse embryos. *Blood* **112**: 1720-1729.

Tun T, Hamaguchi Y, Matsunami N, Furukawa T, Honjo T, Kawaichi M. 1994. Recognition sequence of a highly conserved DNA binding protein RBP-J kappa. *Nucleic Acids Res* **22**: 965-971.

Tzima E, Irani-Tehrani M, Kiosses WB, Dejana E, Schultz DA, Engelhardt B, Cao G, DeLisser H, Schwartz MA. 2005. A mechanosensory complex that mediates the endothelial cell response to fluid shear stress. *Nature* **437**: 426-431.

Ueno H, Weissman IL. 2006. Clonal analysis of mouse development reveals a polyclonal origin for yolk sac blood islands. *Dev Cell* **11**: 519-533.

Uyttendaele H, Marazzi G, Wu G, Yan Q, Sassoon D, Kitajewski J. 1996. Notch4/int-3, a mammary proto-oncogene, is an endothelial cell-specific mammalian Notch gene. *Development* **122**: 2251-2259.

Uyttendaele H, Ho J, Rossant J, Kitajewski J. 2001. Vascular patterning defects associated with expression of activated Notch4 in embryonic endothelium. *Proc Natl Acad Sci USA* **98**: 5643-5648.

Venkatesh DA, Park K, Harrington A, Miceli-Libby L, Yoon JK, Liaw L. 2008. Cardiovascular and hematopoietic defects associated with Notch1 activation in embryonic Tie2-expressing populations. *Circ Res* **103**: 423-431.

Venuti JM, Morris JH, Vivian JL, Olson EN, Klein WH. 1995. Myogenin is required for late by not early aspects of myogenesis during mouse development. *J Cell Biol* **128**: 563-576.

Villa N, Walker L, Lindsell CE, Gasso J, Iruela-Arispe ML, Weinmaster G. 2001. Vascular expression of Notch pathway receptors and ligands is restricted to arterial vessels. *Mech Dev* **108**: 161-164.

Vuorela P, Hatva E, Lymboussaki A, Kaipainen A, Joukov V, Persico MG, Alitalo K, Halmesmaki E. 1997. Expression of vascular endothelial growth factor and placenta growth factor in human placenta. *Biol Reprod* **56**: 489-494.

Wedge SR, Ogilive DJ, Dukes M, Kendrew J, Curwen JO, Hennequin LF, Thomas AP, Stokes ES, Curry B, Richmond GH, Wadsworth PF. 2000. ZD4190: an orally active inhibitor of vascular endothelial growth factor signaling with broad-spectrum antitumor efficacy. *Cancer Res* **60**: 970-975.

Weinmaster G. 1998. Notch signaling: direct or what? *Curr Opin Genet Dev* **228**: 151-165.

Whelan JT, Forbes SL, Bertrand FE. 2007. CBF-1 (RBP-J kappa) binds to the PTEN promoter and regulates PTEN gene expression. *Cell Cycle* **6**: 80-84.

Wood JM, Bold G, Buchdunger E, Cozens R, Ferrari S, Frei J, Hofmann F, Mestan J, Mett H, O'Reilly T, Persohn E, Rosel J, Schnell C, Stover D, Theuer A, Towbin H, Wenger F, Woods-Cook K, Menrad a, Siemeister G, Schirner M, Thierauch KH, Schneider MR, Drevs J, Martiny-Baron F, Totzke F. 2000. PTK787/ZK 22584, a novel and potent inhibitor of vascular endothelial growth factor receptor tyrosine kinases, impairs vascular endothelial growth factor-induced responses and tumor growth after oral administration. *Cancer Res* **60**: 2178-2189.

Xue Y, Gao X, Lindsell CE, Norton CR, Chang B, Hicks C, Gendron-Maguire M, Rand EB, Weinmaster G, Gridley T. 1999. Embryonic lethality and vascular defects in mice lacking the Notch ligand Jagged1. *Hum Mol Genet* **8**: 723-730.

Yancopoulos GD, Davis S, Gale NW, Rudge JS, Wiegand SJ, Holash J. 2000. Vascular-specific growth factors and blood vessel formation. *Nature* **407**: 242-248.

Zeng G, Taylor SM, McColm JR, Kappas NC, Kearney JB, Williams LH, Hartnett ME, Bautch VL. 2007. Orientation of endothelial cell division is regulated by VEGF signaling during blood vessel formation. *Blood* **109:** 1345-1352.

Zhao Q, Egashira K, Hiasa KI, Ishibashi M, Inoue S, Ohtani K, Tan C, Shibuya M, Takeshita A, Sunagawa K. 2004. Essential role of vascular endothelial growth factor and Flt-1 signals in neointimal formation after periadventitial injury. *Arterioscler Thromb Vasc Biol* **24**: 2284-2289.

Appendix I

Microarray data of EC-N1ICD Yolk Sacs*

AI-1 Top 50 Upregulated genes

Gene Symbol	Gene Name	Probe	Fold change
Ankrd1	ankyrin repeat domain 1	1420991_at	11.89
Upk3a	uroplakin 3A	1449104_at	11.23
Myh6	myosin, heavy polypeptide 6, cardiac muscle, alpha	1448826_at	6.04
Cyp2f2	cytochrome P450, family 2, subfamily f, polypeptide 2	1448792_a_at	6.01
Rgs5	regulator of G-protein signaling 5	1420941_at	5.97
Ntn4	netrin 4	1439794_at	5.76
Actc1	actin, alpha, cardiac	1415927_at	5.48
Heyl	hairy/enhancer-of-split related with YRPW motif-like	1438886_at	5.45
Ifi202b	interferon activated gene 202B	1452349_x_at	5.38
Ly86	lymphocyte antigen 86	1422903_at	5.23
Spib	Spi-B transcription factor (Spi-1/PU.1 related)	1460407_at	5.04
Irx5	Iroquois related homeobox 5 (Drosophila)	1421072_at	5.03
Col8a1	collagen, type VIII, alpha 1	1455627_at	4.88
Fabp7	fatty acid binding protein 7, brain	1450779_at	4.8
Tbx18	T-box18	1429974_at	4.77
Ttn	titin	1427445_a_at	4.68
Rrad	Ras-related associated with diabetes	1422562_at	4.61
Gbp2	guanylate nucleotide binding protein 2	1435906_x_at	4.48
C1qb	complement component 1, q subcomponent, beta polypeptide	1417063_at	4.42
Gbp4	guanylate nucleotide binding protein 3	1418392_a_at	4.36
Pscdbp	pleckstrin homology, Sec7 and coiled-coil domains, binding protein	1451206_s_at	4.36
Oasl2	2'-5' oligoadenylate synthetase-like 2	1453196_a_at	4.33
Tgtp	T-cell specific GTPase	1449009_at	4.32
Myl7	myosin, light polypeptide 7, regulatory	1449071_at	4.23

Ifit1	interferon-induced protein with tetratricopeptide repeats 1	1450783_at	4.16
Crlf1	cytokine receptor-like factor 1	1418476_at	4.04
Vldlr	very low density lipoprotein receptor	1434465_x_at	4.04
Nrarp	Notch-regulated ankyrin repeat protein	1417985_at	4.02
Olfm3	olfactomedin 3	1425898_x_at	3.97
Cdh2	cadherin 2	1418815_at	3.88
Hoxa9	homeo box A9	1455626_at	3.87
Igfbp3	insulin-like growth factor binding protein 3	1423062_at	3.85
Amacr	alpha-methylacyl-CoA racemase	1417208_at	3.82
Ifih1	interferon induced with helicase C domain 1	1426276_at	3.82
Sox11	SRY-box containing gene 11	1436790_a_at	3.8
Jun	Jun oncogene	1417409_at	3.79
Foxq1	forkhead box Q1	1438558_x_at	3.78
Emr4	EGF-like module containing, mucin-like, hormone receptor-like sequence 4	1451563_at	3.73
Crabp1	cellular retinoic acid binding protein I	1448326_a_at	3.72
Vegfc	vascular endothelial growth factor C	1439766_x_at	3.65
Pilra	paired immunoglobin-like type 2 receptor alpha	1427327_at	3.61
Sh3bgr	SH3-binding domain glutamic acid-rich protein	1422644_at	3.6
Ubap2	ubiquitin-associated protein 2	1442375_at	3.59
Cbx7	chromobox homolog 7	1420039_s_at	3.59
Magel2	melanoma antigen, family L, 2	1417217_at	3.55
Ptk2	PTK2 protein tyrosine kinase 2	1440082_at	3.54
Hey1	hairy/enhancer-of-split related with YRPW motif 1	1415999_at	3.53
Tbx4	T-box 4	1456033_at	3.44
Esm1	endothelial cell-specific molecule 1	1449280_at	3.41
Gucy2c	guanylate cyclase 2c	1436370_at	3.38

AI-2 Top 50 Downregulated genes

Gene Symbol	Gene Name	Probe	Fold change
Cxcl7	chemokine (C-X-C motif) ligand 7	1418480_at	-7.69
Calml4	calmodulin-like 4	1424713_at	-7.34
Mpo	myeloperoxidase	1415960_at	-5.48
Csf2rb1	colony stimulating factor 2 receptor, beta 1, low-affinity (granulocyte-macrophage)	1421326_at	-5.18
Eif2s1	eukaryotic translation initiation factor 2, subunit 1 alpha	1420491_at	-5.18
Gypa	glycophorin A	1423016_a_at	-4.48
Cxcl4	chemokine (C-X-C motif) ligand 4	1448995_at	-4.22
Rgs18	regulator of G-protein signaling 18	1420398_at	-4.07
Prap1	proline-rich acidic protein 1	1455996_x_at	-3.97
Fbp2	fructose bisphosphatase 2	1449088_at	-3.88
Atp10d	ATPase, Class V, type 10D	1436544_at	-3.73
Oit3	oncoprotein induced transcript 3	1425125_at	-3.7
Abcb1a	ATP-binding cassette, sub-family B (MDR/TAP), member 1A	1419758_at	-3.69
Map3k7	mitogen-activated protein kinase kinase kinase 7	1433270_at	-3.55
Ppargc1a	peroxisome proliferative activated receptor, gamma, coactivator 1 alpha	1434100_x_at	-3.5
Ncf4	neutrophil cytosolic factor 4	1418465_at	-3.4
Dscr6	Down syndrome critical region homolog 6 (human)	1420459_at	-3.32
Plxnc1	plexin C1	1450905_at	-3.3
Hif3a	hypoxia inducible factor 3, alpha subunit	1425429_s_at	-3.28
Haao	3-hydroxyanthranilate 3,4-dioxygenase	1432492_a_at	-3.27
Cited4	Cbp/p300-interacting transactivator, with Glu/Asp-rich carboxy-terminal domain, 4	1425400_a_at	-3.19
Eif5b	eukaryotic translation initiation factor 5B	1435592_at	-3.13
Vat1	vesicle amine transport protein 1 homolog (T californica)	1423726_at	-3.11
Taok1	TAO kinase 1	1459770_at	-3.09
Fcgr3	Fc receptor, IgG, low affinity IIb	1448620_at	-3.09
Pi4k2b	phophatidylinositol 4-kinase type 2 beta	1420411_a_at	-3.02
Pde10a	phosphodiesterase 10A	1439618_at	-2.99
Cyp2a4	cytochrome P450, family 2, subfamily a, polypeptide 4	1422230_s_at	-2.99
Spred2	sprouty protein with EVH-1 domain 2, related sequence	1436892_at	-2.97
Tfrc	transferrin receptor	1452661_at	-2.95

Xdh	xanthine dehydrogenase	1451006_at	-2.94
Agtrl1	apelin receptor	1438651_a_at	-2.93
Asb17	ankyrin repeat and SOCS box-containing protein 17	1420468_at	-2.92
Myo7b	myosin VIIb	1420426_at	-2.92
Hba-a1	hemoglobin alpha, adult chain 1	1417714_x_at	-2.83
Itga3	integrin alpha 3	1421997_s_at	-2.82
Slc6a19	solute carrier family 6 (neurotransmitter transporter), member 19	1428595_at	-2.77
Lgals3	lectin, galactose binding, soluble 3	1426808_at	-2.77
Timm50	translocase of inner mitochondrial membrane 50 homolog	1441819_x_at	-2.75
Casq2	calsequestrin 2	1454395_at	-2.69
Foxh1	forkhead box H1	1422213_s_at	-2.65
Ywhaz	tyrosine 3-monooxygenase/tryptophan 5-monooxygenase activation protein, zeta polypeptide	1416103_at	-2.64
Wdtc1	WD and tetratricopeptide repeats 1	1434560_at	-2.64
Pof1b	premature ovarian failure 1B	1427492_at	-2.64
Ell2	elongation factor RNA polymerase II 2	1450744_at	-2.63
Cd36	CD36 antigen	1450884_at	-2.6
Epb4.2	erythrocyte protein band 4.2	1417337_at	-2.57
Sftpd	surfactant associated protein D	1420378_at	-2.56
Nudt4	nudix (nucleoside diphosphate linked moiety X)-type motif 4	1449107_at	-2.55
Mscp	solute carrier family 25, member 37	1417750_a_at	-2.55

* Microarray data was deposited to the Gene Expression Omnibus (GSE22418)

Appendix II

Microarray data of EC-Rbpj-KO Yolk Sacs*

AII-1 Top 50 Upregulated genes

Gene Symbol	Gene Name	Probe	Fold change
Rps9	ribosomal protein S9	1434624_x_at	28.01
Ifi202b	interferon activated gene 202B	1457666_s_at	9.68
Kcnj11	potassium inwardly rectifying channel, subfamily J, member 11	1455417_at	8.12
Ly86	lymphocyte antigen 86	1422903_at	8.04
Kcne3	potassium voltage-gated channel, Isk-related subfamily, gene 3	1418499_a_at	6.14
Dkk1	dickkopf homolog 1 (Xenopus laevis)	1420360_at	6.03
Plcxd1	phosphatidylinositol-specific phospholipase C, X domain containing 1	1437842_at	5.96
Ppp1r3c	protein phosphatase 1, regulatory (inhibitor) subunit 3C	1433691_at	5.94
Cx3cr1	chemokine (C-X3-C) receptor 1	1450020_at	5.63
Ndrg1	N-myc downstream regulated gene 1	1423413_at	5.33
Spon2	spondin 2, extracellular matrix protein	1417860_a_at	4.96
Fbp1	fructose bisphosphatase 1	1448470_at	4.77
Slc6a20	solute carrier family 6 (neurotransmitter transporter), member 20B	1436667_at	4.74
Vtn	vitronectin	1420484_a_at	4.73
Adamtsl4	ADAMTS-like 4	1451932_a_at	4.63
Olfm3	olfactomedin 3	1425898_x_at	4.62
Gm1381	family with sequence similarity 47, member E	1455383_at	4.55
Fbxo39	F-box protein 39	1443698_at	4.51
Cd52	CD52 antigen	1460218_at	4.44
Igsf4c	cell adhesion molecule 4	1426263_at	4.38
Cfc1	cripto, FRL-1, cryptic family 1	1421524_at	4.37
Ctss	cathepsin S	1448591_at	4.28
Lrrc39	leucine rich repeat containing 39	1453592_at	4.26
Ch25h	cholesterol 25-hydroxylase	1449227_at	4.20
Lamb3	laminin, beta 3	1417812_a_at	4.19
Kcnj8	potassium inwardly-rectifying channel, subfamily J, member 8	1418142_at	4.14
Ddit4	DNA-damage-inducible transcript 4	1428306_at	4.10
Igfbp3	insulin-like growth factor binding protein 3	1423062_at	4.05

Lst1	leukocyte specific transcript 1	1425548_a_at	4.01
Hspa1a	heat shock protein 1A	1452388_at	3.95
Leap2	liver-expressed antimicrobial peptide 2	1427480_at	3.94
Adm	adrenomedullin	1447839_x_at	3.91
Ces1	carboxylesterase 1G	1449486_at	3.83
Gadd45b	growth arrest and DNA-damage-inducible 45 beta	1450971_at	3.81
Lyzs	lysozyme 2	1439426_x_at	3.81
Cd200	CD200 antigen	1448788_at	3.72
Ndrl	N-myc downstream regulated gene 1	1420760_s_at	3.71
Amdhd1	amidohydrolase domain containing 1	1427370_at	3.69
Gys2	glycogen synthase 2	1424815_at	3.68
B3galt6	UDP-Gal:betaGal beta 1,3-galactosyltransferase, polypeptide 6	1435252_at	3.68
D17892	expressed sequence D17892	1447986_at	3.67
Slc22a3	solute carrier family 22 (organic cation transporter), member 3	1420444_at	3.66
Rprm	reprimo, TP53 dependent G2 arrest mediator candidate	1422552_at	3.63
Ms4a6b	membrane-spanning 4-domains, subfamily A, member 6B	1418826_at	3.60
H2-Q8	histocompatibility 2, Q region locus 8	1430802_at	3.54
Esm1	endothelial cell-specific molecule 1	1449280_at	3.51
Gja5	gap junction protein, alpha 5	1429101_at	3.48
Blnk	B-cell linker	1451780_at	3.47
Vcam1	vascular cell adhesion molecule 1	1448162_at	3.45
Lzp-s	lysozyme 1	1436996_x_at	3.45

AII-2 Top 50 downregulated genes

Gene Symbol	Gene Name	Probe	Fold change
Prlpe	prolactin family 7, subfamily a, member 1	1449529_s_at	-32.36
Ctsj	cathepsin J	1416413_at	-17.92
Plf	prolactin family 2, subfamily c, member 2	1427760_s_at	-16.32
Mtmr7	myotubularin related protein 7	1447831_s_at	-15.36
Csh1	prolactin family 3, subfamily d, member 1	1439002_s_at	-11.68
Abcb1b	ATP-binding cassette, sub-family B (MDR/TAP), member 1B	1418872_at	-10.68
Plekha6	pleckstrin homology domain containing, family A	1427149_at	-10.3
Dusp4	dual specificity phosphatase 4	1428834_at	-9.6
Csh2	prolactin family 3, subfamily b, member 1	1415835_at	-9.27
Slc39a8	solute carrier family 39 (metal ion transporter),	1448482_at	-8.43
Prlpa	prolactin family 4, subfamily a, member 1	1448572_at	-8.02
Prlpk	prolactin family 2, subfamily b, member 1	1426730_a_at	-7.02
Myo1b	myosin IB	1447364_x_at	-6.7
Mfap3l	microfibrillar-associated protein 3-like	1428804_at	-6.68
Pi4k2b	phosphatidylinositol 4-kinase type 2 beta	1420411_a_at	-5.86
Fgl1	fibrinogen-like protein 1	1424599_at	-5.6
Eomes	eomesodermin homolog (Xenopus laevis)	1435172_at	-5.48
Bach2	BTB and CNC homology 2	1437667_a_at	-4.95
Dusp6	dual specificity phosphatase 6	1415834_at	-4.83
Ceacam1	carcinoembryonic antigen-related cell adhesion	1425538_x_at	-4.78
Tmem27	transmembrane protein 27	1435064_a_at	-4.69
Hdc	histidine decarboxylase	1454713_s_at	-4.68
Abca1	ATP-binding cassette, sub-family A (ABC1),	1421840_at	-4.59
Hsf2bp	heat shock transcription factor 2 binding protein	1428640_at	-4.56
Kndc1	kinase non-catalytic C-lobe domain (KIND) containing 1	1428599_at	-4.43
Birc1a	NLR family, apoptosis inhibitory protein 1	1425298_a_at	-4.32
Fcgr3	Fc receptor, IgG, low affinity III	1448620_at	-4.26
Spred2	sprouty-related, EVH1 domain containing 2	1434403_at	-4.26
Cd59a	CD59a antigen	1418710_at	-4.09
Rgl1	ral guanine nucleotide dissociation stimulator, -like 1	1418535_at	-4.04
Coro2a	coronin, actin binding protein 2A	1436199_at	-3.92
Gm440	RUN domain containing 3B	1434456_at	-3.86
Bat2d	proline-rich coiled-coil 2C	1429432_at	-3.85
Tfrc	transferrin receptor	1422967_a_at	-3.85
Tulp2	tubby-like protein 2	1417276_at	-3.84

Abcb1a	ATP-binding cassette, sub-family B (MDR/TAP), member 1A	1419758_at	-3.83
B4galt6	UDP-Gal:betaGlcNAc beta 1,4-galactosyltransferase, polypeptide 6	1450913_at	-3.79
Dnahc8	dynein, axonemal, heavy chain 8	1424936_a_at	-3.66
Frmd4b	FERM domain containing 4B	1426594_at	-3.64
Slc23a1	solute carrier family 23 (nucleobase transporters), member 1	1450404_at	-3.63
Tipin	timeless interacting protein	1459720_x_at	-3.62
Tle6	transducin-like enhancer of split 6, homolog of Drosophila E(spl)	1448727_at	-3.51
Prlpm	prolactin family 2, subfamily a, member 1	1449032_at	-3.49
Skil	SKI-like	1452214_at	-3.37
Vwf	Von Willebrand factor homolog	1435386_at	-3.35
Tmem54	transmembrane protein 54	1417895_a_at	-3.35
Myo6	myosin VI	1421120_at	-3.35
Sgk	serum/glucocorticoid regulated kinase 1	1416041_at	-3.29
Rnf125	ring finger protein 125	1429399_at	-3.29
Spsb4	splA/ryanodine receptor domain and SOCS box containing 4	1451419_at	-3.28

* Microarray data was deposited to the Gene Expression Omnibus (GSE22418)

Appendix III

Microarray data of Dox Treated Ainv15-N1-ICD ES cells

AIII-1 Top 50 Upregulated genes

Gene Symbol	Gene Name	Probe	Fold change
Hes5	hairy and enhancer of split 5 (Drosophila)	1456010_x_at	22.84
Pik3cd	phosphatidylinositol 3-kinase catalytic delta polypeptide	1453281_at	5.88
Trh	thyrotropin releasing hormone	1418756_at	5.82
Fabp7	fatty acid binding protein 7, brain	1450779_at	5.80
Endod1	endonuclease domain containing 1	1426541_a_at	5.29
Nrarp	Notch-regulated ankyrin repeat protein	1417985_at	5.09
Spib	Spi-B transcription factor (Spi-1/PU.1 related)	1460407_at	4.94
Rhobtb3	Rho-related BTB domain containing 3	1447869_x_at	4.51
D7Ertd715e	DNA segment, Chr 7, ERATO Doi 715, expressed	1436964_at	4.42
Cenpe	centromere protein E	1439040_at	4.16
Lefty2	Left-right determination factor 2	1436227_at	3.97
Rerg	RAS-like, estrogen-regulated, growth-inhibitor	1451236_at	3.89
Has3	hyaluronan synthase 3	1420589_at	3.76
Ramp2	receptor (calcitonin) activity modifying protein 2	1418188_a_at	3.75
Id4	inhibitor of DNA binding 4	1423259_at	3.74
Pax6	paired box gene 6	1452526_a_at	3.58
F5	coagulation factor V	1449269_at	3.58
Msi2h	Musashi homolog 2 (Drosophila)	1435521_at	3.50
Kalrn	kalirin, RhoGEF kinase	1429796_at	3.40
Nebl	nebulette	1438452_at	3.25
Ptges	prostaglandin E synthase	1439747_at	3.23
Prpf38b	PRP38 pre-mRNA processing factor 38 (yeast) domain containing B	1456506_at	3.14
Fjx1	four jointed box 1 (Drosophila)	1422733_at	3.12
Spsb4	splA/ryanodine receptor domain and SOCS box containing 4	1451418_a_at	3.08
Zfhx1b	zinc finger homeobox 1b	1422748_at	3.06
Prtg	protogenin homolog (Gallus gallus)	1438333_at	3.04
Smc2l1	SMC2 structural maintenance of chromosomes 2-like 1 (yeast)	1429658_a_at	3.01
Falz	fetal Alzheimer antigen	1427311_at	2.95

Trpm1	transient receptor potential cation channel, subfamily M, member 1	1437445_at	2.88
Col13a1	procollagen, type XIII, alpha 1	1422866_at	2.88
Prickle1	prickle like 1 (Drosophila)	1452249_at	2.87
Depdc6	DEP domain containing 6	1419963_at	2.86
Paqr8	progestin and adipoQ receptor family member VIII	1444468_at	2.86
Apobec2	apolipoprotein B editing complex 2	1417889_at	2.81
Dnajb14	DnaJ (Hsp40) homolog, subfamily B, member 14	1430561_at	2.79
Tmc7	transmembrane channel-like gene family 7	1456981_at	2.75
Cidea	cell death-inducing DNA fragmentation factor,	1417956_at	2.73
Scgb3a1	secretoglobin, family 3A, member 1	1419699_at	2.71
Cpd	carboxypeptidase D	1418018_at	2.68
Wfdc2	WAP four-disulfide core domain 2	1424351_at	2.68
Ddx6	DEAD (Asp-Glu-Ala-Asp) box polypeptide 6	1424598_at	2.65
Spsb1	splA/ryanodine receptor domain and SOCS box containing 1	1449752_at	2.65
Fut9	fucosyltransferase 9	1457409_at	2.63
Rian	RNA imprinted and accumulated in nucleus	1452899_at	2.60
Stk25	serine/threonine kinase 25 (yeast)	1416770_at	2.60
Alcam	activated leukocyte cell adhesion molecule	1426301_at	2.59
Atp6v1h	ATPase, H+ transporting, lysosomal V1 subunit H	1457639_at	2.57
Ttyh1	tweety homolog 1 (Drosophila)	1422694_at	2.53
Akap9	A kinase (PRKA) anchor protein (yotiao) 9	1455151_at	2.53
Zbtb16	zinc finger and BTB domain containing 16	1439163_at	2.52
Mia3	melanoma inhibitory activity 3	1459984_at	2.52
Ank3	ankyrin 3, epithelial	1452124_at	2.51
Bub3	budding uninhibited by benzimidazoles 3 homolog (S. cerevisiae)	1459104_at	2.50

AIII-2 Top 50 Downregulated genes

Gene Symbol	Gene Name	Probe	Fold change
Insm1	insulinoma-associated 1	1421399_at	-4.61
Dll1	delta-like 1 (Drosophila)	1419204_at	-3.96
Lef1	lymphoid enhancer binding factor 1	1421299_a_at	-3.93
Lbxcor1	ladybird homeobox 1 homolog (Drosophila) corepressor 1	1437880_at	-3.88
Ung2	uracil DNA glycosylase 2	1455114_at	-3.87
Bnip3	BCL2/adenovirus E1B interacting protein 1, NIP3	1422470_at	-3.49
Adm	adrenomedullin	1447839_x_at	-3.38
Ascl2	achaete-scute complex homolog-like 2 (Drosophila)	1432018_at	-3.31
En2	engrailed 2	1418868_at	-3.14
Cbfa2t1h	CBFA2T1 identified gene homolog (human)	1444615_x_at	-3.07
Mlana	melan-A	1430635_at	-3.01
Cd80	CD80 antigen	1457952_at	-2.98
Pou3f1	POU domain, class 3, transcription factor 1	1422068_at	-2.94
Neurod1	neurogenic differentiation 1	1426413_at	-2.88
Bnipl	BCL2/adenovirus E1B 19kD interacting protein like	1420683_at	-2.6
Ssty1	spermiogenesis specific transcript on the Y 1	1449467_at	-2.54
Foxd3	forkhead box D3	1422210_at	-2.51
Samd9l	sterile alpha motif domain containing 9-like	1460603_at	-2.49
Cyp2s1	cytochrome P450, family 2, subfamily s, polypeptide 1	1428283_at	-2.49
Mucdhl	mucin and cadherin like	1426014_a_at	-2.49
Zfp526	zinc finger protein 526	1443585_at	-2.48
Trp53	transformation related protein 53	1457623_x_at	-2.48
Ptk9l	protein tyrosine kinase 9-like (A6-related protein)	1431292_a_at	-2.46
Prmt8	protein arginine N-methyltransferase 8	1435204_at	**-2.45**
Plb1	phospholipase B1	1431535_at	-2.45
Sorbs2	sorbin and SH3 domain containing 2	1446744_at	-2.43
Gpha2	glycoprotein hormone alpha 2	1421497_at	-2.43
Grhl2	grainyhead-like 2 (Drosophila)	1429086_at	-2.41
Zcchc6	zinc finger, CCHC domain containing 6	1430573_s_at	-2.39
Aoc3	amine oxidase, copper containing 3	1449396_at	-2.38
Ndrg1	N-myc downstream regulated gene 1	1450976_at	-2.37
Aqp8	aquaporin 8	1417828_at	-2.36
Plcxd1	phosphatidylinositol-specific phospholipase C, X domain containing 1	1437842_at	-2.36

Lrp2bp	Lrp2 binding protein	1436538_at	-2.36
Fkbp4	FK506 binding protein 4	1458729_at	-2.36
Slc5a11	solute carrier family 5 (sodium/glucose cotransporter), member 11	1428752_at	-2.34
Thap4	THAP domain containing 4	1443311_at	-2.33
Hat1	histone aminotransferase 1	1420237_at	-2.31
Agxt2l1	alanine-glyoxylate aminotransferase 2-like 1	1452975_at	-2.31
Il1r2	interleukin 1 receptor, type II	1419532_at	-2.31
Tmem25	transmembrane protein 25	1452962_at	-2.3
Camk2b	calcium/calmodulin-dependent protein kinase II, beta	1455869_at	-2.29
Npc1l1	NPC1-like 1	1438514_at	-2.28
Ebna1bp	EBNA1 binding protein 2	1437512_x_at	-2.28
Xkr4	X Kell blood group precursor related family member 4	1456572_x_at	-2.27
Bcl11a	B-cell CLL/lymphoma 11A (zinc finger protein)	1419406_a_at	-2.25
Sbk1	SH3-binding kinase 1	1423978_at	-2.25
D7Wsu1	DNA segment, Chr 7, Wayne State University 128,	1456217_at	-2.24
Rgs3	regulator of G-protein signaling 3	1454026_a_at	-2.24
Hes6	hairy and enhancer of split 6 (Drosophila)	1452021_a_at	-2.24

Appendix IV

Microarray data of differentiated Ainv15-N1-ICD ES cells

AIV-1 Top 50 Upregulated genes

Gene Symbol	Gene Name	Probe	Fold change
Afp	alpha fetoprotein	1416645_a_at	393.11
Cdh11	cadherin 11	1450757_at	233.59
Nr2f1	nuclear receptor subfamily 2, group F, member 1	1418157_at	168.81
Ttr	transthyretin	1454608_x_at	167.13
Hand2	heart and neural crest derivatives expressed transcript 2	1436041_at	165
Hbb-y	hemoglobin Y, beta-like embryonic chain	1436823_x_at	141.59
Col3a1	collagen, type III, alpha 1	1427884_at	141.24
Rgs5	regulator of G-protein signaling 5	1420941_at	136.24
Hbb-bh1	hemoglobin Z, beta-like embryonic chain	1437990_x_at	112.41
Asb4	ankyrin repeat and SOCS box-containing 4	1433919_at	108.43
Dkk1	dickkopf homolog 1 (Xenopus laevis)	1420360_at	107.91
Dnm3os	dynamin 3, opposite strand	1452382_at	99.89
Igfbp5	insulin-like growth factor binding protein 5	1452114_s_at	89.57
Tbx2	T-box 2	1422545_at	84.14
Hba-a1	hemoglobin alpha, adult chain 1	1452757_s_at	80.61
Ptn	pleiotrophin	1416211_a_at	79.87
Lum	lumican	1423607_at	76.96
Nrp1	neuropilin 1	1448943_at	74.97
Frzb	frizzled-related protein	1448424_at	73.44
Tcf21	transcription factor 21	1417447_at	70.8
Isl1	ISL1 transcription factor, LIM/homeodomain	1450723_at	65.59
Prrx1	paired related homeobox 1	1425528_at	64.87
Igf2	insulin-like growth factor 2	1415931_at	63.34
Rbms3	RNA binding motif, single stranded interacting protein	1436938_at	60.41
Fli1	Friend leukemia integration 1	1433512_at	57.36
Rkhd3	mex3 homolog B (C. elegans)	1437152_at	56.4
Agtrl1	apelin receptor	1438651_a_at	54.44
Postn	periostin, osteoblast specific factor	1423606_at	54.16
Emcn	endomucin	1425582_a_at	53.35
Pdgfra	platelet derived growth factor receptor, alpha polypeptide	1421917_at	52.75
Flrt2	fibronectin leucine rich transmembrane protein 2	1455096_at	52.53

Tshz2	teashirt zinc finger family member 2	1435385_at	51.34
Capn6	calpain 6	1421952_at	49.86
Adam12	a disintegrin and metallopeptidase domain 12 (meltrin alpha)	1421171_at	47.36
Ptprd	protein tyrosine phosphatase, receptor type, D	1429052_at	46.8
Col9a1	collagen, type IX, alpha 1	1428571_at	46.27
Nr2f2	nuclear receptor subfamily 2, group F, member 2	1416158_at	45.62
Edg3	sphingosine-1-phosphate receptor 3	1438658_a_at	44.9
Islr	immunoglobulin superfamily containing leucine-rich repeat	1418450_at	44.63
Dlk1	delta-like 1 homolog (Drosophila)	1449939_s_at	44.17
Fbn2	fibrillin 2	1422831_at	43.81
Pcdh7	protocadherin 7	1449249_at	43.58
Fat4	FAT tumor suppressor homolog 4 (Drosophila)	1460574_at	43.29
Sema6d	sema domain, transmembrane domain (TM), and cytoplasmic domain, (semaphorin) 6D	1453055_at	42.75
Plagl1	pleiomorphic adenoma gene-like 1	1426208_x_at	42.08
Tgfbi	transforming growth factor, beta induced	1448123_s_at	41.94
Tshz1	teashirt zinc finger family member 1	1427233_at	40.84
Unc5c	unc-5 homolog C (C. elegans)	1419592_at	39.76
Hoxd10	homeobox D10	1418606_at	38.15
Ctla2a	Ctla2a	1448471_a_at	37.86

AIV-2 Top 50 Downregulated genes

Gene Symbol	Gene Name	Probe	Fold change
Tdgf1	teratocarcinoma-derived growth factor 1	1450989_at	-36.66
Sycp3	synaptonemal complex protein 3	1449534_at	-35.26
Aass	aminoadipate-semialdehyde synthase	1423523_at	-33.58
Fgf4	fibroblast growth factor 4	1420085_at	-29.8
Gad1	glutamic acid decarboxylase 1	1416561_at	-26.29
Eras	ES cell-expressed Ras	1456511_x_at	-25.74
Klf9	Kruppel-like factor 9	1436763_a_at	-23.04
Neurod1	neurogenic differentiation 1	1426412_at	-21.88
Ndg2	coiled-coil-helix-coiled-coil-helix domain containing 10	1433720_s_at	-20.64
Dpys	dihydropyrimidinase	1436291_a_at	-19.81
Lefty1	left right determination factor 1	1417638_at	-19.55
Pou5f1	POU domain, class 5, transcription factor 1	1417945_at	-19.22
Dnahc8	dynein, axonemal, heavy chain 8	1424936_a_at	-19.14
Dmrt1	doublesex and mab-3 related transcription factor 1	1423582_at	-19.05
Slc27a2	solute carrier family 27 (fatty acid transporter), member 2	1416316_at	-18.44
Gm397	zinc finger and SCAN domain containing 4C	1457033_at	-17.86
Ddx4	DEAD (Asp-Glu-Ala-Asp) box polypeptide 4	1427242_at	-17.64
Clca6	chloride channel calcium activated 6	1443256_at	-17.48
Pla2g1b	phospholipase A2, group IB, pancreas	1437015_x_at	-17.45
Esrrb	phospholipase A2, group IB, pancreas	1436926_at	-17.35
Mael	maelstrom homolog (Drosophila)	1436837_at	-16.62
Prmt8	protein arginine N-methyltransferase 8	1435204_at	-16.01
Nanog	Nanog homeobox	1429388_at	-15.93
Atp1a3	ATPase, Na+/K+ transporting, alpha 3 polypeptide	1427481_a_at	-15.67
Psma8	proteasome (prosome, macropain) subunit, alpha type, 8	1427170_at	-15.6
Hck	hemopoietic cell kinase	1449455_at	-15.21
Fut9	fucosyltransferase 9	1435308_at	-15.04
Morc1	microrchidia 1	1419418_a_at	-14.79
Prdm14	PR domain containing 14	1444390_at	-14.56
Jam2	junction adhesion molecule 2	1431417_at	-14.55
Dnmt3l	DNA (cytosine-5-)-methyltransferase 3-like	1425035_s_at	-14.37
Hook1	hook homolog 1 (Drosophila)	1439173_at	-13.58
Nefh	neurofilament, heavy polypeptide	1424847_at	-13.4
Zfp42	zinc finger protein 42	1418362_at	-13.38
Lrrc2	leucine rich repeat containing 2	1453628_s_at	-13.2

Rex2	reduced expression 2	1438237_at	-12.79
Nr0b1	nuclear receptor subfamily 0, group B, member 1	1417760_at	**-12.7**
Pycard	PYD and CARD domain containing	1417346_at	-12.4
Ina	internexin neuronal intermediate filament protein, alpha	1448991_a_at	-12.3
Rasd2	RASD family, member 2	1427344_s_at	-12.24
Cobl	cordon-bleu	1434917_at	-12.19
Gbx2	gastrulation brain homeobox 2	1420337_at	-12.1
Gng3	guanine nucleotide binding protein (G protein), gamma 3	1417428_at	-12.02
Tcfcp2l1	transcription factor CP2-like 1	1418091_at	-12.02
Lrrc34	leucine rich repeat containing 34	1429366_at	-11.98
Fbxo15	F-box protein 15	1427238_at	-11.59
Syt9	synaptotagmin IX	1423258_at	-11.5
Hsf2bp	heat shock transcription factor 2 binding protein	1428640_at	-11.33
Dppa2	developmental pluripotency associated 2	1429654_at	-11.26
Pipox	pipecolic acid oxidase	1449374_at	-11.03

Appendix V

Curriculum Vitae

Jessica N. Copeland
Department of Pathology and Laboratory Medicine
Division of Cancer and Developmental Biology
University of Kansas Medical Center
Kansas City, KS 66160
office (913) 588-0458
fax (913) 588-8287
jcopeland@kumc.edu

ACADEMIC AFFILIATIONS

University of Kansas Medical Center Department of Pathology and Laboratory Medicine

EDUCATION

May 2004	**University of Missouri-Rolla** Department of Biological Sciences **B.S.**, Biological Sciences
August 2004-present	**University of Kansas Medical Center** Department of Pathology and Laboratory Medicine

RESEARCH EXPERIENCE

Jan 2005-present	**University of Kansas Medical Center,** Kansas City, KS Department of Pathology and Laboratory Medicine Graduate Training Assistant, laboratory of Jay Vivian, Ph.D. Dissertation studies: Vascular differentiation and Notch signaling in the mouse embryo.
June 2003-Aug 2003	**Los Alamos National Laboratory**, Los Alamos, NM REU Laboratory Technician Independent research using rDNA of yeast to examine DNA repair.
May 2002-Dec 2002	**University of Missouri - Rolla**, Rolla, MO Department of Biological Sciences

	Laboratory Technician, EPA CAFO Project Participated in experiments utilizing gas chromatography and C.O.D.

FELLOWSHIPS AND RECOGNITION

October 2009	Trainee Poster Award **6th Annual Gilbert S. Greenwald Symposium** Kansas City, MO
July 2009 – July 2010	Predoctoral Fellowship **Biomedical Research Training Program** University of Kansas Medical Center, Kansas City, KS
June 2007-June 2009	Predoctoral Fellowship **American Heart Association Heartland Affiliate**
June 2006	Best Poster Competition Honorable Mention **Society of Developmental Biology 65th Annual Meeting** Ann Arbor, MI
Aug 2005-present	Graduate Teaching Assistantship, **Department of Pathology and Laboratory Medicine** University of Kansas Medical Center, Kansas City, KS

TEACHING EXPERIENCE

Aug 2003-Dec 2003	**University of Missouri - Rolla,** Rolla, MO Department of Biological Sciences Zoology Teaching Assistant
Aug 2002-Dec 2002	**University of Missouri - Rolla**, Rolla, MO Department of Biological Sciences Cell Biology Teaching Assistant

POSTERS AND ORAL PRESENTATIONS

October 2010	Poster Session presentation **7th Annual Gilbert S. Greenwald Symposium** Kansas City, MO
October 2009	Poster Session presentation **6th Annual Gilbert S. Greenwald Symposium** Kansas City, MO
April 2008	Oral Session presentation **2008 Annual Experimental Biology Meeting** San Diego, CA
April 2008	Poster Session presentation

	2008 Annual Experimental Biology Meeting San Diego, CA
October 2007	Poster Session presentation **4th Annual Gilbert S. Greenwald Symposium** Kansas City, MO
June 2007	Poster Session presentation **First Pan American Congress in Developmental Biology** Cancun Mexico
April 2007	Oral Session presentation **University of Kansas Medical Center Student Research Forum** Kansas City, KS
October 2006	Poster Session presentation **3rd Annual Gilbert S. Greenwald Symposium** Kansas City, MO
June 2006	Poster Session presentation **Society of Developmental Biology 65th Annual Meeting** Ann Arbor, MI

PUBLISHED ABSTRACTS

Copeland J, Vivian JL. 2008. Notch signaling in early embryonic vascular differentiation. *FASEB* **22:** 522.2.
Copeland J, Vivian JL. 2007. Notch can regulate VEGF-related signaling in embryonic vascular differentiation. *Dev Biol* **306**: 445.
Copeland J, Katayama H, Vivian JL. 2006. Vascular differentiation defects associated with activated Notch signaling in endothelia of the mouse embryo. *Dev Biol* **295**: 394.

PUBLICATIONS

Copeland JN, Vivian JL. Overexpression of placental growth factor in the early embryo disrupts vascular differentiation. *In Preparation*.
Copeland JN, Feng Y, Neradugomma NK, Fields PE, Vivian JL. Notch signaling regulates remodeling and vessel diameter in the extraembryonic yolk sac. *BMC Dev Biol* **11**: 12.
Feng Y, Yang Y, Ortega MM, **Copeland JN**, Zhang M, Jacob JB, Fields TA, Vivian JL, Fields PE. 2010. Early mammalian erythropoiesis requires the Dot1L methyltransferase. *Blood* **116**: 4483-4491.